Philippine Society of Pathologists, Inc.

Vol. 11 No. 1 June 2026
ISSN 2507-8364 (Online)

PHILIPPINE JOURNAL OF PATHOLOGY

The Official Journal of the Philippine Society of Pathologists, Inc.

IN THIS ISSUE:

ALLIED HOSPITAL SUPPLY INTERNATIONAL CORP.

VALUE FOR MONEY

RAPID TEST KIT

ONSET refers to beginning which is align for early detection which one of the primary objective of RDT. Onset also has positive connotation-action, timing and proactive which is the essence of early diagnosis". Onset brand demonstrate High sensitivity and specificity.

onset

WEBSITE

8-928-4649

Philippine Journal of Pathology
Vol. 11 No. 1 June 2026 | ISSN 2507-8364 (Online)
https://philippinejournalofpathology.org

Philippine Journal of Pathology

The Philippine Journal of Pathology (PJP) is an open-access, peer-reviewed, English language, medical science journal published by the Philippine Society of Pathologists, Inc. Committee on Publications. It shall serve as the official platform for publication of high quality original articles, case reports or series, feature articles, and editorials covering topics on clinical and anatomic pathology, laboratory medicine and medical technology, diagnostics, laboratory biosafety and biosecurity, as well as laboratory quality assurance. The journal's primary audience are Filipino laboratorians, diagnosticians, laboratory managers, pathologists, medical technologists, and all other medical and scientific disciplines interfacing with the laboratory. The PJP follows the **ICMJE Recommendations for the Conduct, Reporting, Editing and Publication of Scholarly Work in Medical Journals, EQUATOR Network Guidelines,** and **COPE Guidelines.** The PJP does not charge any article processing or submission fees from authors. It does not charge any subscription fees or download fees to access content.

IN THIS ISSUE

Greetings to all our members.

It is both a privilege and an honor to write this message as your President. At the same time, I am deeply mindful of the tremendous responsibility that comes with this position, especially in this era of rapid advancements in pathology.

In this context, I would like to extend my heartfelt congratulations to Dr. Amado O. Tandoc III for his unwavering dedication to the advancement of our very own Philippine Journal of Pathology. Without his leadership, commitment, and the tireless efforts of the editorial staff, the revival of our beloved PJP would not have come to fruition. More importantly, through their collective resolve and hard work, the PJP has now been indexed in Scopus, a milestone that further enhances the journal's credibility, visibility, and standing within the scientific community.

As someone who strongly advocates for the vital role of research and scholarly publication in advancing the field of pathology—particularly in a developing country such as the Philippines—I sincerely hope that more of our members will find the time and inspiration to engage in research and contribute their work to our journal. Through our collective efforts, we can continue to strengthen the body of local scientific knowledge and elevate the practice of pathology in our country.

I encourage each of you to support and contribute to the continued growth and success of the Philippine Journal of Pathology.

Thank you, and I look forward to working with all of you in advancing our profession.

Jeffrey S. So, MD, FPSP
President, Philippine Society of Pathologists, Inc.

*Cavatina**

There is a reason some melodies linger long after the performance has ended. Not because they are triumphant, but because they carry memory gently. They remind us that meaning is often found not in fanfare, but in persistence, in the patient work of returning, rebuilding, and remaining.

This issue of the *Philippine Journal of Pathology* comes at the end of a season of milestones for the journal, and perhaps also a season of reflection.

In December 2025, during the Annual Convention of the Philippine Association of Medical Journal Editors (PAMJE), whose theme was *Publishing for National Relevance: Aligning Medical Journals with the National Unified Health Research Agenda (NUHRA)*, we were given the opportunity to share the experiences of the *Philippine Journal of Pathology* in reestablishing itself as a local medical journal striving to remain both nationally meaningful and internationally visible. The conversation was not merely about indexing, metrics, or platforms, but about survival, and about the continuing relevance of Philippine scholarship in an increasingly crowded scientific landscape.

That same month, the journal formally released its Policy on the Use of Artificial Intelligence. Like many journals across the world, we recognize that artificial intelligence will shape the future of scientific communication in profound ways. Yet amid rapid technological change, the fundamental obligations of scientific publishing remain unchanged: transparency, accountability, integrity, and trust.

In February 2026, the *Philippine Journal of Pathology* was accepted into Scopus. For many journals, indexing represents arrival. For us, it feels more like responsibility. Visibility widens readership, but it also deepens our obligation to uphold rigor, ethics, and relevance. The work ahead remains substantial, but this milestone belongs not only to the Editorial Board, reviewers, and staff, but to every Filipino pathologist, researcher, and author who believed that a Philippine journal deserved to endure.

In March 2026, during the PAMJE Educational Forum held on the occasion of the 44th anniversary of the DOST–PCHRD, we discussed the 2026 updates to the ICMJE Recommendations. These updates remind us that scientific publishing is constantly evolving, challenged by emerging technologies, changing authorship practices, predatory behavior, and increasing public scrutiny. Yet they also reaffirm that journals are not merely repositories of papers; they are stewards of scientific credibility.

https://doi.org/10.21141/PJP.2026.647

*Italian for "a Little Song."

Perhaps the most personal moment came during the 2026 Convention of the Philippine Society of Pathologists, where I was deeply honored to receive the Distinguished Service Award for work related to the journal. My daughter helped prepare an audiovisual presentation tracing the journey of the *Philippine Journal of Pathology*. We took it as an opportunity to honor the late Dr. Jose Ma. Avila, adviser to the journal and former Editor-in-Chief of *Acta Medica Philippina*, whose guidance and faith in Philippine medical publishing helped shape many of us.

Accompanied by the piece *Cavatina* by Stanley Myers, some pathologists later remarked that the presentation sounded sad.

Maybe it did.

But not all quiet music is sorrowful. Some melodies simply carry the weight of memory. They acknowledge that institutions are built not only through achievement, but through sacrifice, uncertainty, fatigue, and the often invisible labor of people who believed in something before others did. In many ways, journals resemble such music: sustained not by spectacle, but by endurance.

The work of rebuilding the *Philippine Journal of Pathology* has never been the work of one person alone. It has depended on editors, reviewers, authors, society leaders, mentors, staff, and readers who continued to contribute despite limitations familiar to many journals in low- and middle-income countries. It has required faith that local scholarship matters, that Philippine data deserve visibility, and that our scientific voice should not disappear into silence.

As we release this June 2026 issue, we do so with gratitude: for those who built before us, for those who continue the work now, and for those who will inherit it afterward.

Like a Cavatina, perhaps the role of a journal is not always to be loud. Sometimes its task is simply to remain clear, honest, and enduring enough for others to hear themselves within it.

Amado O. Tandoc III, MD, FPSP
Editor-in-Chief

OPEN ACCESS – FEATURE ARTICLE

Strengthening Diagnostic Approach for Emerging Pathogens in the Philippines Through TEM-based Ultrastructural Pathology

Maria Sarah Lenon, Jhunel Vinarao, Danielle Aquino

Research Institute for Tropical Medicine, Alabang, Muntinlupa, Philippines

ABSTRACT

The emergence of novel pathogens poses significant challenges to public health systems worldwide, demanding rapid and coordinated outbreak response mechanisms. The case of "Pathogen X," a hypothetical novel pathogen, highlights the complexity of such efforts, which require rapid identification, diagnostic readiness, and effective containment strategies. Leveraging recent advances in ultrastructural pathology and genomics is essential to ensure a timely and robust response. Within this diagnostic framework, transmission electron microscopy (TEM) serves as a powerful imaging modality at high magnification that enables direct visualization of pathogen particles and infection-induced ultrastructural cellular changes. Unlike molecular techniques that infer presence through nucleic acids, TEM offers same-day morphological triage, confirmation of pathogen presence, and identification of co-infections. Through techniques such as negative staining and ultrathin sectioning, TEM reveals hallmark structural features that not only support provisional taxonomic classification and biosafety risk assessment but also inform the design and quality control of downstream assays such as metagenomic next-generation sequencing (mNGS) and targeted PCR. As such, TEM significantly accelerates and reinforces the overall outbreak investigation workflow. Its high-resolution imaging capabilities make it particularly valuable in situations where speed, morphological clarity, and pathogen diversity necessitate a direct visualization approach.

Key words: electron microscopy, transmission electron microscopy, ultrastructural pathology, emerging pathogens, Pathogen X

ISSN 2507-8364 (Online)
Printed in the Philippines.

Received: 18 December 2025.
Accepted: 18 December 2025.
Published online first: 10 June 2026.
https://doi.org/10.21141/PJP.2026.571

Corresponding author: Maria Sarah L. Lenon, MD
E-mail: sarahlenon@gmail.com
ORCiD: https://orcid.org/0000-0002-4257-9212

ELECTRON MICROSCOPY AS REVOLUTIONARY TECHNOLOGY

The first prototype of the electron microscope was developed in 1931, engineered by Ernst Ruska and Max Knoll in Berlin, revolutionizing how scientists visualize life at the smallest scales.[1] This groundbreaking invention laid the foundation for modern electron microscopy. In 1939, the first commercially available electron microscope was introduced by Siemens, with Ernst Ruska playing a key role in its development. Following World War II, numerous companies developed commercial electron microscopes, notably JEOL in Japan and Philips in Europe, leading to widespread adoption in biological and materials research.[2]

Today, modern transmission electron microscopes (Figure 1), with resolutions reaching as fine as 0.23 nm and magnification exceeding 2 million times, can reveal structures far beyond the reach of conventional light microscopy.[3,4] From viruses and bacterial ultrastructure to molecular-level entities such as prions, TEM provides an unparalleled window into the architecture of disease. For researchers at the forefront of pathogen detection, this translates to faster diagnostics, deeper understanding of novel threats, and a critical advantage in pandemic prevention.

Recent advancements in TEM protocols have significantly expanded its diagnostic applications across infectious agents. Ranjan et al. demonstrated that negative staining enables sample preparation for foot-and-mouth disease virus detection in under 10 minutes, highlighting TEM's

Figure 1. ***JEOL JEM-F200 Transmission Electron Microscope*** installed at the Research Institute for Tropical Medicine.

Photo taken by J.G. Vinarao.

efficiency in urgent diagnostic settings.[5] Laue further emphasized the evolution of diagnostic electron microscopy from a routine laboratory method to a specialized tool increasingly used in outbreak investigations and pathogen characterization.[6] Notably, SARS-CoV-2 was initially identified using TEM, which provided rapid morphological insights into viral particles before genomic data were available, thereby guiding subsequent metagenomic sequencing efforts.[6,7]

In addition to structural visualization, TEM techniques such as immunogold labeling have proven valuable for biochemical and functional characterization. This approach enhances the detection of specific antigens and extracellular vesicles associated with pathogens, offering insights into mechanisms of disease transmission and immune evasion.[8] Such capabilities position TEM not only as an imaging modality but also as a functional diagnostic tool. Further illustrating its versatility, Jiao et al. employed TEM to trace virion assembly and intracellular movement in plant virology, demonstrating its applicability across diverse biological systems.[9]

CELLULAR, TISSUE, AND BACTERIAL CROSS-SECTION ULTRASTRUCTURAL ANALYSIS

Transmission electron microscopy remains indispensable for nanoscale visualization of pathogens and host cellular architecture. High-quality ultrastructural imaging requires advanced instrumentation, meticulous specimen preparation, and specialized technical expertise. At the Research Institute for Tropical Medicine (RITM), personnel

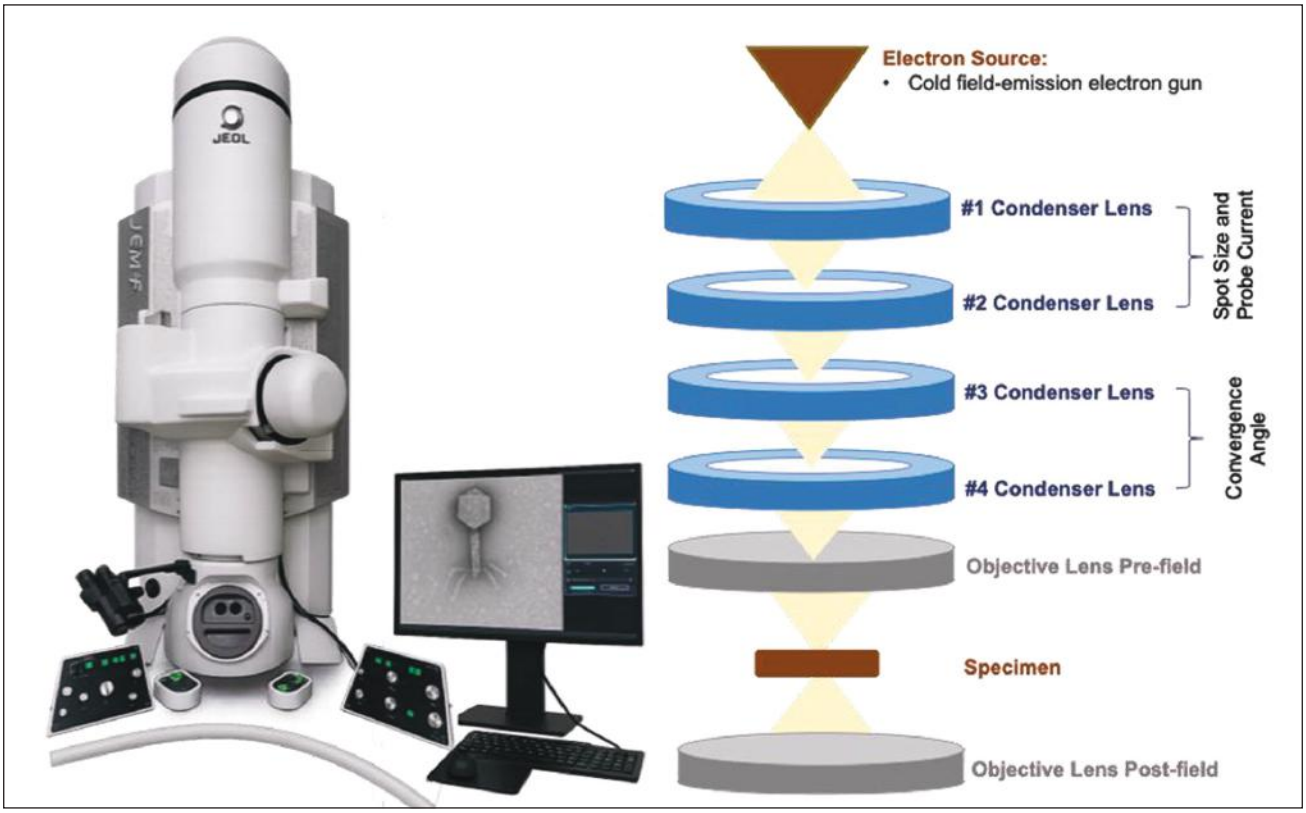

Figure 2. ***JEOL JEM-F200 transmission electron microscope and its lens system.*** The JEM-F200 is equipped with a cold field emission gun (CFEG), producing a highly coherent electron beam with low energy spread, ideal for resolving nanoscale viral structures. The condenser lens system (CL1 and CL2) modulates beam intensity and spot size, enabling optimization for imaging and analytical techniques such as energy-dispersive X-ray spectroscopy and electron energy loss spectroscopy. The specimen stage is positioned at the center of the column, where the objective lens—critical for high-resolution imaging—focuses transmitted electrons. Downstream intermediate and projector lenses determine final magnification and imaging mode, supporting applications ranging from low-magnification surveys to high-resolution diagnostics.[10]

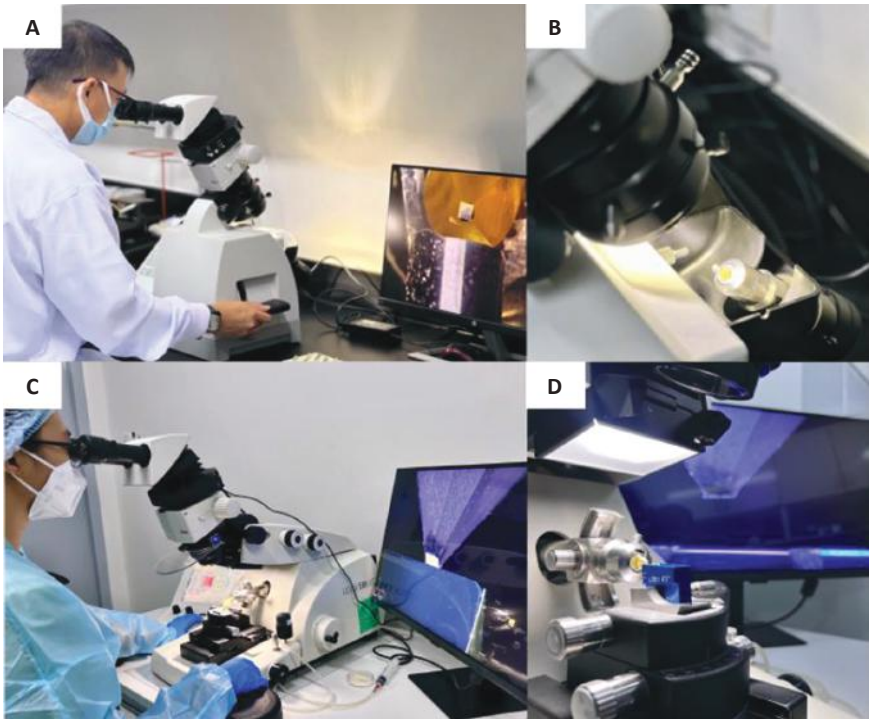

Figure 3. ***Transmission electron microscopy sample preparation procedures:*** **(A and B)** semi-thin and **(C and D)** ultra-thin sectioning using a diamond knife.

utilize modern TEM (Figure 2) platforms alongside the Leica UC7 ultramicrotome, enabling the production of ultrathin sections essential for ultrastructural analysis (Figure 3). Preparation workflows include negative and positive staining as well as ultrathin sectioning at sub-micron thicknesses, procedures that demand exceptional technical proficiency.

Beyond imaging, ultrastructural analysis plays a key role in elucidating pathogen-induced cellular disruption. Yang et al. demonstrated that duck Tembusu virus compromises the blood–brain barrier, revealing novel cytopathological changes through TEM that shed light on neuropathogenesis.[11] In bacterial infections, Liss and Hensel identified previously unrecognized ultrastructural features in *Salmonella enterica*-infected cells, challenging existing models of intracellular bacterial environments.[12] Similarly, Schulte et al. showed that ultrastructural heterogeneity among bacterial morphotypes correlates with physiological states, offering insight into bacterial viability and stress responses.[13]

Collectively, these studies underscore the ability of ultrastructural methods to reveal biological features that may be overlooked by molecular or immunological assays. Integrating TEM into pathogen detection workflows enhances characterization of emerging agents, refines disease definitions, and may facilitate discovery of novel diagnostic biomarkers.

TEM IN VIRAL DIAGNOSTICS AND INTEGRATION WITH GENOMICS

Transmission electron microscopy continues to serve as a critical diagnostic modality, particularly for rapid detection of viral and atypical pathogens. Negative staining (Figure 4) allows rapid preparation and high-contrast visualization of viral particles (Figure 5) using electron-dense stains such as uranyl acetate or phosphotungstic acid. Jiang et al. demonstrated that TEM with negative staining can identify multiple pathogens from bronchoalveolar lavage fluid within 48 hours, outperforming many molecular diagnostics in turnaround time.[14] Importantly, TEM's reagent-independent nature makes it especially valuable for detecting unknown or emerging pathogens.

While metagenomic next-generation sequencing has revolutionized infectious disease diagnostics through hypothesis-free detection of known and novel pathogens, TEM remains a vital complementary tool. Unlike sequencing methods that infer pathogen presence from genetic material, TEM provides direct visual confirmation and enables assessment of infection-induced cellular pathology. Although mNGS excels at detecting unexpected or co-infecting organisms,[15] its sensitivity can be limited by high host DNA background unless extensive enrichment strategies are applied.[16]

Advances such as cryo-electron tomography and immunogold labeling have further expanded TEM's capabilities, enabling molecular-level visualization of pathogen–host interactions.[17] Integration of TEM into public health and reference laboratories strengthens surveillance and outbreak response capacity, particularly for morphologically distinctive or highly transmissible agents. A synergistic diagnostic framework combining TEM's specificity with the broad detection range of NGS offers a more robust and accurate approach to infectious disease diagnosis.

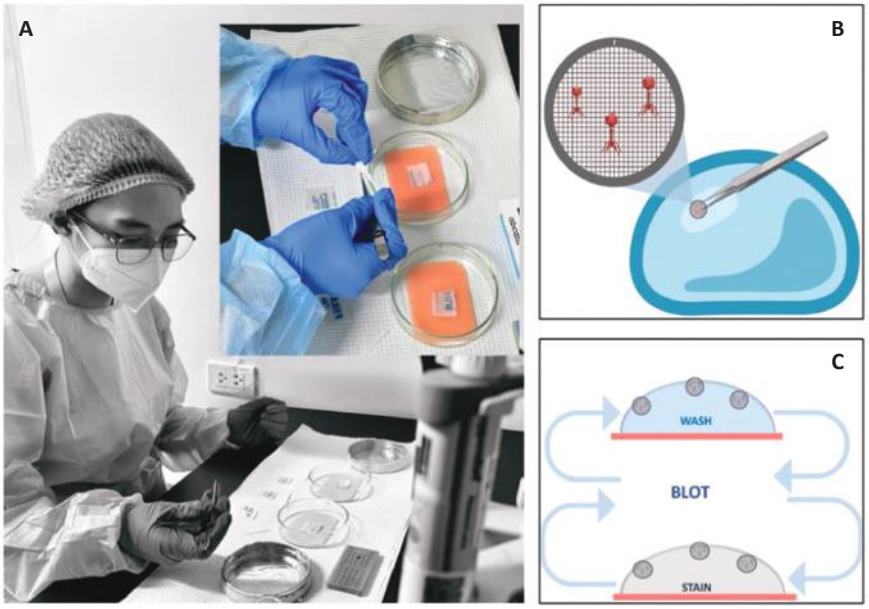

Figure 4. ***Negative staining workflow for enhanced ultrastructural visualization of viral particles.*** **(A)** Setup of the negative staining station, including essential tools and reagents; **(B)** Schematic representation of the staining procedure showing sample adherence to grids, followed by **(C)** sequential washing, blotting, and drying steps.

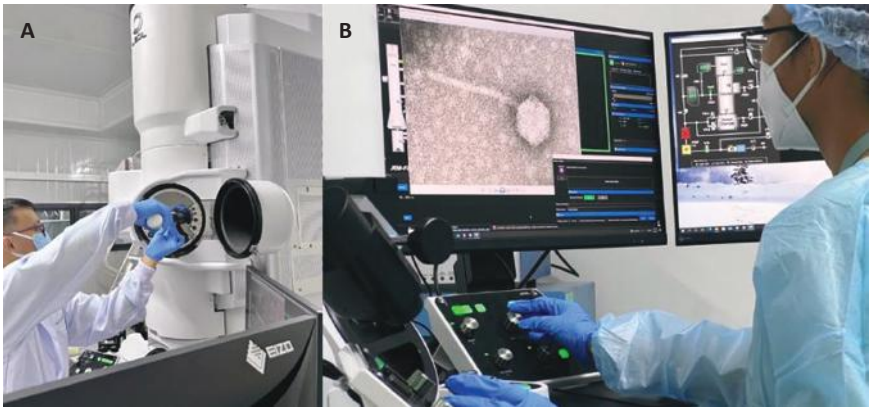

Figure 5. ***Generating electron micrographs using the transmission electron microscope (TEM).*** **(A)** Insertion of the sample holder into the TEM column; **(B)** Operation of the TEM user interface for image acquisition and parameter adjustment.

CONCLUSION

Seeing the unseen and future-facing vision

As the world confronts emerging and re-emerging pathogens—including Ebola, Zika, COVID-19, and avian influenza—early detection has become a cornerstone of public health preparedness. The upgraded TEM laboratory at RITM was established to strengthen national capacity for infectious disease surveillance, diagnostics, and outbreak response. In this context, TEM serves not merely as an instrument but as a sentinel technology, bridging classical microscopy and modern molecular diagnostics.

The commissioning of this advanced TEM system marks a significant step forward in the Philippines' preparedness for biological threats. Beyond diagnostics, it enables cutting-edge research in structural virology, vaccine development, nanomedicine, and materials science, reinforcing its role as a cornerstone of future-facing infectious disease research.

STATEMENT OF AUTHORSHIP

All authors certified fulfillment of ICMJE authorship criteria.

AUTHOR DISCLOSURE

The authors declared no conflict of interest.

DATA AVAILABILITY STATEMENT

The data that support the findings of this study are available from the corresponding author upon reasonable request.

FUNDING SOURCE

None.

REFERENCES

1. Asarnow D, Becker VA, Bobe D, et al. Recent advances in infectious disease research using cryo-electron tomography. Front Mol Biosci. 2024;10:1296941. PMID: 38288336 PMCID: PMC10822977 DOI: 10.3389/fmolb.2023.1296941
2. Chua TH, Punjabi LS, Khor LY. Tissue pathogens and cancers: a review of commonly seen manifestations in histo- and cytopathology. Pathogens. 2021;10(11): 1410. PMID: 34832566 PMCID: PMC8624235 DOI: 10.3390/pathogens10111410
3. Čižmár P, Yuana Y. Detection and characterization of extracellular vesicles by transmission and cryo-transmission electron microscopy. Methods Mol Biol. 2017;1660:221-32. PMID: 28828660 DOI: 10.1007/978-1-4939-7253-1_18
4. Harris PJF. Transmission electron microscopy of carbon: a brief history. C. 2018;4(1):4. DOI: 10.3390/c4010004.
5. JEOL Ltd. JEM-F200 multipurpose electron microscope. JEOL Ltd.; n.d. Accessed August 8, 2025. https://www.jeol.com/products/scientific/tem/JEM-F200.php
6. Jiang J, Hu C. Li Y, et al. Transmission electron microscopy improves diagnostic sensitivity in nonbacterial etiology of severe pneumonia: a retrospective study. Am J Med Sci. 2019;357(4): 289-95. PMID: 30638601 PMCID: PMC7093854 DOI: 10.1016/j.amjms.2018.11.012
7. Jiao M, Yin Y, Tian Y, et al. Adoption of the 2A ribosomal skip principle to track assembled virions of pepper mild mottle virus in Nicotiana benthamiana. Plants (Basel). 2024;13(7):928. PMID: 38611458 PMCID: PMC11013369 DOI: 10.3390/plants13070928
8. Laue M. Diagnostic electron microscopy in human infectious diseases—methods and applications. J Microsc. 2025;299(3):186-205. PMID: 39560601 PMCID: PMC12352021 DOI: 10.1111/jmi.13370
9. Liss V, Hensel M. Take the tube: remodelling of the endosomal system by intracellular Salmonella enterica. Cell Microbiol. 2015;17(5):639-47. PMID: 25802001 DOI: 10.1111/cmi.12441
10. Max Planck Institute for Colloids and Interfaces. JEOL JEM-F200 scanning transmission electron microscope [Internet]. Max Planck Institute for Colloids and Interfaces; n.d. Accessed August 8, 2025. https://www.mpikg.mpg.de/6727477/scanning-transmission-electron-microscope-jeol-jem-f200
11. Ranjan R, Biswal JK, Singh RP. Optimization and development of protocol for detection of foot-and-mouth disease virus by negative staining using transmission electron microscopy. Acta Sci Vet Sci. 2023;5(2):18-23. DOI: 10.31080/asvs.2023.05.0597.
12. Schulte M, Hensel M, Mi□kiewicz K. Exposure to stressors and antimicrobials induces cell-autonomous ultrastructural heterogeneity of an intracellular bacterial pathogen. Front Cell Infect Microbiol. 2022; 12:963354. PMID: 36457851 PMCID: PMC9705743 DOI: 10.3389/fcimb.2022.963354
13. Smith Y. History of the electron microscope. News-Medical. Published August 23, 2018. Accessed August 8, 2025. https://www.news-medical.net/life-sciences/History-of-the-Electron-Microscope.aspx
14. Simner PJ, Miller S, Carroll KC. Understanding the promises and hurdles of metagenomic next-generation sequencing as a diagnostic tool for infectious diseases. Clin Infect Dis. 2018;66(5):778-88. PMID: 29040428 PMCID: PMC7108102 DOI: 10.1093/cid/cix881
15. Yang S, Shi Y, Wu J, Chen Q. Ultrastructural study of the duck brain infected with duck tembusu virus. Front Microbiol. 2023;14:1086828. PMID: 36891400 PMCID: PMC9987711 DOI: 10.3389/fmicb.2023.1086828
16. Zhao X, Ge Y, Zhang Y, et al. Pathogen diagnosis value of nanopore sequencing in severe hospital-acquired pneumonia patients. Infect Drug Resist. 2023;16: 3293-303. PMID: 37260782 PMCID: PMC10228525 DOI: 10.2147/IDR.S410593
17. Zhu N, Zhang D, Wang W, et al. A novel coronavirus from patients with pneumonia in China, 2019. N Engl J Med. 2020;382(8):727-33. PMID: 31978945 PMCID: PMC7092803 DOI: 10.1056/NEJMoa2001017

OPEN ACCESS – ORIGINAL ARTICLE

Utilization of *in silico*-designed primers for SARS-CoV-2 Molecular Surveillance using Direct PCR Product Sequencing Surveillance (DPPSS) Method

Sarah Jane Datay-Lim,[1,2] Flyndon Mark Dagalea,[2,3] Michael Reigh Guevarra,[2] Kristine Avila,[2] Kim Claudette Fernandez,[2] Francisco Heralde III[2]

[1]*Department of Laboratory Medicine and Pathology, The Medical City, Pasig City, Philippines*
[2]*Department of Biochemistry and Molecular Biology, College of Medicine, University of the Philippines Manila*
[3]*Department of Chemistry, College of Science, University of Eastern Philippines*

ABSTRACT

Background. The COVID-19 pandemic caused by SARS-CoV-2 significantly strained healthcare systems in the Philippines, highlighting the critical importance of reliable molecular diagnostics and genomic surveillance. Although vaccination efforts and public health measures mitigated disease impact, the continued emergence of viral variants underscores the need for sustainable local surveillance strategies. Strengthening in-country capacity through the development of *in silico*–designed primers and cost-effective sequencing approaches can enhance rapid variant detection and improve preparedness for future emerging infectious diseases.

Objective. This paper offers a method in detecting the SARS-CoV-2 virus and its variants. A direct PCR product sequencing surveillance or DPPSS offers a new possibility of detecting emerging disease by using PCR products and using it as templates in determining the base sequence.

Methodology. A total of 20 random positive samples for SARS-CoV-2 from March 2022 sample pool in Metro Manila, Philippines was used in this study. The RNA was extracted using Purelink™ RNA Mini Kit, quantified with NanoDrop, and subjected to one-step RT-PCR. An in-house designed *in silico* primers were used in this study by using thermodynamic parameters to optimize specificity and amplification efficiency, considering GC contents, balanced Tm, minimal secondary structures and cross-dimers and *in silico* validation via Basic Local Alignment Search Tool (BLAST) against reference databases.

Amplicons were analyzed through gel electrophoresis, sequenced, and analyzed using BioEdit software. A nucleotide BLAST search identified COVID-19 variants, confirmed using Cov-Lineages website.

Results. *In silico* designed primers (S1, S2, E/M, Orf1ab) collectively exhibited 100% sensitivity in detecting SARS-CoV-2 in nasopharyngeal swab samples. Individual primer sensitivities varied, with Orf1ab at 58.82% and E/M at 90.91%. Our analysis revealed the prevalence of Omicron sublineage BA.2 in the Philippines, aligning with local data showing more BA.2 cases than the global predominance of BA.1.

Conclusion. Combined *in silico* primers (S1, S2, E/M, ORF1ab) accurately detect SARS-CoV-2 and its variants. This method provides a valuable diagnostic and surveillance tool for public health management.

Key words: COVID-19, virus variants, PCR, sequencing, molecular diagnostic techniques

ISSN 2507-8364 (Online)
Printed in the Philippines.

Received: 18 February 2026.
Accepted: 31 March 2026.
Published online first: 24 June 2026.
https://doi.org/10.21141/PJP.2026.609

Corresponding author: Sarah Jane L. Datay-Lim, MD
E-mail: sldataylim@themedicalcity.com
ORCiD: https://orcid.org/0000-0002-9874-7019

INTRODUCTION

In early 2020, the world faced a novel public health crisis caused by SARS-CoV-2, the etiologic agent of Coronavirus 2019 (COVID-19). The virus primarily affects the respiratory system, causing symptoms ranging from mild upper respiratory illness to severe pneumonia.[1,2] As of January 2026, the World Health Organization (WHO) reported 779,102,516 confirmed cases globally,[3] while the Philippine Department of Health documented 4,140,383 cases nationwide.[4] Multiple variants have since emerged, including Alpha, Beta, Gamma, Delta, Epsilon, Eta, Iota, Kappa, Zeta, Mu, and Omicron, with Omicron classified as a Variant of Concern and others as Variants Being Monitored.[1,2]

The pandemic highlighted the critical role of laboratory diagnostics. Nucleic acid amplification tests, particularly reverse transcription- polymerase chain reaction (RT-PCR), remain the gold standard for COVID-19 diagnosis due to their high sensitivity and specificity. However, limitations such as reduced detection in low viral load samples and resource-intensive requirements restrict widespread implementation in low- and middle-income countries.[5,6] Rapid antigen and antibody-based assays support surveillance but require confirmatory testing due to lower sensitivity. Meanwhile, genomic surveillance through next-generation and whole-genome sequencing is essential for variant characterization, though high costs limit routine clinical use.[5]

Although the WHO declared the end of COVID-19 as a global health emergency in May 2023,[7] continued viral evolution underscores the need for sustainable and cost-effective molecular surveillance strategies. SARS-CoV-2 continues to acquire mutations that influence transmissibility, immune escape, and therapeutic effectiveness. Strengthening local capacity for variant detection and preparedness remains imperative.

This study introduces Direct PCR Product Sequencing Surveillance (DPPSS) as a low-cost alternative for molecular surveillance. Direct sequencing of PCR-amplified products enables rapid base sequence determination with minimal processing errors,[8] offering a practical approach for resource-limited settings such as the Philippines. Primer design targeted key genomic regions of SARS-CoV-2, including the spike (S), envelope (E), membrane (M), and open reading frame (ORF) regions.[9-11] The S primer targets the spike protein gene associated with viral entry; the EM primer aligns with envelope and membrane regions critical for viral assembly; and the O primer spans open reading frames to provide broader genomic coverage.[12-14] These targeted regions support effective and efficient variant monitoring using the DPPSS method.

As we utilize PCR surveillance sequencing as a cornerstone in tracking and understanding the evolution of SARS-CoV-2, the chosen primers enhance the specificity and sensitivity of the assay, ensuring accurate detection and surveillance. The strategic placement of primers allows for targeted amplification of regions crucial for both diagnostic and epidemiological purposes.

This paper aims to present an evaluation *in silico*-designed primers using the DPPSS method being developed for the detection of SARS-CoV-2 variants among RNA samples extracted from SARS-CoV-2 positive nasopharyngeal swab specimens. Likewise, this paper will identify the sensitivity of the designed primers to detect the SARS-CoV-2 virus, determine the type and frequency of SARS-CoV-2 variants in the positive specimens, and correlate the relationship of the detected variants with the clinical and epidemiological data during the time of collection.

METHODOLOGY

Sampling

A total of 20 random nasopharyngeal/ oropharyngeal positive samples for SARS-CoV-2 after RT-PCR testing were taken from March 2022 sample pool in Metro Manila, Philippines.

RNA extraction

The viral RNA of the samples was extracted using the PureLink™ Viral RNA Mini Kit (Invitrogen®) by following the manufacturer's protocol. Essentially, proteinase K and a lysis buffer were used to open cells and obtain RNA. Following this, RNA binding was performed using spin-columns. Wash buffers were used for the RNA washing step and lastly, the RNA was eluted through centrifugation. The eluted RNA was stored in -20°C.

Nucleic acid quantification

The RNA extracts were quantified using the Thermo Scientific NanoDrop™ 1000 Spectrophotometer. First, the device was cleaned using sterile distilled water and bleach in an alternate manner for 2 mins each. Following this step, "blank" measurements were made by dispensing 1 μL of buffer onto the lower optical surface. Upon completing the cleaning and blank reading steps, quantification of the samples was performed by loading 1 μL of the sample onto the device. To accurately assess sample quality, 260/280 or 260/230 ratios was analyzed in combination with overall spectral quality. Pure nucleic acids typically yield a 260/280 ratio of ~1.8 and a 260/280 ratio of ~2.0 for DNA and RNA, respectively.

DPPSS primer

In silico–designed oligonucleotide primer sets targeting the ORF1ab, S1, S2, E, and M genomic regions of SARS-CoV-2 (See Table 1). The table summarizes the target gene, primer designation (forward and reverse), nucleotide sequence (5′–3′), predicted amplicon length (bp), GC content (%), and calculated melting temperature (Tm, °C). Primer design was performed using thermodynamic parameters to optimize specificity and amplification efficiency, with selection criteria including appropriate GC content, balanced Tm between primer pairs, absence of significant secondary structures (hairpins and self-dimers), minimal cross-dimer formation, and *in silico* specificity verification through Basic Local Alignment Search Tool (BLAST) analysis against reference genomic databases. It was then sent for synthesis to Macrogen, Inc. (South Korea).

One step RT-PCR

The one-step RT-PCR was performed using the SuperScript™ III One-Step RT-PCR System with Platinum Taq DNA Polymerase (Invitrogen®, USA). Following the manufacturer's protocol, each 10 μL reaction contained 2 μL of 2x Reaction buffer, 0.4 μL DNTPs, 0.6 μL of each forward and reverse primers, 0.4 μL Taq polymerase enzyme, 1 μL RNA template, and 5 μL distilled, nuclease-free water. The touchdown amplification was carried out using the T100™ thermal cycler (Bio-Rad, Japan). The thermal cycling conditions consisted of 30 mins at 50°C for reverse transcription, 15 mins at 95°C for Taq polymerase activation, 10 cycles of touchdown PCR set at 94°C for 1 min denaturation, 55°C for 1 min annealing, and 72°C for 1 min extension. After this, the final PCR profile is set at 20 cycles consisting of 94°C for 1 min denaturation, 58°C for 1 min annealing, and 72°C for 1 min extension. The final extension profile is set at 72°C for 10 mins and the reaction is terminated and held at 4°C.

Table 1. *In silico*-designed primers featuring the following target genes: ORF1ab, S1, S2, E, and M

Target Gene	Primer Name	Primer Pair Sequence (5'→3')	Product size (bp)	GC content	Tm
ORF1ab	SARS-CoV-2_Var_01	*Forward primer 01* *ACCAATGTGCTATGAGGCCC*	818	55%	60.11
		Reverse primer 01 *CATCACCCAACTAGCAGGCA*		55%	60.04
S	SARS-CoV-2_Var_S1	*Forward primer S1* *CAAATCGCTCCAGGGCAAAC*	1362	55%	60.11
		Reverse primer S1 *GTGGCAAAACAGTAAGGCCG*		55%	60.04
S	SARS-CoV-2_Var_S2	*Forward primer S2* *GTCCTTCCCTCAGTCAGCAC*	655	60%	60.00
		Reverse primer S2 *GACTCCTTTGAGCACTGGCT*		55%	59.96
E,M	SARS-CoV-2_Var_EM1	*Forward primer EM1* *CGATTGTGTGCGTACTGCTG*		55%	59.01

Detection of the RT-PCR product

The amplicons were subjected to electrophoresis using a 1.0% agarose gel and were stained using gel red. The gels were quantified by using a nanodrop and were visualized under UV light using XR+ Gel Documentation System (Bio-rad, Japan).

Sequencing

Around 20 μL of the RT-PCR amplicons were packaged by wrapping parafilm wax around the lid of the PCR reaction tubes. The tubes were placed inside sealable bags and were sent for sequencing as per the service provider instructions (Macrogen Inc., South Korea).

Sequence analysis

The resulting sequencing results were visualized and analyzed using the BioEdit software. A consensus sequence was generated by aligning the forward and reverse sequence of the sample. Note that the reverse sequence is in the 3' to 5' orientation, thus the sequence should be flipped first to set the orientation to the 5' direction. After ensuring that both sequences were in the 5' direction, the sequence alignment was run using the ClustalW function of the software. After alignment, the sequence was edited by removing the lagging sequence strand first, followed by the removal of the leading sequence. Once completed, a consensus sequence was generated by using the Consensus Sequence generator function of the software.

BLAST search and lineage identification

A BLAST analysis was performed to determine the variant identity of the viral samples using the online platforms provided by the National Center for Biotechnology Information (NCBI) and the China National Center for Bioinformation. The consensus sequence of each sample was initially used as the query sequence for BLAST analysis, and the corresponding description, species identification, and accession number of the top hits were recorded. In cases where the consensus sequence failed to yield BLAST results, the forward sequencing read was used. If no significant match was obtained, the reverse sequence was reverse-complemented and subsequently analyzed. The resulting BLAST hits were documented accordingly. Using the recorded description and accession number, the SARS-CoV-2 variant was determined through the SARS-CoV-2 epidemiological lineage assignment tool available on the Cov-Lineages website.

RESULTS

A total of 16 samples were subjected to RNA extraction using PureLink™ Viral RNA/DNA kit and one-step RT-PCR assays. After extraction, the samples' concentration and purity were determined using NanoDrop™. The samples with good concentration and purity were included for further analysis. Pre-amplification RNA integrity and post-amplification product specificity were evaluated by agarose gel electrophoresis. Expected amplicon sizes for the DPSS primer sets were confirmed as follows: SARS-CoV-2_Var_S1 (1362 bp), SARS-CoV-2_Var_S2 (655 bp), SARS-CoV-2_Var_EM1 (658 bp), and SARS-CoV-2_Var_O1 (818 bp).

Figure 1 shows the post-PCR agarose gel electrophoresis result of samples 6, 7, 8, 10, 101, 128, 130, 133, 140, 143, 146, 147, 152, and 156 using SARS-CoV-2_Var_EM1 primer. Samples 7, 10, 143, 146, and 152 were the best samples in this primer showing a product size of more than 600 bp and a band greater than 60 ng. Only the PCR products meeting these criteria were selected for sequencing.

The raw sequence data were quality-checked, trimmed and assembled to generate consensus sequence and alighted to the SARS-CoV-2 reference genome and lineage classification performed using the Pango nomenclature system based on characteristic mutation profiles within the amplified regions. The assigned lineages are summarized in Table 3.

DISCUSSION

The results showed that the four (4) *in silico*-designed primers used for this study: S1, S2, E/M and Orf1ab had a sensitivity of 100% when used in combination to detect previously tested known nasopharyngeal/ oropharyngeal swab samples positive for SARS-CoV-2. Each primer had different sensitivities, with Orf1ab being the lowest at 58.82% and the E/M the highest at 90.91% (Table 4). The AGE for the E/M also had the highest number of bands noted (Figure 1). This is in contrast with other studies that

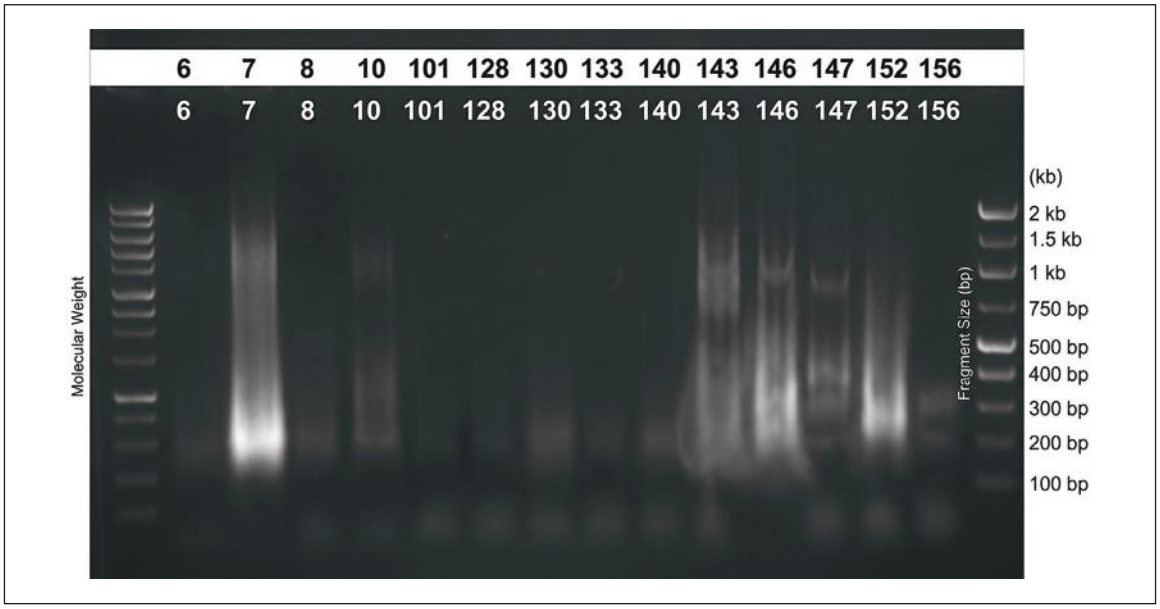

Figure 1. Post PCR agarose gel electrophoresis result for E/M primer (left to right: Samples 6, 7, 8, 10, 101, 128, 130, 133, 140, 143, 146, 147, 152 and 156).

show Orf1ab, N, and Rdrp as having the highest sensitivities among the different evaluated gene target primers.[12,15]

Designing primers for a virus that frequently mutates such as SARS-CoV-2 is challenging. Ideally, the target must be an area that is conserved in the genome so that it can still detect the virus. One possible explanation for the high sensitivity of E/M in our study can be attributed to the lack of mutation detected in the E/M gene from the samples included (Appendix 1). All the samples had multiple mutations in the S and ORF1ab proteins which is compatible with the variant classification of most samples under Omicron. This is similar to the study by Mentes et al., showed that the E gene had the lowest mutation rate from their experiment.[16] Further supporting this is a local study on the genome sequences in the Philippines during the start of the pandemic also showed that the most conserved among the different proteins is the envelope protein, 224 with 100% sequence similarity at both nucleotide and amino acid levels relative to the reference.[17]

The total number of mutations across the target regions, as well as the type (example: point mutation vs. deletion) can damage it significantly, leading to potential misclassification and affect the accuracy of diagnostics employing the primers. It can also affect primer and probe hybridization, causing amplification failure in real time polymerase chain reaction (RT-PCR), the gold standard for SARS-CoV-2 diagnosis. This is the reason why multiple primers or primer sets are used for SARS-CoV-2 diagnostics as recommended also by different studies[12,16,18] and supports our finding of high sensitivity for combined four primers rather than individual ones. Any conflicting results warrants repeat RT-PCR and agarose gel electrophoresis to exclude technical variability and persistent discordance maybe resolved by sequencing the amplified products. The sequencing data can be used to identify genomic regions and assess mutations that can affect primer binding sites that can explain amplification failures in certain targets.

The mutations in the samples were in the S and ORF1ab proteins, but the primers were still able to detect bands in the S protein but were not as successful in the ORF1ab (Appendix 1). No cross-reactivity was noted. The use of multiple targets therefore enhances overall diagnostic sensitivity by showing that there can be target-specific sequence variation rather than false positive or negative results through repeat testing and sequencing confirmation utilized by the DPPSS method.

There have been reports that variants of SARS-CoV-2 can affect the diagnostic accuracy of RT-PCR testing.[19] As mentioned, the mutations and other changes can affect the target regions of the primers designed to capture the virus. In this study, the sample sequencing revealed the different virus strains and classification (Table 2). The three WHO groups of COVID-19 virus variants are: variants of concern (VOCs), variants under monitoring (VUMs), and variants of interest (VOIs).[20] The most common VOC detected in this study was the Omicron, but others present during that time such as Delta were seen as well. This reflects the epidemiological data during the time the swabs were collected in 2021, with each primer showing specificity with different variants (Table 3). This also proves that this particular primer set can detect SARS-CoV-2 across different variants and mutations.

It could be recalled that three prominent waves have been noted since the COVID-19 pandemic was declared in 2020. The first wave was dominated by two VOC one after the other: alpha and delta until the first half of 2021.[20,21] Other variants with higher pathogenicity than alpha variants such as Beta (B.1.351) and Gamma (P.1) were also present during that time. The first Omicron (B.1.1.529) was reported in November 2021 from Botswana, South Africa. It was declared a VOC by the WHO because of its high transmissibility and virulence, related to the numerous mutations (26-32) in spike proteins, N terminal domain and receptor binding sites.[20] In the Philippines,

Table 2. Identified SARS-CoV-2 variants through BLAST using DPPSS primers

Sample	Primer Name		BLAST Result	SARS-CoV-2 Variant
AG	SARS-CoV-2_Var_S1	forward	**No significant similarity found.*	
		reverse		
		consensus	XBB.1.5.48	Omicron
AN	SARS-CoV-2_Var_S2	forward	FL.1.1 XBB.1.5.85	Omicron
		reverse	BA.2.3.1 BF.7.14.1	Omicron
		consensus	**No significant similarity found.*	
AZ	SARS-CoV-2_Var_S2	forward	FL.1 XBB.1.5.28	Omicron
		reverse	**No significant similarity found.*	
		consensus		
BO	SARS-CoV-2_Var_EM1	forward	**No significant similarity found.*	
		reverse		
		consensus	FL.1.5.1	Omicron
L	SARS-CoV-2_Var_EM1	forward	XBB.1.41.1 FL.1.5.1 EG.5.1.1	Omicron
		reverse	FY.3.1 XCF GP.2	Omicron
		consensus	**No significant similarity found.*	
Y	SARS-CoV-2-Var_S1	forward	BA.2.7 BA.2.1	Omicron
BG	SARS-CoV-2_Var_EM1	forward	XBB.1.28	Omicron
S	SARS-CoV-2_Var_O1	reverse	B.1.274	
AI	SARS-CoV-2_Var_S1	forward	BA.2.40.1	Omicron
		reverse	**No significant similarity found.*	
		consensus		
AM	SARS-CoV-2_Var_S2	forward	BA.5.2.2	Omicron
			AY.106	Delta
		reverse	BA.2.6.1 XBB.1.22.2	Omicron
		consensus	**No significant similarity found.*	
M	SARS-CoV-2_Var_EM1	forward	**No significant similarity found.*	
		reverse		
		consensus		
C	SARS-CoV-2_Var_S1	forward	**No significant similarity found.*	
		reverse		
		consensus		
G	SARS-CoV-2_Var_S2	forward	**No significant similarity found.*	
		reverse		
		consensus	FL.14 XBB.2.3.9 BA.5.1.38	Omicron
H	SARS-CoV-2_Var_S2	forward	**No significant similarity found.*	

the first cases of Omicron infection from the data of Philippine Genome Center (PGC) were reported in December of 2021 but unlike the worldwide data which showed predominance of BA.1 sublineage, there were more BA.2 cases observed locally.[22-24] Our findings showed concordance with this report.

Unlike the other VOCs with a convergent evolution pattern, Omicron is highly antigenically divergent. There is continuous antigenic drift that gives rise to sub lineages that have higher neutralization escape, decreasing the vaccination effectiveness.[25] This highlights the value of genomic surveillance even in the face of lower positivity rates, mortality and morbidity caused by the virus. Although VOC may still be responsive to current treatments and developed vaccines, there may be some standalone single nucleotide polymorphisms (SNPs) such as Spike mutation E484K that lowers sensitivity to antiviral drugs.[21]

While positivity rates were elevated during the height of the pandemic, they have since declined significantly in the current period. In a resource limited country, it is challenging to follow the international recommendations[26,27] on genomic SARS-CoV-2 monitoring which should be a threshold minimum of 2.5% or ideally 1% of a particular variant among all variants within one unit of time.[26] Sequencing was performed locally in several institutions (e.g., Philippine Genome Center), with a requirement of CT value of less than <30, positive for any SARS-CoV-2 specific target genes sent within 24 hours upon release of RT-PCR result.[28] There are higher CT values from positive samples detected in the current situation, further decreasing the

Table 3. Designed DPPSS primers specificity

		Primer	Name	Target Gene	Length	Tm	GC%	Specificity and date detected
1	fw	CAAATCGCTCCAGGGCAAAC	SARS-CoV-2_Var_S1	S	20	60.11	55	XBB.1.5 (Oct 2022) BA.2.1 (Late 2021) BA.2.7 (June 2022) BA.2.40.1 (Mid 2022)
	rv	GTGGCAAAACAGTAAGGCCG			20	60.04	55	
2	fw	GTCCTTCCCTCAGTCAGCAC	SARS-CoV-2_Var_S2	S	20	60.04	60	FL.1 (Late 2022) FL.1.1 (Mid 2023) XBB.1.5.28 (2022) XBB.1.5.85 (2022) BA.5.2.2 (Mid 2022) AY.106 (2020-Mid 2021)
	rv	GACTCCTTTGAGCACTGGCT			20	59.96	55	BA.2.3.1 (Early 2022) BA.2.6.1 (Early 2022) BF.7.14.1 (Late 2022) XBB.1.22.2 (Feb 2023)
3	fw	CGATTGTGTGCGTACTGCTG	SARS-CoV-2_Var_EM1	E & M	20	59.01	55	FL.1.5.1 (2023) EG.5.1.1 (2023) XBB.1.28 (Late 2022) XBB.1.41.1 (2023)
	rv	AGGTCCTTGATGTCACAGCG			20	60.04	55	FY.3.1 (2023) XCF (2022) GP.2 (2022)
4	fw	ACCAATGTGCTATGAGGCCC	SARS-CoV-2_Var_O1	ORF1ab	20	60.11	55	
	rv	CATCACCCAACTAGCAGGCA			20	60.04	55	B.1.274 (2020)

Note: The forward (fw) and reverse (rv) primer sequences are directed from 5′ to 3′.

Table 4. Designed DPPSS primers sensitivity

Primer	Sensitivity	Confidence Interval
S1	66.67%	47.19%-82.71%
S2	83.33%	62.62%-95.26%
E/M	90.91%	70.84%-98.88%
Orf1ab	58.82%	40.7%-75.35%
Combined 4 primers	100.00%	83.16%-100.00%

samples sent for genomic surveillance.[29] Hence, we might be missing out on important mutations and changes in the virus and the current epidemiologic data may not be representative of what is currently happening.

With locally designed primers such as the ones featured in our study, we highlight the importance of genomic surveillance on a broader geographical coverage to combat issues such as presence of immune escape variants,[29] as well as optimizing workflow for early detection of emerging variants. The DPPSS provides a rapid-cost effective and targeted surveillance tool for monitoring known variants in a resource limited setting. Compared with sequencing, this method is simple because it utilizes existing equipment available locally and in routine molecular laboratories such as PCR machines and electrophoresis, with a straightforward, simple workflow. Results can also be analyzed with a shorter turn-around time (TAT) because the scope of detection focuses on predefined genomic regions with no extensive bioinformatics requirement or need for high-throughput sequencing machine and extensive library preparations. In depth and comprehensive analysis can then be reserved for sequencing should the need arise.

Since Omicron, known to have S gene drop out, is currently the most widespread VOC, it is imperative that appropriately designed primers with other targets are included in the testing. Even though there are a lot of commercially available kits, some of them have undisclosed primer set sequences which may not be optimized leading to false positive results.[10] A study by Park et al., showed that under-optimized primer sets containing long and short dimer bands were present in commercial kits that could potentially cause false positive results. Continuous monitoring is needed to ensure that diagnostic tests can still detect SARS-CoV-2, maintaining the accuracy of kits available for detection.

The information from genomic data can also help in vaccine improvement and monitoring viral variability and genotypic features that impacts antigenicity, infectivity, pathogenicity and susceptibility to treatment and vaccines.[25] Aside from samples collected from patients, other surveillance methods such as wastewater monitoring[12] can also use the primer sets in this study to serve as an early warning for transmission trends. With recent Emerging/Re-emerging Infections Diseases (EREIDS) such as Nipah virus (NiV)[30] (reported in patients in Bangladesh, India who experienced severe neurological and respiratory symptoms) and epidemic-prone Water, Sanitation and Hygiene (WASH) pathogens, locally available methods for developing diagnostic tools must be available for swift response. This is applicable not just to emerging viral pathogens but also to other infectious agents of public health importance. We recommend that continuous surveillance must be performed to be prepared to manage any public health threat such as NiV and prevent re-emergence of SARS-CoV-2 pandemic.

CONCLUSION

The combined used of four *in silico*-designed primer sets (S1, S2, E/M and ORF1ab) demonstrated accurate detection of SARS-CoV-2 in previously confirmed RT-PCR-positive samples, including variants with S gene mutations such as Omicron. The multi-target design improves assay reliability despite the viral evolution.

The Direct PCR Product Sequencing Surveillance (DPPSS) approach provides a simple and cost-effective method that enables both detection and mutation monitoring. This makes it a practical tool for genomic surveillance in resource-limited settings. In the Philippines, DPPSS and similar Laboratory Developed Tests (LDTs) may be integrated into existing diagnostic workflows, subject to appropriate validation and regulatory compliance, to strengthen decentralized testing and support national surveillance efforts. It also ensures a stronger and prepared response to emerging global threats.

ACKNOWLEDGMENTS

The authors would like to thank the Department of Biochemistry and Molecular Biology Laboratory, College of Medicine, University of the Philippines Manila, for providing the laboratory facilities and equipment necessary to complete this research.

STATEMENT OF AUTHORSHIP

The authors certified fulfillment of ICMJE authorship criteria.

AUTHOR DISCLOSURE

The authors declared no conflicts of interest.

DATA AVAILABILITY STATEMENT

The datasets used and/or analyzed during the current study are available from the corresponding author upon reasonable request.

FUNDING SOURCE

None.

REFERENCES

1. Centers for Disease Control and Prevention. About COVID-19. Updated 2023. https://cdc.gov/coronavirus/2019-ncov
2. Centers for Disease Control and Prevention. SARS-CoV-2 variant classifications and definitions. Updated 2023. https://stacks.cdc.gov/view/cdc/107682
3. World Health Organization. WHO COVID-19 dashboard. 2026. https://data.who.int/dashboards/covid19/cases
4. Department of Health Republic of the Philippines. COVID-19 case tracker. 2024. https://doh.gov.ph/diseases/covid-19/covid-19-case-tracker/
5. Falzone L, Gattuso G, Tsatsakis A, Spandidos DA, Libra M. Current and innovative methods for diagnosis of COVID-19 infection (review). Int J Mol Med. 2021;47(6):100. PMID: 33846767 PMCID: PMC8043662 DOI: 10.3892/ijmm.2021.4933
6. Rai P, Kumar BK, Deekshit VK, Karunasagar I, Karunasagar I. Detection technologies and recent developments in the diagnosis of COVID-19 infections. Appl Microbiol Biotechnol. 2021;105(2):441-55. PMID: 33394144 PMCID: PMC7780074 DOI: 10.1007/s00253-020-11061-5
7. UN News. WHO chief declares end to COVID-19 as a global health emergency. Published May 5, 2023. https://news.un.org/en/story/2023/05/1136367
8. Dorit RL, Ohara O, Hwang CBC, Kim JB, Blackshaw S. Direct DNA sequencing of PCR products. Curr Protoc Mol Biol. 2001;Chapter15:Unit 15.2. PMID: 18265116 DOI: 10.1002/0471142727.mb1502s56
9. Huang Y, Yang C, Xu XF, Liu SW. Structural and functional properties of SARS-CoV-2 spike protein: potential antiviral drug development for COVID-19. Acta Pharmacol Sin. 2020;41(9):1141-9. PMID: 32747721 PMCID: PMC7396720 DOI: 10.1038/s41401-020-0485-4
10. Thomas S. The structure of the membrane protein of SARS-CoV-2 resembles the sugar transporter SemiSWEET. Pathog Immun. 2020;5(1):342-63. PMID: 33154981 PMCID: PMC7608487 DOI: 10.20411/pai.v5i1.377
11. V'kovski P, Kratzel A, Steiner S, Stalder H, Thiel V. Coronavirus biology and replication: implications for SARS-CoV-2. Nat Rev Microbiol. 2021;19:155-70. PMID: 33116300 PMCID: PMC7592455 DOI: 10.1038/s41579-020-00468-6
12. Mollaei HR, Afshar AA, Kalantar-Neyestanaki D, Fazlalipour M, Aflatoonian B. Comparison of five primer sets from different genome regions of COVID-19 for detection of virus infection by conventional RT-PCR. Iran J Microbiol. 2020;12(3):185-93. PMID: 32685113 PMCID: PMC7340604
13. Park M, Won J, Choi BY, Lee CJ. Optimization of primer sets and detection protocols for SARS-CoV-2 using PCR and real-time PCR. Exp Mol Med. 2020;52(6):963-77. PMID: 32546849 PMCID: PMC7295692 DOI: 10.1038/s12276-020-0452-7
14. Qu W, Li J, Cai H, Zhao D. PCR primer design for the rapidly evolving SARS-CoV-2 genome. Methods Mol Biol. 2022;2392:185-97. PMID: 34773624 DOI: 10.1007/978-1-0716-1799-1_14
15. Otero MCB, Murao LAE, Limen MAG, et al. Multifaceted assessment of wastewater-based epidemiology for SARS-CoV-2 in selected urban communities in Davao City, Philippines: a pilot study. Int J Environ Res Public Health. 2022;19(14):8789. PMID: 35886640 PMCID: PMC9324557 DOI: 10.3390/ijerph19148789
16. Mentes A, Papp K, Visontai D, et al. Identification of mutations in SARS-CoV-2 PCR primer regions. Sci Rep. 2022;12(1):18651. PMID: 36333366 PMCID: PMC9636223 DOI: 10.1038/s41598-022-21953-3
17. Tablizo F, Lapid C, Maralit B, et al. Analysis of SARS-CoV-2 genome sequences from the philippines: genetic surveillance and transmission dynamics. medRxiv. Published 2020. DOI: 10.1101/2020.08.22.20180034
18. Saldivar-Espinoza B, Garcia-Segura P, Novau-Ferré N, et al. The mutational landscape of SARS-CoV-2. Int J Mol Sci. 2023;24(10):9072. PMID: 37240420 PMCID: PMC10219494 DOI: 10.3390/ijms24109072
19. Jain A, Rophina M, Mahajan S, et al. Analysis of the potential impact of genomic variants in global SARS-CoV-2 genomes on molecular diagnostic assays. Int J Infect Dis. 2021;102:460-2. PMID: 33181329 PMCID: PMC7834429 DOI: 10.1016/j.ijid.2020.10.086

20. Yadav S, Zaman K, Bashyal P, et al. Newer emerging SARS-CoV-2 variant: Omicron EG.5. Ann Med Surg (Lond). 2023;85(12):5845-6. PMID: 38098560 PMCID: PMC10718343 DOI: 10.1097/MS9.0000000000001386
21. Grimaldi A, Panariello F, Annunziata P, et al. Improved SARS-CoV-2 sequencing surveillance allows identification of new variants and signatures in infected patients. Genome Med. 2022;14(1):90. PMID: 35962405 PMCID: PMC9372932 DOI: 10.1186/s13073-022-01098-8
22. Philippine Genome Center. PGC SARS-CoV-2 Bulletin No. 8: Detection of the first 500 SARS-CoV-2 Omicron Variant in the Philippines. Published January 20, 2022. https://pgc.up.edu.ph/detection-of-the-sars-cov-2-omicron-variant-in-the-philippines/
23. Tablizo FA, Saloma CP, Castro MJR, et al. Detection and genome sequencing of SARS-CoV-2 variants belonging to the B.1.1.7 lineage in the Philippines. Microbiol Resour Announc. 2021;10(18):e00219-21. PMID: 33958417 PMCID: PMC8103862 DOI: 10.1128/MRA.00219-21
24. Li YT, Polotan FGM, Sotelo GIS, et al. Lineage BA.2 dominated the Omicron SARS-CoV-2 epidemic wave in the Philippines. Virus Evol. 2022;8(2):veac078. PMID: 36090771 PMCID: PMC9452094 DOI: 10.1093/ve/veac078
25. Markov PV, Katzourakis A, Stilianakis NI. Antigenic evolution will lead to new SARS-CoV-2 variants with unpredictable severity. Nat Rev Microbiol. 2022;20(5):251-2. PMID: 35288685 PMCID: PMC8919145 DOI: 10.1038/s41579-022-00722-z
26. European Centre for Disease Prevention and Control. Guidance for representative and targeted genomic SARS-CoV-2 monitoring. Published 2021. https://www.ecdc.europa.eu/en/publications-data/guidance-representative-and-targeted-genomic-sars-cov-2-monitoring
27. World Health Organization. Guidance for surveillance of SARS-CoV-2 variants. Published 2021. https://iris.who.int/server/api/core/bitstreams/f641d2bb-08c6-46a4-afc8-a7267885569a/content
28. Department of Health. DOH Circular 2020-042: Sending of samples for sequencing at Philippine Genome Center. Published December 30, 2020.
29. Tomar SS, Khairnar K. Challenges of SARS-CoV-2 genomic surveillance in India during low positivity rate scenario. Front Public Health. 2023;11:1117602. PMID: 37441634 PMCID: PMC10335399 DOI: 10.3389/fpubh.2023.1117602
30. Asokan S, Luke MS, Atiyah HM, et al. Nipah virus as a pandemic threat: current knowledge, diagnostic gaps, and future research priorities. Diagn Microbiol Infect Dis. 2026;114(2):117141. PMID: 41092535 DOI: 10.1016/j.diagmicrobio.2025.117141

OPEN ACCESS – ORIGINAL ARTICLE

Concordance Between the Ki-67 and Proliferation Index of Molecular Signature Tests (MammaPrint and OncotypeDX) Among Filipino Patients in two St. Luke's Medical Center Facilities: An Analytical Cross-sectional Study

Rebecca Nagtalon and Manuelito Madrid

St. Luke's Medical Center-Global City, Philippines

ABSTRACT

Background. Breast cancer remains a leading malignancy among women globally. In addition to established factors like histopathology, hormone receptor status, and lymph node involvement, tools such as immunohistochemistry and molecular tests have been developed to assess tumor behavior and recurrence risk.

Objective. This study investigates the concordance between the Ki-67 proliferation index measured by immunohistochemistry and the recurrence risk scores obtained from molecular genomic testing in patients with invasive breast cancer.

Methodology. This cross-sectional study included patients with invasive breast carcinoma at St. Luke's Medical Center from 2019 to 2024, who underwent biopsy or mastectomy, with hormone status and Ki-67 index assessed by immunohistochemistry. All patients also had molecular genomic testing using either MammaPrint or OncotypeDX. Concordance between Ki-67 and the genomic recurrence risk score was evaluated using Kappa statistics, and results were further analyzed according to clinical risk and hormone receptor status.

Results. Fifty-eight (58) patients met the study criteria. Most had grade 2, hormone receptor-positive, HER2-negative, and node-negative tumors, with high clinical risk based on Adjuvant! Online criteria (adapted from the MINDACT trial). The agreement between categorical Ki-67 and molecular recurrence risk was only fair: 66.7% for MammaPrint (kappa = 0.35) and 60% for OncotypeDX (kappa = 0.29) using a 30% Ki-67 cutoff.

Conclusion. There is a fair agreement between Ki-67 and the molecular genomic tests. These findings are consistent with prior studies reporting weak to moderate association. Despite the limited sample size, Ki-67 remains a practical and accessible risk stratification tool, particularly where genomic assays are unavailable. The study supports integrating Ki-67 with clinicopathologic and genomic data to guide therapy, reflecting current best-practice recommendations.

Key words: breast cancer, Ki-67, OncotypeDX, MammaPrint

ISSN 2507-8364 (Online)
Printed in the Philippines.

Received: 19 April 2026.
Accepted: 14 June 2026.
Published online first: 25 June 2026.
https://doi.org/10.21141/PJP.2026.631

Corresponding author: Rebecca R. Nagtalon, MD, DPSP
E-mail: rrnagtalon@stlukes.com.ph
ORCiD: https://orcid.org/0000-0002-4925-4381

INTRODUCTION

There is an increasing worldwide cancer burden. According to the Global cancer statistics for 2020, an estimated 19.3 million new cancer cases and almost 10 million cancer deaths occurred worldwide. Breast cancer is one of the most prevalent types of cancer and has surpassed lung cancer as the most diagnosed malignancy. Among Filipino women, breast cancer is the most common cause of malignancy accounting for 31.4% of cases. This remains a significant public health concern, particularly in developing countries such as the Philippines.[1-4] When screened, the proportion of breast tumors that are malignant varies depending on the population studied and the diagnostic methods employed. The overall malignancy rates for all breast tumors varies from 10 to 20% but depending on the age and imaging characteristics, studies show that the rates may go as high as 40%.[5-11]

Breast cancer treatment is expensive. Majority of payments for these treatments come from out-of-pocket expenses. Though available, the PhilHealth packages cover only a portion of the total cost of treatment. In a study by Ngelangel et al., approximately PhP 180,000 pesos in out-of-pocket expenditures were spent on cancer treatment. Government agencies help shoulder some of these expenses such as the *Malasakit* center, Breast Cancer Medicine awareness program and the PhilHealth the Z-package, however, the financial burden still exists. Surgery alone entails a big financial burden on the patient. The addition of neoadjuvant or adjuvant chemotherapy causes greater physical, and financial impact to Filipino patients.[1,12,13]

In breast cancer, the clinicopathologic features such as age, tumor size and grade, hormone receptor status, and axillary lymph node involvement affect the treatment protocol for each patient. The National Comprehensive Cancer Network (NCCN) guidelines recommend the determination of biomarkers such as estrogen receptor (ER), progesterone receptor (PR), HER2 status, and testing for Ki-67, especially if hormone receptor-positive, HER2-negative and considering adjuvant abemaciclib.[14] The determination of these biomarkers using immunohistochemistry (IHC) and fluorescence in-situ hybridization (FISH) subclassify breast cancer to its major molecular subtypes: Luminal-types A and B, HER2-enriched, and Triple negative. The luminal subtypes are differentiated according to their hormone receptor expression and Ki-67 expression. Luminal A is ER+, PR high, HER2 -, and Ki-67 <20%, while Luminal B is ER+, PR low or intermediate +, HER2 + or HER2 -, and Ki-67 ≥20%.[15-17] Aside from these, biomarkers such as Ki-67, alongside molecular signature tests like MammaPrint and OncotypeDX, are crucial in guiding the prognosis and treatment planning.

Ki-67 is a nuclear protein associated with cell proliferation. It has been widely used as a prognostic and predictive marker in cancer.[18] Ki67 is expressed in actively dividing cells. Its signal increases as cells move through the different phases of the cell cycle. In tumors, these Ki-67 positive cells generally correlated with more aggressive behavior and worse clinical course.[19,20] It is particularly useful in distinguishing between luminal A and luminal B subtypes, which have different treatment approaches and prognoses.[17,21]

Ki-67 for breast cancer can be used for monitoring neoadjuvant chemotherapy and prognostication purposes. In the 2021 St. Gallen consensus a definite cut-off for recommending chemotherapy in ER-positive node negative breast cancer could not be completely established.[22,23] The recommendations for giving or withholding chemotherapy was only recommended in Ki-67 percentages of <5% or ≥30%. In a study by Huang et al, the most common expression range of Ki-67 in hormone receptor positive, HER2-negative breast cancer is 10-30%.[24] This shows that a great proportion of breast cancer patients will fall into this category, urging us to find a more cost-effective biomarker that can clinch and guide treatment considering all the factors. Several studies have demonstrated that high Ki-67 levels correlate with poorer prognosis and increased likelihood of recurrence.[25,26] However, standardization issues in Ki-67 assessment methods have led to variations in clinical interpretation. Prospective studies that looked onto molecular genomic tests such as MINDACT, ADAPT, TAILORx, and RxPonder were done to fill the gap.[27-30]

MammaPrint and OncotypeDX are genomic assays designed to stratify breast cancer patients based on their risk of recurrence and response to chemotherapy. MammaPrint is a 70-gene expression profile that categorizes patients into high-risk and low-risk groups.[23,24] OncotypeDX, on the other hand, is a 21-gene assay that provides a Recurrence Score (RS) to predict the likelihood of distant recurrence and chemotherapy benefit in hormone receptor-positive, HER2-negative breast cancer patients.[25] Studies have shown that both tests help personalize treatment decisions and reduce unnecessary chemotherapy exposure.[26] One of the largest studies performed is the MINDACT trial (Microarray In Node Negative Disease may Avoid Chemotherapy). This was launched with the aim of prospectively validating the performance of the Amsterdam 70-gene profiler MammaPrint. Using high-throughput microarray analysis, MammaPrint can accurately select early-stage breast cancer patients who are highly likely to develop distant metastases or recurrence and, therefore, may benefit the most from adjuvant chemotherapy. The MammaPrint results were correlated to the clinical risk as well. In the MINDACT trial, low clinical risk in ER+/HER2- breast cancer was defined as a 10-year breast cancer-specific survival probability of greater than 88% without adjuvant systemic therapy. They determined this by using a modified version of Adjuvant! Online, considering tumor size, grade, nodal status, hormone and HER2 receptor status. The low clinical risk was defined by specific criteria for tumor size and grade, with variations depending on the presence or absence of lymph node involvement.[22-24] The use of Mammaprint and other genomic profiling tests such as BluePrint and OncoType DX have been utilized in the Philippines. In a study by Kho et al, all low-risk Filipinos patients in their study underwent adjuvant endocrine therapy alone and foregone otherwise clinically recommended chemotherapy. Gene profiling of breast cancer in a resource-limited setting is feasible and imperative to avoid chemotherapy and/or overtreatment.[27]

It was recognized in the 2021 St. Gallen International Consensus guidelines for treatment of early breast cancer that genomic assays are highly recommended, but they understand that access to such testing is not available to most women around the world. While governance should improve this disparity, the availability of Ki-67 scores may serve as a surrogate for defining proliferation and biological risk.[16] Thus, the concordance of Ki-67 index to the molecular gene panel, MammaPrint and OncotypeDX, can be useful in determining breast cancer treatment. Several studies have explored the relationship between the Ki-67 index and molecular signature tests. A meta-analysis by Petrelli et al. (2015) found a moderate correlation between Ki-67 and OncotypeDX RS, suggesting that while Ki-67 provides valuable proliferation information, molecular assays offer a more comprehensive genomic risk assessment.[28] Additionally, research has shown that Ki-67 alone may not fully capture the tumor's biological complexity, necessitating the integration of molecular tests for a more accurate prognosis.[26] Recent research

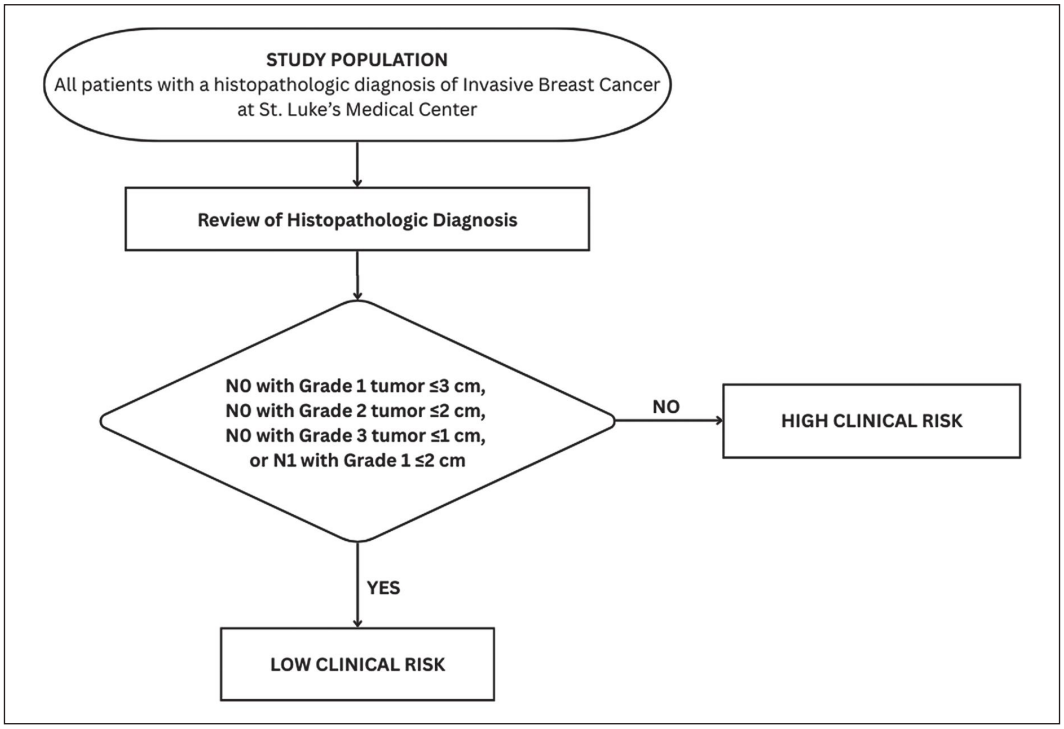

Figure 1. Assignment of clinical risk.

continues to underscore the prognostic value of Ki-67 in breast cancer. A 2023 study by Lee et al., examined the association between Ki-67 levels, the 21-gene Recurrence Score (OncotypeDX), endocrine resistance, and survival outcomes. The study found that higher Ki-67 levels were linked to increased endocrine resistance and poorer survival rates, highlighting Ki-67's role in predicting treatment response and prognosis.[29] The relationship between Ki-67 and molecular assays like OncotypeDX has been further explored in recent studies. Lee et al.,'s 2023 research demonstrated that while both Ki-67 and the 21-gene Recurrence Score are valuable, they provide complementary information. Ki-67 offers immediate proliferation data, whereas molecular assays deliver a broader genomic risk assessment, suggesting that integrating both markers could enhance prognostic accuracy.[28-33]

The Ki-67 proliferation index and molecular signature tests such as MammaPrint and OncotypeDX play vital roles in breast cancer prognosis and treatment stratification. While Ki-67 is a widely accessible marker, molecular tests provide a broader genomic perspective. However, given the high cost and limited accessibility to genomic tests like MammaPrint and Oncotype DX in the Philippines, investigating Ki-67 as a cost-effective surrogate marker to aid clinicians in risk stratification and treatment decisions, especially considering the ethnic and genetic diversity in breast cancer should be explored. Utilizing Ki-67 may also help patients who could benefit from adjuvant chemotherapy, thereby optimizing treatment plans without incurring the high costs associated with genomic testing.[34-37]

The study aimed to evaluate the concordance of Ki-67 index score using immunohistochemistry and the recurrence score using the molecular genomic tests (MammaPrint and OncotypeDX) among Filipino patients with Invasive Breast Cancer seen in SLMC in the said time frame. The concordance between Ki-67 and molecular genomic tests (MammaPrint and OncotypeDX) in determining the risk of recurrence based on Kappa statistics was also analyzed overall, by age group, by clinical risk, by estrogen and progesterone receptor status, and by Her2/neu status. Understanding the concordance between these markers in Filipino patients, may potentially improve individualized breast cancer management in the local setting.

METHODOLOGY

Study design

This is an analytic cross-sectional study which included patients with Invasive Breast Carcinoma in St. Luke's Medical Center (SLMC) from January 1, 2019, to December 31, 2024. Data was collected via retrospective review of medical charts through the hospital's electronic medical records and laboratory information system.

Risk assessment

The clinical risk or the probability of breast cancer survival without systemic therapy was based on the MINDACT trial using the Adjunct Online! tool.[31] Figure 1 illustrates the assigned the risk based on the data from the histopathology report. "Low clinical risk" was defined as: N0 with Grade 1 tumor ≤3 cm, N0 with Grade 2 tumor ≤2 cm, N0 with Grade 3 tumor ≤1 cm, or N1 with Grade 1 ≤2 cm. All other tumor grades or nodal stage that did not fit this category was defined as "high clinical risk."

Inclusion and exclusion criteria

The study included all patients 18 years old and above and must have had their breast biopsy or mastectomy done in SLMC. The histopathology report must have included

the diagnosis of Invasive breast carcinoma with reports of the tumor size, histologic grade, histologic subtype, and lymphovascular invasion. Additional pathology reports should also have Ki-67, hormone status (ER, PR), and HER2/neu using IHC or FISH done in the same institution. Only those whose biopsy specimens sent out through the SLMC laboratory for molecular genomic testing for OncotypeDX or MammaPrint were included in the study. Those with incomplete reports and other organs or biopsy sites that were not the breast were excluded from the study.

Sample size

PASS 2021 software was used to compute the minimum sample size requirement. Parameters were obtained from a previous study by Amezcua-Gálvez et al.[38] A minimum of 59 patients were required to achieve 90% statistical power given a kappa of 0.35 and alpha set at 0.05. Although a minimum sample size was computed, the researchers performed total enumeration technique wherein all eligible patients will be included in the study.

Data collection and analysis

Data was encoded in MS Excel by the researcher. Stata MP version 17 software was used for data processing and analysis. Continuous variables were presented as mean/standard deviation (SD) and median/interquartile range (IQR) depending on the data distribution. Shapiro Wilk test was used to assess the normality of data. Categorical variables were expressed as frequencies and percentages.

The concordance of Ki-67 with MammaPrint and OncotypeDX was examined using percent agreement and Cohen's Kappa statistics. Cohen's kappa was interpreted as poor (<0.00), slight (0.00-0.20), fair (0.21-0.40), moderate (0.41-0.60), substantial (0.61-0.80), and almost perfect (0.81-1.00) agreement. Subgroup analyses by clinical risk was performed. Sensitivity analyses excluding PR- and HER2+ were also done. Missing data were neither replaced nor estimated.

Ethical considerations

This research protocol was reviewed and approved by the St. Luke's Medical Center Institutional Ethics Assess Committee. The study involved retrospective data collection from patients admitted between January 2019 and December 2024, for which a waiver of informed consent was granted due to the absence of direct patient contact. All patient information was anonymized using coded identifiers and securely stored in password-protected electronic files and locked physical cabinets accessible only to authorized personnel. Privacy and confidentiality were maintained throughout, with data remaining for five years before destruction. The research was conducted in accordance with the Declaration of Helsinki (2013) and the ICH-GCP guidelines.

RESULTS

A total of 58 patients were included in the study. Table 1 presents the characteristics of the included patients. The mean age of the cohort was 57.1 years. Based on these criteria, the clinical risk stratification is 43% (n = 25) were considered low risk and 57% (n=33) were categorized as high risk. The median tumor size was 1.6 cm.

Table 1. Demographic and clinical characteristics of invasive breast cancer patients, SLMC

Characteristics	n (%) Mean ± SD
Age (in years), mean	57.1 ± 10.4
<50 years	15 (26)
≥50 years	43 (74)
Clinical risk	
Low risk	25 (43)
High risk	33 (57)
Tumor size (in cm), median	1.6 [IQR: 1.2, 2.5]
Nodal status	
N0	45 (78)
N1	13 (22)
N2	0
N3	0
Histologic grade	
G1	10 (17)
G2	36 (62)
G3	12 (21)
Lymphovascular invasion	
Yes	17 (29)
No	41 (71)
ER	
Positive	58 (100)
Negative	0
PR	
Positive	56 (97)
Negative	2 (3)
HER-2-neu	
Positive	3 (5)
Negative	55 (95)
Ki67, median	30 [IQR: 15, 40]
<30%	28 (48)
≥30%	30 (52)
Mammaprint, mean [n = 33]	-0.1 ± 0.3
Low risk	13 (39)
High risk	20 (61)
Oncotype DX, median [n = 25]	21 [IQR: 14-24]
Low-to-medium risk	20 (80)
High risk	5 (20)

Majority of cases were node-negative (N0) with a histologic grade 2 (G2). Lymphovascular invasion was identified in 29% (n=17) of patients. All tumors were estrogen receptor-positive (ER+, 100%, n=58). Progesterone receptor (PR) status was positive in 97% (n = 56) and negative in 3% (n=2). On HER-2-neu assessment, only 5% (n=3) of tumors were positive, while the majority (95%, n=55) were negative.

The median Ki67 proliferation index in the study was 30%. The percentage of patients who had a Ki-67 greater than 30% was 52% Genomic risk assessment using MammaPrint was performed in 33 patients, yielding a mean score of -0.1 ± 0.3. Thirteen patients (39%) were classified as low-risk and 20 (61%) as high-risk. Oncotype DX testing was carried out in 25 patients, with a median score of 21. Of these, 80% (n=20) fell within the low-to-medium risk category and 20% (n = 5) were identified as high risk.

Table 2. Concordance of Ki67 and MammaPrint (n = 33)

Ki67	Mammaprint		
	High risk	Low risk	Total
≥30%	12	3	15
<30%	8	10	18
Total	20	13	33

Table 3. Concordance of Ki67 and Oncotype DX (n = 25)

Ki67	Oncotype DX		
	High risk	Low-to-medium risk	Total
≥30%	5	10	15
<30%	0	10	10
Total	5	20	25

Concordance of Ki67 and molecular genomic tests

As summarized in Table 2, concordant classification between the Ki-67 proliferation index and MammaPrint genomic risk was observed in 22 of 33 patients, corresponding to an agreement rate of 66.67% (95% CI: 49.69–83.64%). Cohen's kappa was 0.35, indicating fair agreement between the two measures, and this association was statistically significant ($p = 0.035$).

When comparing Ki-67 and OncotypeDX, concordant results were found in 15 of 25 patients, yielding an agreement rate of 60% (15/25; 95% CI: 39.40–80.64%). All patients with Ki67 <30% (n = 10) were classified as low-to-medium risk by Oncotype DX, while among patients with Ki67 ≥30% (n=15), 5 were high risk and 10 were low-to-medium risk by Oncotype DX. Cohen's kappa statistic for the agreement between Ki67 and Oncotype DX was 0.29, indicating fair agreement, though not statistically significant ($p = 0.031$).

Concordance of Ki67 and molecular genomic tests by age group

For Ki-67 and MammaPrint, concordance was lower in younger patients, with only 4 of 9 women under 50 years (44.44%; 95% CI, 3.93–84.96%) showing matching risk classifications, corresponding to slight agreement (kappa = 0, $p = 1.000$). In contrast, among patients aged 50 years and above, 18 of 24 (75.0%; 95% CI, 56.32–93.68%) had concordant results, indicating moderate agreement between Ki-67 and MammaPrint (kappa = 0.50, $p = 0.010$).

A similar pattern was seen for Ki-67 and Oncotype DX: in those younger than 50 years, 4 of 6 patients (66.67%; 95% CI, 12.47–100%) showed concordance, reflecting fair agreement (kappa = 0.33, $p = 0.337$). Among patients ≥50 years, concordant Ki-67 and Oncotype DX classifications were observed in 11 of 19 cases (57.89%; 95% CI, 33.45–82.34%), also consistent with fair agreement (kappa = 0.27, $p = 0.067$).

Concordance of Ki67 and molecular genomic tests by clinical risk

In subgroup analyses by clinical risk, Ki-67 showed different patterns of concordance with the two genomic assays. For Ki-67 and MammaPrint, agreement was higher in the low-risk group: 10 of 13 low clinical risk patients (76.92%; 95% CI, 50.42–100%) had concordant results, with moderate agreement (kappa = 0.53, $p = 0.051$), compared with 12 of 20 high-risk patients (60.00%; 95% CI, 36.48–83.52%) and only fair agreement (kappa = 0.24, $p = 0.198$). In contrast, for Ki-67 and Oncotype DX, the concordance tended to be better in the high-risk group, where 9 of 13 patients (69.23%; 95% CI, 40.20–98.26%) showed concordant classifications with moderate agreement (kappa = 0.43, $p = 0.052$). Among low clinical risk patients, only 6 of 12 (50.00%; 95% CI, 16.82–83.18%) had concordant Ki-67 and Oncotype DX results, corresponding to slight agreement (kappa = 0.12, $p = 0.356$).

Concordance of Ki67 and molecular genomic tests by receptor status

Sensitivity analyses were conducted in hormone receptor–positive, HER2-negative subgroups, as all tumors were ER-positive, and the small number of HER2-positive cases (n = 3) precluded meaningful separate analysis. Among PR-positive patients assessed with Ki-67 and MammaPrint (n = 33), 22 showed concordant risk classifications, corresponding to an agreement of 66.67% (95% CI, 49.69–83.64%) and fair agreement (kappa = 0.35, $p = 0.035$). Similarly, for PR-positive patients evaluated with Ki-67 and

Table 4. Concordance of Ki67 and MammaPrint by age group

Ki67	<50 years (n = 9)			≥50 years (n = 24)		
	Mammaprint			Mammaprint		
	High risk	Low risk	Total	High risk	Low risk	Total
≥30%	2	1	3	10	2	12
<30%	4	2	6	4	8	12
Total	6	3	9	14	10	24

Table 5. Concordance of Ki67 and Oncotype DX by age group

Ki67	<50 years (n = 9)			≥50 years (n = 24)		
	Oncotype DX			Oncotype DX		
	High risk	Low-to-medium risk	Total	High risk	Low-to-medium risk	Total
≥30%	1	2	3	4	8	12
<30%	0	3	3	0	7	7
Total	1	5	6	4	15	19

Table 6. Concordance of Ki67 and MammaPrint by clinical risk

Ki67	High clinical risk (n = 20)			Low clinical risk (n = 13)		
	Mammaprint			Mammaprint		
	High risk	Low risk	Total	High risk	Low risk	Total
≥30%	8	1	9	4	2	6
<30%	7	4	11	1	6	7
Total	15	5	20	5	8	13

Table 7. Concordance of Ki67 and Oncotype DX by clinical risk

Ki67	High clinical risk (n = 13)			Low clinical risk (n = 12)		
	Oncotype DX			Oncotype DX		
	High risk	Low-to-medium risk	Total	High risk	Low-to-medium risk	Total
≥30%	4	4	8	1	6	7
<30%	0	5	5	0	5	5
Total	4	9	13	1	11	12

Oncotype DX (n = 23), 14 had concordant results, yielding an agreement of 60.87% (95% CI, 39.29–82.45%) and again a fair level of agreement (kappa = 0.30, p = 0.033).

A comparable pattern was observed when the analyses were restricted to HER2-negative patients. Among the 30 HER2-negative women who underwent both Ki-67 and MammaPrint testing, 20 had concordant classifications (66.67%; 95% CI, 48.76–84.57%), with fair agreement (kappa = 0.35, p = 0.048). In the HER2-negative subgroup assessed with Ki-67 and Oncotype DX (n = 25), concordance was seen in 15 patients, corresponding to an agreement of 60.00% (95% CI, 39.36–80.64%) and fair agreement (kappa = 0.29, p = 0.031). Overall, concordance between Ki-67 and both genomic assays remained consistently in the fair range across PR-positive and HER2-negative subgroups, with slightly higher agreement rates for MammaPrint than for Oncotype DX.

DISCUSSION

This study appraises the real-world concordance between the Ki-67 proliferation index determined by immunohistochemistry and risk strata from molecular signature assays—specifically MammaPrint and OncotypeDX—in Filipino patients with predominantly hormone receptor-positive, node-negative, early-stage breast cancer.

Clinical and genomic risk stratification in a Filipino context

Consistent with global epidemiologic trends reported in GLOBOCAN and CA: A Cancer Journal for Clinicians, breast cancer remains the most frequently diagnosed malignancy among women in the Philippines and a major contributor to cancer mortality, underscoring the need for context-appropriate risk stratification strategies.[2-4,39,40] In our cohort, most cases were hormone receptor-positive, node-negative, early-stage tumors, mirroring the profile of contemporary HR-positive/HER2-negative populations in large international trials and registry studies, but genomic testing revealed a spectrum of recurrence risk despite this apparently favorable clinicopathologic profile.

Our findings further demonstrate that most of Filipino patients treated in this tertiary center are categorized as high clinical risk and would traditionally be considered candidates for adjuvant chemotherapy. Clinical risk in this study was assigned using the modified Adjuvant! Online–

Table 8. Concordance of Ki67 and MammaPrint among PR+ patients (n = 33)

Ki67	Mammaprint		
	High risk	Low risk	Total
≥30%	12	3	15
<30%	8	10	18
Total	20	13	33

Table 9. Concordance of Ki67 and Oncotype DX among PR+ patients (n = 23)

Ki67	Oncotype DX		
	High risk	Low-to-medium risk	Total
≥30%	5	9	14
<30%	0	9	9
Total	5	18	23

Table 10. Concordance of Ki67 and MammaPrint among HER2- patients (n = 30)

Ki67	Mammaprint		
	High risk	Low risk	Total
≥30%	10	3	13
<30%	7	10	17
Total	17	13	30

Table 11. Concordance of Ki67 and Oncotype DX among HER2- patients (n = 25)

Ki67	Oncotype DX		
	High risk	Low-to-medium risk	Total
≥30%	5	10	15
<30%	0	10	10
Total	5	20	25

based approach adopted in the MINDACT trial, which integrates age, tumor size, nodal status, histologic grade, and hormone receptor status to estimate relapse risk and to compare clinicopathologic risk with genomic signatures such as MammaPrint. This approach is comparable to other breast cancer clinical decision support systems (CDSSs)—including PREDICT, ONCOassist, CancerMath, CTS5, and residual cancer burden calculators—which similarly combine standard prognostic variables to refine adjuvant treatment recommendations. A systematic review by Mazo et al., reported that CDSSs improve consistency and transparency in complex adjuvant therapy decisions, particularly when used alongside multigene assays such as Oncotype DX and MammaPrint, although further integration of individualized and real-world data is needed to optimize their impact on patient outcomes.[41]

The molecular genomic assays utilized in this study includes MammaPrint and OncotypeDX. Data from prior studies indicate that both assays facilitate individualized treatment decision-making and help reduce unnecessary chemotherapy administration. MammaPrint employs a 70-gene signature to stratify patients into high-risk and low-risk categories, whereas OncotypeDX analyzes a 21-gene panel to generate a Recurrence Score (RS) for prognostication and therapeutic guidance.[29-31] Although standardized treatment algorithms, such as those outlined in the NCCN Clinical Practice Guidelines, provide a framework for managing early breast cancer, molecular assays refines a more precise clinical risk estimates beyond traditional factors like tumor size, grade, nodal status, and hormone receptor profile.[14,15]

Biomarker concordance and clinical interpretation

Based on the 2021 St. Gallen International Consensus, adjuvant chemotherapy in ER-positive, HER2-negative, node-negative breast cancer is most clearly supported at the extremes of proliferation, with Ki-67 values ≤5% arguing against chemotherapy and Ki-67 ≥30% favoring its use.[16] Because no institutional cutoff had been established, we adopted the ≥30% threshold recommended by St. Gallen to define a high Ki-67 category in our cohort. Using this cutoff, we observed only fair concordance between Ki-67 and the molecular genomic assays, with agreement rates of 66.7% for MammaPrint (kappa = 0.35) and 60.0% for Oncotype DX (kappa = 0.29).

This modest agreement aligns with prior reports showing weak to moderate correlation between Ki-67 and multigene signatures, including studies and meta-analyses indicating that Ki-67 alone cannot fully recapitulate the composite genomic risk captured by assays such as Oncotype DX and MammaPrint. Several series have reported low or non-significant linear correlations between Ki-67 and the 21-gene Recurrence Score, despite both being proliferation-linked, and kappa coefficients in the low to fair range when dichotomized risk groups are compared. Taken together with our data, these findings support the use of Ki-67 as a helpful, accessible surrogate marker, but reinforce that treatment decisions should ideally integrate Ki-67 with clinicopathologic features and, where available, genomic assay results rather than relying on Ki-67 alone.[22,23,29,30,42-45]

Technical limitations in Ki-67 assessment likely contribute substantially to the discordance we observed between Ki-67 and multigene assays. Antibody clone selection, fixation and staining protocols, pre-analytical handling, subjective visual scoring, and the lack of universally adopted thresholds (and alignment between manual and digital image analysis) are all well-described sources of variability.[46] Studies by Copur et al. and Selmani et al., have reported only low to moderate concordance between Ki-67 and Oncotype DX, regardless of whether Ki-67 is measured by conventional immunohistochemistry or more quantitative approaches, underscoring that technical and methodological differences limit interchangeability.[30,42] Further comparisons, including those by Tian et al., Nguyen et al, and Pons et al., reinforce that heterogeneity in Ki-67 scoring methods and population differences impact reliability and interchangeability across molecular and protein markers.[44-46] To mitigate these issues in our study, we restricted inclusion to these two tertiary centers with uniform tissue processing and IHC protocols, with most Ki-67 readings were rendered by one pathologist, which likely reduced—but did not eliminate—measurement variability.

Subgroup analyses suggested that patient characteristics also modulate concordance patterns. Among women aged ≥50 years, Ki-67 and MammaPrint showed moderate agreement, whereas only slight agreement was seen in those <50 years, a difference that is probably influenced by the very small number of younger patients and wide confidence intervals in this group. This age-related trend is compatible with prior reports that proliferation indices and genomic risk scores may behave differently in younger versus older hormone receptor-positive cohorts, particularly where chemotherapy benefit and endocrine sensitivity differ.[41,42]

When stratified by clinical risk, agreement between Ki-67 and MammaPrint was highest in the low clinical risk group (moderate agreement, kappa = 0.53) and only fair in the high-risk group (kappa = 0.24), suggesting that Ki-67 may align better with genomic risk at the more favorable end of the spectrum. In contrast, Ki-67 and Oncotype DX showed the opposite pattern, with moderate agreement in clinically high-risk patients and only slight agreement in those at low clinical risk (kappa = 0.12, p = 0.356), indicating that the two genomic platforms may weigh proliferative and non-proliferative genes differently across risk strata. Similar 'fair' levels of concordance were observed in sensitivity analyses restricted to PR-positive and HER2-negative subgroups, reinforcing the notion that Ki-67 and multigene assays capture overlapping but distinct dimensions of tumor biology rather than being directly interchangeable measures.

Our findings are consistent with meta-analyses and key primary studies that attribute discrepancies between Ki-67 and multigene assays to technical variability, differences in laboratory protocols, inter-observer subjectivity, heterogeneous laboratory practices, and the absence of universally applied cut-offs. Recognizing these challenges, the International Ki-67 in Breast Cancer Working Group and related expert panels have issued detailed recommendations to standardize pre-analytical

handling, scoring methodology, and reporting of Ki-67, with the goal of improving reproducibility, enabling more reliable cross-study comparisons, and clarifying how Ki-67 should be integrated with genomic assays in routine practice.[22,23,29,30,42-48]

Limitations and directions for future research

The relatively small sample size limited the power of this study to perform more granular subgroup analyses, and the retrospective design may have introduced selection bias. In addition, only a subset of eligible patients underwent molecular genomic testing, reflecting both physician-driven test ordering and substantial out-of-pocket costs, which in the Philippines are estimated at approximately PHP 200,000–300,000 (USD 3,000–5,000) per assay. Even in a tertiary center such as St. Luke's Medical Center, multigene assays are not requested routinely, further constraining the number of cases available for concordance analyses. Another limitation is that we were unable to correlate Ki-67 and genomic test results with long-term outcomes such as recurrence or metastasis, preventing direct comparison of their prognostic performance in this cohort. Prospective studies with larger, more diverse populations and systematic follow-up will be necessary to clarify how surrogate markers like Ki-67 relate to in-vivo tumor biology and to validate their use alongside, or in place of, multigene assays in resource-constrained settings.

CONCLUSION

Given persistent financial barriers in the Philippines, Ki-67 remains a pragmatic and widely accessible option for initial risk stratification in settings where multigene assays cannot be routinely performed. However, our findings support integrating Ki-67 with clinicopathologic and genomic information whenever feasible, in line with contemporary best-practice recommendations.[14-16,28,31] Consistent with the ESMO guidelines for early breast cancer, pretreatment assessment should include histological type and grade, IHC evaluation of estrogen receptor (ER), progesterone receptor (PR) and human epidermal growth factor receptor 2 (HER2) biomarkers and a proliferation marker such as Ki-67. Furthermore, gene expression assays (e.g., EndoPredict, MammaPrint, Oncotype DX, Prosigna and others) are primarily recommended for HR-positive, HER2-negative tumors at immediate clinical risk based on conventional pathology and IHC, and only one of these assays should be used for each individual patient.[48]

Looking forward, research must focus on optimizing Ki-67 cut-offs for Filipino and broader Southeast Asian populations, ensuring assay standardization, and further validating risk models that accommodate local clinical realities and resource limitations. And while Ki-67 and further molecular genomic tests have yet to be included in the National Clinical Practice Guidelines for Breast Cancer, collaboration between clinicians, pathologists, and health policymakers—especially those involved in national health insurance reforms and cancer access programs—will be key to implementing findings from cutting-edge genomic research for the benefit of Filipino patients.[49]

ACKNOWLEDGMENTS

The authors thank the Institute of Pathology and Institutional Ethics Review Committee of the St. Luke's Medical Center for their technical support, assistance, and unwavering support of research.

STATEMENT OF AUTHORSHIP

The authors certified fulfillment of ICMJE authorship criteria.

AUTHOR DISCLOSURE

The authors declared no conflicts of interest.

DATA AVAILABILITY STATEMENT

The data that support the findings of this study are retained at St. Luke's Medical Center. Restrictions apply to the availability of these data, which were used under license/ethical approval for the current study, and so are not publicly available. Data requests may be submitted to the Institutional Ethics Review Committee of St. Luke's Medical Center for researchers who meet the criteria for access to confidential data.

FUNDING SOURCE

None.

REFERENCES

1. Ngelangel CA, Lam HY, Rivera AS, Kimman ML, Real IO, Balete SL. Philippine costs in oncology (peso): describing the economic impact of cancer on Filipino cancer patients using the ASEAN costs in oncology study dataset. Acta Med Philippina. 2018;52(2):125-33. DOI: 10.47895/amp.v52i2.418
2. Sung H, Ferlay J, Siegel RL, et al. Global cancer statistics 2020: GLOBOCAN estimates of incidence and mortality worldwide for 36 cancers in 185 countries. CA Cancer J Clin. 2021;71(3):209-49. PMID: 33538338 DOI: 10.3322/caac.21660
3. World Health Organization. International Agency for Research on Cancer. Breast fact sheet. GLOBOCAN 2020; 2020. Accessed August 23, 2022. https://gco.iarc.fr/today/data/factsheets/cancers/20-Breast-fact-sheet.pdf
4. World Health Organization. International Agency for Research on Cancer. Philippines fact sheet. GLOBOCAN 2020; 2020. Accessed August 23, 2022. https://gco.iarc.fr/today/data/factsheets/populations/608-philippines-fact-sheets.pdf
5. Bent C, Bassett LW, D'Orsi CJ, Sayre JW. The positive predictive value of BI-RADS microcalcification descriptors and final assessment categories. AJR Am J Roentgenol. 2010;194(5):1378-83. PMID: 20410428 DOI: 10.2214/AJR.09.3423

6. Berg WA, Zhang Z, Lehrer D, et al. Detection of breast cancer with addition of annual screening ultrasound or a single screening MRI to mammography in women with elevated breast cancer risk. JAMA. 2012;307(13):1394-404. PMID: 22474203 PMCID: PMC3891886 DOI: 10.1001/jama.2012.388
7. Wiratkapun C, Bunyapaiboonsri W, Wibulpolprasert B, Lertsithichai P. Biopsy rate and positive predictive value for breast cancer in BI-RADS category 4 breast lesions. J Med Assoc Thai. 2010;93(7):830-7. PMID: 20649064
8. Mohapatra SK, Mishra A, Sahoo TK, et al. The positive predictive values of the breast imaging reporting and data system (BI-RADS) 4 lesions and its mammographic morphological features. Indian J Surg Oncol. 2021;12(1):182-9. PMID: 33814852 PMCID: PMC7960818 DOI: 10.1007/s13193-020-01274-5
9. Paulinelli RR, Freitas-Júnior R, Rebouças Moreira MA, et al. Risk of malignancy in solid breast nodules according to their sonographic features. J Ultrasound Med. 2005;24(5):635-41. PMID: 15840795 DOI: 10.7863/jum.2005.24.5.635
10. Liberman L, Abramson AF, Squires FB, Glassman JR, Morris EA, Dershaw DD. The breast imaging reporting and data system: positive predictive value of mammographic features and final assessment categories. AJR Am J Roentgenol. 1998;171(1):35-40. PMID: 9648759 DOI: 10.2214/ajr.171.1.9648759
11. Berg WA, Campassi CI, Ioffe OB. Cystic lesions of the breast: sonographic-pathologic correlation. Radiology. 2003;227(1):183-91. PMID: 12668745 DOI: 10.1148/radiol.2272020660
12. Department of Health. What is breast cancer medicines access program (bcmap)? 2022. Accessed August 22, 2022.
13. PhilHealth. The guiding principles of the Z benefits, Circular No. 2021-0022. 2021. Accessed August 23, 2022. https://www.philhealth.gov.ph/circulars/2021/circ2021-0022.pdf
14. National Comprehensive Cancer Network. NCCN Clinical Practice Guidelines in Oncology: Breast cancer. Version 4.2025. National Comprehensive Cancer Network. 2025. Accessed October 29, 2025. https://www.nccn.org
15. Catedral LI, Tan HN, Chua AJ, Sacdalan DB, Sacdalan DL. Patterns of biomarker use in cancer treatment among medical oncologists in the Philippines. JCO Glob Oncol. 2020;6:1593-608. PMID: 33079606 PMCID: PMC7605373 DOI: 10.1200/GO.20.00265
16. Burstein HJ, Curigliano G, Thürlimann B, et al. Customizing local and systemic therapies for women with early breast cancer: the St. Gallen International Consensus Guidelines for treatment of early breast cancer 2021. Ann Oncol. 2021;32(10):1216-35. PMID: 34242744 PMCID: PMC9906308 DOI: 10.1016/j.annonc.2021.06.023
17. Inic Z, Zegarac M, Inic M, et al. Difference between luminal A and luminal B subtypes according to Ki-67, tumor size, and progesterone receptor negativity providing prognostic information. Clin Med Insights Oncol. 2014;8:107-11. PMID: 25249766 PMCID: PMC4167319 DOI: 10.4137/CMO.S18006
18. Scholzen T, Gerdes J. The Ki-67 protein: from the known and the unknown. J Cell Physiol. 2000;182(3):311-22. PMID: 10653597 DOI: 10.1002/(SICI)1097-4652(200003)182:3<311::AID-JCP1>3.0.CO;2-9
19. Davey MG, Hynes SO, Kerin MJ, Miller N, Lowery AJ. Ki-67 as a prognostic biomarker in invasive breast cancer. Cancers. 2021;13(17):4455. PMID: 34503265 PMCID: PMC8430879 DOI: 10.3390/cancers13174455
20. Inwald EC, Klinkhammer-Schalke M, Hofstädter F, et al. Ki-67 is a prognostic parameter in breast cancer patients: results of a large population-based cohort of a cancer registry. Breast Cancer Res Treat. 2013;139(2):539-52. PMID: 23674192 PMCID: PMC3669503 DOI: 10.1007/s10549-013-2560-8
21. Gnant M, Thomssen C, Harbeck N. St. Gallen/Vienna 2015: a brief summary of the consensus discussion. Breast Care. 2015;10(2):124-30. PMID: 26195941 PMCID: PMC4464099 DOI: 10.1159/000430488
22. Maltoni R, Palleschi M, Ravaioli S, Tumedei MM, Altini M, Bravaccini S. Spotlight on Ki67 as a prognostic marker in early breast cancer: all that glitters may not be gold. Diagn Pathol. 2020;15(1):109. PMID: 32917222 PMCID: PMC7488398 DOI: 10.1186/s13000-020-01024-9
23. Randhawa AS, Roy PS, Hazarika M, Ahmed S. Retrospective analysis of Ki-67 as a predictive and prognostic marker for pathological complete response to neoadjuvant chemotherapy in breast cancer. J Clin Oncol. 2023;41(16_suppl):e12610. DOI: 10.1200/JCO.2023.41.16_suppl.e12610
24. Ma Q, Liu YB, She T, Liu XL. The role of Ki-67 in HR+/HER2− breast cancer: a real-world study of 956 patients. Breast Cancer (Dove Med Press). 2024;16:117-26. PMID: 38476641 PMCID: PMC10929654 DOI: 10.2147/BCTT.S451617
25. Dowsett M, Nielsen TO, A'Hern R, et al. Assessment of Ki67 in breast cancer: recommendations from the International Ki67 in Breast Cancer Working Group. J Natl Cancer Inst. 2011;103(22):1656-64. PMID: 21960707 PMCID: PMC3216967 DOI: 10.1093/jnci/djr393
26. Varga Z, Li Q, Jocjum W, et al. Ki-67 assessment in early breast cancer: SAKK28/12 validation study on the IBCSG VIII and IBCSG IX cohort. Sci Rep. 2019;9:13534. DOI: 10.1038/s41598-019-49638-4
27. Paik S, Shak S, Tang G, et al. A multigene assay to predict recurrence of tamoxifen-treated, node-negative breast cancer. N Engl J Med. 2004;351(27):2817-26. PMID: 15591335 DOI: 10.1056/NEJMoa041588
28. Petrelli F, Viale G, Cabiddu M, Barni S. Prognostic value of different cut-off levels of Ki-67 in breast cancer: a systematic review and meta-analysis of 64,196 patients. Breast Cancer Res Treat. 2015;153(3):477-91. PMID: 26341751 DOI: 10.1007/s10549-015-3559-0
29. Lee J, Lee Y, Bae SJ, et al. Ki-67, 21-gene recurrence score, endocrine resistance, and survival in patients with breast cancer. JAMA Netw Open. 2023;6(8):e2330961. PMID: 37647069 PMCID: PMC10469325 DOI: 10.1001/jamanetworkopen.2023.30961

30. Copur MS, Peterson T, Tun SM, et al. The relationship of oncotype Dx Recurrence Score (RS) with Ki 67 in early stage breast cancer patients in a community based cancer center in rural central Nebraska. J Clin Oncol. 2022;40(16_suppl):e12566. DOI:10.1200/JCO.2022.40.16_suppl.e12566
31. Mook S, Van't Veer LJ, Rutgers EJ, Piccart-Gebhart MJ, Cardoso F. Individualization of therapy using Mammaprint®: from development to the MINDACT Trial. Cancer Genomics Proteomics. 2007;4(3):147-55. PMID: 17878518
32. Cardoso F, Piccart-Gebhart M, Van't Veer L, Rutgers E; TRANSBIG Consortium. The MINDACT trial: the first prospective clinical validation of a genomic tool. Mol Oncol. 2007;1(3):246-51. PMID: 19383299 PMCID: PMC5543876 DOI: 10.1016/j.molonc.2007.10.004
33. Sparano JA, Gray RJ, Makower DF, et al. Adjuvant chemotherapy guided by a 21-gene expression assay in breast cancer. N Engl J Med. 2018;379(2):111-21. PMID: 29860917 PMCID: PMC6172658 DOI: 10.1056/NEJMoa1804710
34. Ngo MJN, Kho MR. Gene expression profiling for breast cancer in the Philippines: real-world data on feasibility, possible disparities, and clinical implications for LMICs. J Clin Oncol. 2022;40(16_suppl):e12569. DOI: 10.1200/JCO.2022.40.16_suppl.e12569
35. Bösl A, Spitzmüller A, Jasarevic Z, Rauch S, Jäger S, Offner F. MammaPrint versus EndoPredict: Poor correlation in disease recurrence risk classification of hormone receptor positive breast cancer. PLoS One. 2017;12(8):e0183458. PMID: 28850621 PMCID: PMC5574574 DOI: 10.1371/journal.pone.0183458
36. Bustreo S, Osella-Abate S, Cassoni P, et al. Optimal Ki-67 cut-off for luminal breast cancer prognostic evaluation: a large case series study with a long-term follow-up. Breast Cancer Res Treat. 2016;157(2):363-71. PMID: 27155668 PMCID: PMC4875067 DOI: 10.1007/s10549-016-3817-9
37. Lombardi A, Lazzeroni R, Bersigotti L, Vitale V, Amanti C. The proper Ki-67 cut-off in hormone responsive breast cancer: a monoinstitutional analysis with long-term follow-up. Breast Cancer (Dove Med Press). 2021;13:213-21. PMID: 33854368 PMCID: PMC8039013 DOI: 10.2147/BCTT.S305440
38. Amezcua-Gálvez JE, Lopez-Garcia CA, Villarreal-Garza C, et al. Concordance between Ki-67 index in invasive breast cancer and molecular signatures: EndoPredict and MammaPrint. Mol Clin Oncol. 2022;17(3):132. PMID: 35949891 PMCID: PMC9353786 DOI: 10.3892/mco.2022.2565
39. Siegel RL, Kratzer TB, Giaquinto AN, Sung H, Jemal A. Cancer statistics, 2025. CA Cancer J Clin. 2025;75(1):10-45. PMID: 39817679 PMCID: PMC11745215 DOI: 10.3322/caac.21871
40. Gradishar WJ, Moran MS, Abraham J, et al. Breast Cancer, Version 3.2022, Clinical Practice Guidelines in Oncology. J Natl Compr Canc Netw. 2022;20(6):691-722. PMID: 35714673 DOI: 10.6004/jnccn.2022.0030
41. Mazo C, Kearns C, Mooney C, Gallagher WM. Clinical decision support systems in breast cancer: A systematic review. Cancers (Basel). 2020;12(2):369. PMID: 32041094 PMCID: PMC7072392 DOI: 10.3390/cancers12020369
42. Selmani Z, Molimard C, Overs A, et al. Low correlation between Ki67 assessed by qRT-PCR in Oncotype DX test and immunohistochemistry in breast cancer. Sci Rep. 2022;12(1):3617. PMID: 35256657 PMCID: PMC8901910 DOI: 10.1038/s41598-022-07593-7
43. Yang Y, Leenstra JL, Wadhwani N, Ho A, Brown PD, Sachdev S. J Clin Oncol. 2026;44(16_suppl):2089. DOI:10.1200/JCO.2026.44.16_suppl.2089
44. Tian C, He Y, Tan Y, et al. Ki-67 versus MammaPrint/BluePrint for assessing luminal breast cancer biology in Chinese patients. J Clin Oncol. 2020;38(15_suppl):e13673. DOI:10.1200/JCO.2020.38.15_suppl.e13673
45. Nguyen B, Cusumano PG, Deck K, et al. Comparison of molecular subtyping with BluePrint, MammaPrint, and TargetPrint to local clinical subtyping in breast cancer. Ann Surg Oncol. 2012;19(10):3257-63. PMID: 22965266 DOI: 10.1245/s10434-012-2561-6
46. Pons L, Hernández-León L, Altaleb A, et al. Conventional and digital Ki67 evaluation and their correlation with molecular prognosis and morphological parameters in luminal breast cancer. Sci Rep. 2022;12(1):8176. PMID: 35581229 PMCID: PMC9114341 DOI: 10.1038/s41598-022-11411-5
47. Van 't Veer LJ, Dai H, van de Vijver MJ, et al. Gene expression profiling predicts clinical outcome of breast cancer. Nature. 2002;415(6871):530-6. PMID: 11823860 DOI: 10.1038/415530a
48. European Society for Medical Oncology (ESMO). ESMO Clinical Practice Guidelines: Breast Cancer. Accessed November 24, 2025. https://www.esmo.org/guidelines/esmo-clinical-practice-guidelines-breast-cancer
49. Department of Health, East Avenue Medical Center. Breast Cancer National Clinical Practice Guidelines. Manila, Philippines: Department of Health; 2022. Accessed November 24, 2025. https://bit.ly/CPG-BreastCA-2022

OPEN ACCESS – ORIGINAL ARTICLE

Blood Collection Tubes Utilized for Fasting Blood Sugar Measurement: A Source of Variation in Clinical Laboratory Test Results

Jomar Adams Ganding [1,2]

[1]*Department of Medical Technology, School of Health Sciences, Mapua University, Makati City, Philippines*
[2]*Graduate School, Trinity University of Asia. Quezon City, Philippines*

ABSTRACT

Background. Diabetes mellitus (DM) remains a major global health burden, with increasing prevalence in developing countries such as the Philippines. Accuracy of glucose measurement is vital for diagnosis and management; however, preanalytical variables, particularly glycolysis from varying collection tubes, temperature and time interval can significantly affect test results. Despite guideline recommendations favoring plasma, serum is still commonly used in local clinical practice.

Objective. This study evaluated the effectiveness of different commercially available blood collection tubes in preserving glucose stability by minimizing pre-analytical glycolysis.

Methodology. A cross-sectional observational and quasi-experimental study was conducted among 40 healthy adult participants (18–59 years) from a tertiary institution in Quezon City, Philippines. A total of 160 samples were collected using four tube types (one plasma and three serum tubes). Samples were analyzed at varying time intervals (0–180 minutes) and storage conditions (room temperature and 4°C). Glucose levels were measured using the glucose oxidase method. Statistical analysis included Shapiro–Wilk, Kruskal–Wallis H-test, Welch's t-test, and Dwass–Steel–Critchlow–Fligner post hoc comparisons at a 1% significance level.

Results. Glucose concentrations differed significantly across tube types (p <0.001) and time intervals (p <0.001), but not by storage temperature (p = 0.023). Plasma samples demonstrated significantly higher glucose levels than serum samples, with all serum tubes showing a consistent negative bias relative to the fluoride-containing plasma tube. Although differences remained within the ± 6 mg/dL CLIA allowable total error, clinically relevant deviations were observed near diagnostic thresholds. Glucose stability significantly declined beyond 60 minutes, indicating ongoing glycolysis despite sample separation.

Conclusion. Blood collection tube type and delayed processing significantly influence glucose measurements. While acceptable within analytical limits, systematic biases may affect clinical interpretation. Standardization of blood collection practices and stricter pre-analytical protocols are essential to improve diagnostic accuracy for diabetes in the Philippines.

Key words: blood collection tubes, fasting blood sugar (FBS), clinical laboratory science

ISSN 2507-8364 (Online)
Printed in the Philippines.

Received: 8 February 2026.
Accepted: 28 March 2026.
Published online first: 25 June 2026.
https://doi.org/10.21141/PJP.2026.601

Corresponding author: Jomar Adams Ganding, RMT, MSMT
E-mail: jaganding@mapua.edu.ph
ORCiD: https://orcid.org/0009-0002-8516-3601

INTRODUCTION

Diabetes mellitus (DM) is a chronic disease described to be a group of metabolic diseases characterized by abnormally high glucose levels that result from defects in insulin secretion, insulin action or both.[1,2] The global prevalence of DM significantly increased over the last decade.[3] More so, it has a major impact on third-world countries, particularly the Philippines, with a projected 7.5 million cases by 2045. In 2021, there has been 4.3 million Filipinos with DM, while 2.8 million remained undiagnosed.[4] There are four clinical types of Diabetes mellitus described according to etiology, Type 1 DM (formerly insulin dependent diabetes mellitus or juvenile diabetes mellitus): results from autoimmune beta-cell destruction, leading to absolute insulin deficiency, Type 2 DM (formerly non-insulin dependent diabetes mellitus or adult-onset DM): results from a progressive insulin secretory defect in the background of insulin resistance, Gestational diabetes

mellitus (GDM): diabetes first diagnosed during pregnancy, and Secondary diabetes: e.g., genetic defects in beta cell function or insulin action, diabetes of the exocrine pancreas (pancreatitis, cystic fibrosis), drug- or chemical-induced diabetes (such as from the treatment of AIDS, after organ transplantation, glucocorticoids), other endocrine diseases (Cushing's syndrome, hyperthyroidism).[5,6]

Glucose measurement, specifically the fasting blood sugar (FBS) is one of the most commonly done tests in the clinical laboratory. More so, the accurate glucose measurement is key in the diagnosis and management of diabetes patients because this serves as a screening test in detecting hyperglycemia.[7-9] FBS levels of patients with DM are characterized to be >126 mg/dL with a threshold level of >180 mg/dL where insulin therapy should be initiated.[5] Knowing the importance of accuracy in the measurement of blood glucose, the most suitable collection tube for blood glucose determination is still an issue. Previous studies show that the common tube still lacks the ability to immediately prevent clinically significant glycolysis, a process due to the consumption of glucose by the blood cells (RBC, WBC, and platelets), even in so-called gold standard tubes containing sodium fluoride with potassium oxalate. It is also compared to serum tube and citrated tubes which were recommended to be considered for glucose measurement.[10] While a 2019 study by Bonetti, G. et al. shows that tubes with sodium fluoride/citrate buffer liquid mixture and lithium-heparin tube have equal results in avoiding glycolysis completely and within 4 hours.[11] Currently, in the Philippines the majority of clinical laboratories are still using serum rather than plasma as the sample for FBS testing.

This practice is contrary to the Philippines Diabetes Clinical Practice Guidelines (CPG) recommendation, which is to utilize plasma for the said testing. As to the advantage of plasma samples, it allows immediate sample tube centrifugation without waiting for the blood to clot.[12] In this regard, failures in the proper specimen handling and collection is considered as one of the possible sources of variability in the medical laboratory test results as part of the pre-analytical phase errors with the highest percentage of 46% up to 77%, compared to the analytical and post-analytical phases.[13,14]

Moreso, since accurate measurements of blood glucose levels are crucial for the diagnosis of diabetes, proper blood collection tubes should be used to preserve the quality of the samples. In this study, the researcher evaluated the capability of different commercially available serum tubes in preserving the quality of the blood samples by preventing clinically significant glycolysis.

METHODOLOGY

Research design

The research design used in this research is cross-sectional observational and quasi-experimental design, as it attempted to compare the glucose measurements from different collection tubes commonly used in the clinical laboratory. This was the design used because the aim of this research is to observe whether there is relatedness between the glucose levels and the collection tubes used temperature variation and interval in its measurement. Only observation of data was used, and no intervention were used to obtain the results.

Study population, sample and sampling technique

The intended study population for this research are teaching and non-teaching personnel of tertiary institution in Quezon City, Philippines. The age range for that participants were from 18 to 59 years old. The healthy volunteers were recruited from March 2022 to April 2022. Nonprobability sampling was used as the sampling technique for this research. More so, the subjects were required to fast for 8-12 hours. Subjects who exceeded the said fasting requirement were rejected from the study. These patient preparations, data gathering procedures and blood collection procedures were thoroughly discussed to the participants through an orientation prior to specimen collection. The orientation also discussed the contents of the informed consent form, the participants' rights in the study, how their anonymity and confidentiality will be ensured, and the potential risks and mitigations were all given emphasis. Lastly, the orientation was done personally or through an online platform. Once consents were given and the orientation successfully done blood collection started the next day. The samples that were used in this study were the serum and plasma samples collected from the teaching and non-teaching personnel.

A total of one hundred-sixty (160) samples from 40 subjects were analyzed in this study. In addition, any information about the participants that were collected were kept confidential, which only the researcher can access. The information of the patients, such as name, age and birthdate gathered during specimen collection were kept confidential with the use of patient accession number and so their names will not be divulged. Meanwhile, information about the participants were kept in a file with a lock key, for electronic data it was kept in a folder with password and authentication, and it will not be shared with anyone, especially those not related to the research.

The samples from each subject were aliquoted, for each blood collection tube, two tubes were prepared and labelled according to the accession number of the specimens. The serum and plasma were separated from their respective tubes and divided to each tube equally, one to be stored at room temperature, 26.0 °C (range 23.6–28.6 °C) and at refrigerated temperature, 4.0 °C. It was then measured at varying time intervals, immediately after centrifugation, after 30 minutes, after 60 minutes. 120 minutes and 180 minutes.

Research instrument

An informed consent form and questionnaire were given to the teaching and non-teaching personnel of tertiary institution in Quezon City, Philippines who participated in the study. The questionnaire contained questions regarding their relevant clinical history, work experience and environment. These questions focused on recent hospitalization, medication and diet and lifestyle.[11] The equipment used for the collection of samples were evacuated tubes and needles, tourniquet, alcohol pads, gauze pad, and sharps container. The materials used for the glucose measurement are centrifuge, glucose oxidase reagent (Randox), and the Biosystems A15 machine.

Blood collection

Blood samples were collected by a single experienced phlebotomist to minimize venipuncture bias and were carried out between 7 am and 11 am to limit the effects of diurnal and circadian rhythm.[15-17] Samples were collected through an evacuated tube system to minimize contamination and to allow the collection of multiple blood collection tubes from the subjects.[18-20] The room temperature during blood collection was 26.0 °C (range 23.6–28.6 °C). Visibly lipemic, icteric or hemolyzed samples were not included in the study.[19,21-23] The blood collection tubes that used were the plasma tubes from BD Vacutainer sodium fluoride/sodium EDTA 13 x 75 mm (P1 Tube), 2 ml and the serum tubes used were BD Vacutainer plain serum tube 13 x 75 mm (S1 Tube), 4 ml, BD Vacutainer serum tube with clot activator 13 x 75 mm, 4 ml (S2 Tube), and BD Vacutainer serum separator tube (SST) 13 x 100 mm (S3 Tube), 4 ml.[24] Blood collection procedures were carried out following the Clinical and Laboratory Standards Institute (CLSI) Guidelines GP 41. A total of 160 specimens were drawn. Forty (40) tubes for each blood collection tube mentioned above. More so, the samples were collected at the phlebotomy room of the College of Medical Technology Diagnostic laboratory. Therefore, there were no delays in transportation and no effect on environmental temperature.

Specimen processing and aliquot preparation

After collection, serum tubes were allowed to clot for 60 minutes for S1, 20 minutes for S2 and S3;[16] and then all four tubes, including P1 were centrifuged at 1600 × g for 10 minutes using the DSC1512T of Digisystems centrifuge. The aliquot preparation was carried out immediately after centrifugation. Two tubes were labelled according to the accession number of the specimens. The serum and plasma were separated from their respective tubes and aliquots of the samples were prepared, containing approximately 1.0 mL aliquots of plasma and serum. For each blood collection tube, two tubes were prepared and labelled according to the accession number of the specimens, one to be stored at room temperature, 26.0 °C (range 23.6–28.6 °C) and at refrigerated temperature, 4.0 °C. In addition, prior to the measurement of samples visibly lipemic, hemolyzed, and icteric was not included in the study

Glucose measurement

The glucose concentration was determined spectrophotometrically using Biosystem A15 autoanalyzer (Biosystems Inc.) by a glucose oxidase-peroxidase method (Randox).[25] Prior to the measurement, calibration procedures were done. As for the quality control procedures, the researcher ran a two-level of quality control material at the beginning of each working day before starting any measurement. This was conducted by the researcher who is also qualified technical personnel and results were properly documented. All the specimens from the participants were analyzed using the same lot of reagents, eliminating any lot-to-lot variability in the results. The researcher performed the measurements of all study specimens. The glucose concentration was measured immediately after centrifugation x and with intervals of 30 minutes, 60 minutes, 120 minutes, 180 minutes.[26,27]

Inclusion and exclusion criteria

Both teaching and non-teaching personnel of tertiary institution in Quezon City, Philippines who were willing to participate in this study were enrolled. Individuals with comorbidities such as chronic liver disease, malignancy, autoimmune disease, and pregnant women were excluded. In addition, this study did not include individuals with prediabetes, established diabetes, or gestational diabetes mellitus; therefore, the diagnostic impact of the observed plasma–serum and tube-related differences across all glycemic categories could not be fully assessed.

Statistical treatment of data

For the statistical treatment of the data, prior to conducting the analysis, the test of normality was done using Shapiro-Wilk statistics which showed that the assumption of normality was violated, $W = 0.982$, $p = <0.001$. Thus, the researcher used the non-parametric statistical tools, Kruskal-Wallis H-Test as an alternative to one-way ANOVA and Dwass-Steel-Critchlow-Fligner (DSCF) pairwise comparisons for the post-hoc analysis. All of which have a 1% level of significance. These were used in determining if there were significant differences among the glucose measurement using varying blood collection tube, storage temperature and time interval prior to measurement.[12,16]

Ethical clearance

The study was carried out in accordance with the ethical standards set by the Trinity University of Asia—Institutional Ethics Review Committee (TUA—IERC). Most importantly, the research protocol and written informed consent utilized in this study were reviewed and approved by TUA—IERC with a research protocol code number, 2022-009-Ganding-GS-FBS-v2.

RESULTS AND DISCUSSION

A total of 40 subjects participated and provided blood samples for the four different blood collection tubes: BD Vacutainer sodium fluoride/sodium EDTA 13 x 75 mm (P1 Tube), BD Vacutainer plain serum tube 13 x 75 mm (S1 Tube), BD Vacutainer serum tube with clot activator 13 x 75 mm, 4 ml (S2 Tube), and BD Vacutainer serum separator tube (SST) 13 x 100 mm (S3 Tube) for an overall total of 400 blood samples processed during the experiment. After specimen collection, the tubes were inverted following the manufacturer's recommendation then were allowed to clot serum tubes were allowed to clot according to the for 60 minutes for S1, 20 minutes for S2 and S3;[16] and then all four tubes, including P1 will be centrifuged at 1600 × g for 10 min using the DSC1512T of Digisystems centrifuge. The aliquot preparation was carried out immediately after centrifugation. Two tubes were labelled according to the accession number of the specimens. The serum and plasma were separated from their respective tubes and divided to each tubes equally. After the initial glucose measurement, tubes were stored at room temperature (26.0 °C) or at refrigerated temperature (4.0 °C) and measured repeatedly after 30, 60, 120, and 180 minutes.

Since the glucose concentration from the four different tubes, differs significantly at 1% level of significance, $H(3) = 25.3$, $p = <0.001$ as shown in Table 4 a post hoc analysis using DSCF for pairwise comparison was done to specifically

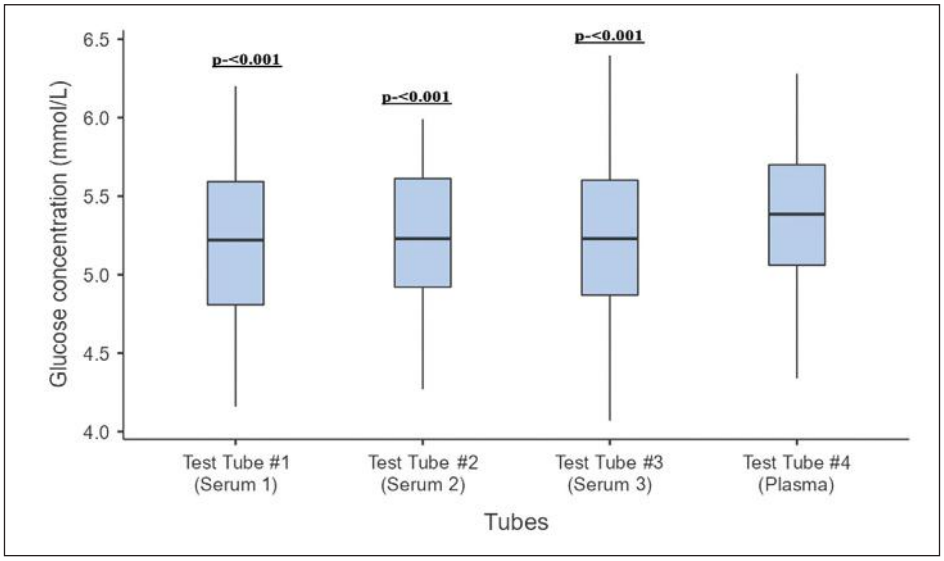

Figure 1. Difference of glucose measurement with varying collection tubes.

Table 1. Post-hoc analysis using Dwass-Steel-Critchlow-Fligner pairwise comparisons on the difference of glucose measurement with varying collection tubes

Pairwise comparisons – Glucose concentration (mmol/L)		W	*p*
Test Tube #1 (Serum 1)	Test Tube #2 (Serum 2)	2.022	0.481
Test Tube #1 (Serum 1)	Test Tube #3 (Serum 3)	0.674	0.964
Test Tube #1 (Serum 1)	Test Tube #4 (Plasma)	6.337	<0.001
Test Tube #2 (Serum 2)	Test Tube #3 (Serum 3)	-1.429	0.744
Test Tube #2 (Serum 2)	Test Tube #4 (Plasma)	4.598	0.006
Test Tube #3 (Serum 3)	Test Tube #4 (Plasma)	5.754	<0.001

Table 2. Glucose concentration in varying temperature storage prior to measurement

Shapiro-Wilk	W	*p*
Glucose concentration (mmol/L)	0.982	<0.001

Note: A low *p*-value suggests a violation of the assumption of normality

Table 3. Homogeneity of variances test (Levene's)

	F	df	*P*
Glucose concentration (mmol/L)	0.712	1	0.399

Note: A low *p*-value suggests a violation of the assumption of equal variances

Table 4. Independent samples t-test

	Welch's t		Cohen's d
	Statistic	*p*	Effect Size
Glucose concentration (mmol/L)	2.28	0.023	0.114

Table 5. Difference of glucose measurement with varying storage temperature

	Group	Mean	Median	SD
Glucose concentration (mmol/L)	Room Temp.	5.28	5.29	0.437
	Refrigerated Temp.	5.23	5.24	0.449

identify the tubes that had a significant difference in their glucose concentration (mmol/L). As shown in Tables 5 and 7, complemented by Figure 5, Test tube 1- Serum 1 (MD = 5.22); Test Tube #2 - Serum 2 (MD = 5.23); and Test Tube #3 - Serum 3 (MD = 5.23) are significantly different from the Test Tube #4 Plasma (MD = 5.38), W = 6.337, p = <0.001, W = 4.598, p = 0.006, W = 5.754, p = <0.001, respectively.

These findings agree with the conclusion of Pant et al., that the use of different tubes for glucose measurement yields varying results. This is contrary with the findings of Winter et al., who mentioned that glucose concentration measured from serum tubes, specifically those with thixotropic gel (S3) would remain unchanged. However, the findings in this study further agrees with Bhatt et al., that the glucose concentration measured from the plasma collected using the gray top tube containing NaF/Na EDTA tube has higher glucose concentration compared to serum tubes. This can be explained and attributed with the additive found in P1, the sodium fluoride (NaF) which is an antiglycolytic agent.[28] Fluoride inhibits enolase, an enzyme involved in glycolysis which requires magnesium for its optimal activity.[7] This is the very reason this tube is also recommended by CLSI and ADA as a gold standard for glucose measurement.

Prior to conducting the analysis, Tables 2 and 3 show the test of normality was examined using Shapiro-Wilk statistics which showed that the assumption of normality was violated, W = 0.982, p = <0.001. Aside from this, test of homogeneity of variance test using Levene's test was utilized and found out that a violation of the assumption of equal variances, F = 0.712, p = 0.399 was violated. Thus, Welch-Test was used as an alternative to parametric T-Test for independent samples.

Table 4 shows the result of Welch-Test reveals that the glucose concentration did not differ significantly among the varying temperatures storage prior to measurement at 1% level of significance, t(1)=2.28, p = 0.023. There is a moderate effect size in this analysis reflected in Cohen's (d = 0.114). In addition, Table 5, complemented

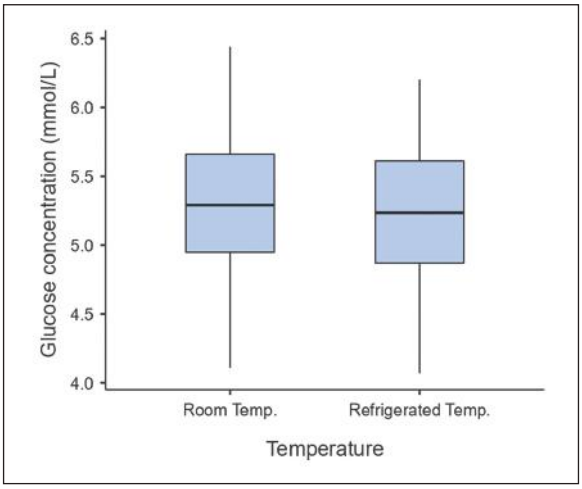

Figure 2. Difference of glucose measurement at varying temperature storage.

by Figure 2, presents the descriptive on the difference of glucose measurement with varying storage temperature.

The findings of this study shows that varying temperature storage prior to measurement is not significant. This suggests that regardless of storage temperature, glucose concentration is unaffected. This is contrary to the findings of Kubihal et al., who mentioned that glucose is only stable at lower temperatures. This may be due to a more robust condition of this study that used a significance level of 1% compared to the other studies that used a 5% level of significance.

Glucose concentration in varying time intervals prior to measurement

Table 6 shows the result of Kruskal-Wallis H-Test reveals that the glucose concentration differs significantly at 1% level of significance among the different time intervals prior to measurement, H(3)=55.3, p = <0.001. There is a weak effect size in this analysis (ε^2 = 0.0346).

Meanwhile, Table 7 shows the Post hoc analysis using DSCF showed that the glucose concentration (mmol/L) at different time interval specifically after 120 minutes (MD = 5.17); after 180 minutes (MD = 5.17); are significantly different from the glucose concentration measured immediately after centrifugation (MD = 5.46), W = -7.36, p = <0.001, W = -8.82, p = <0.001, respectively. In addition, glucose concentration (mmol/L) measured after 120 minutes (MD = 5.17); after 180 minutes (MD = 5.17); are also significantly different from the glucose concentration measured after 60 minutes (MD = 5.36), W = -75.74, p = <0.001, W = -7.08, p = <0.001, respectively.

This study suggests that glucose, whether in plasma and serum, is optimally stable only up to one hour. This agrees with study made by Winter et al., who mentioned that delayed specimen processing and measurement beyond one hour should be avoided. As seen in Table 7, complemented by Table 8, there is significant decrease in glucose concentration with the increasing lapse of time, the difference being more with increase in time gap, which also agrees with the conclusions of Bhargava et al. Currently, the CLSI guidelines would recommend processing of specimens within two hours but based on the results of this study the difference is already significant. This finding aligns with the results of Bhatt et al., The significant decrease may be attributed to the continuous glycolysis due to the presence of red blood cells and white blood cells even after separation of plasma or serum.[11,29]

Although the decreased in the glucose concentration seen from measurements done after two and three hours are statistically significant, the difference is within the ± 6 mg/dL (0.33 mmol/L), which is within the standard acceptable range as defined by the United States Clinical Laboratory Improvement Amendments (CLIA) guideline.[12,16,28] However, in the Philippines, there are no guidelines similar to CLIA yet.

Based on the data collected from this study it shows that over all glucose concentration measured using different blood collection tubes, stored at room and refrigerated temperature and are measured at varying time interval are significantly different. While there is no significant difference in the glucose concentration measured with varying temperature storage prior to measurement. It can be noted that glucose concentration varies significantly when stored in room and refrigerated temperatures. S1 has decreased by 4.05% at room temperature and 2.85% at refrigerated temperature; S2 has decreased by

Table 6. Difference of glucose measurement at varying time intervals prior to measurement

Kruskal-Wallis	χ^2	df	*p*	ε^2
Glucose concentration (mmol/L)	55.3	4	<0.001	0.0346

Table 7. Post-hoc analysis using Dwass-Steel-Critchlow-Fligner pairwise comparisons on the difference of glucose measurement with varying time intervals prior to measurement

Pairwise comparisons – Glucose concentration (mmol/L)		W	*P*
Immediately after centrifugation	30 minutes	-4.39	0.016
	60 minutes	-2.03	0.607
	120 minutes	-7.36	<0.001
	180 minutes	-8.82	<0.001
30 minutes	60 minutes	2.52	0.386
	120 minutes	-3.17	0.163
	180 minutes	-4.48	0.013
60 minutes	120 minutes	-5.74	<0.001
	180 minutes	-7.08	<0.001
120 minutes	180 minutes	-1.18	0.921

Table 8. Descriptive on glucose concentration glucose measured at varying time intervals prior to measurement

	Time	Median
Glucose concentration (mmol/L)	Immediately after centrifugation	5.46
	30 minutes	5.32
	60 minutes	5.36
	120 minutes	5.17
	180 minutes	5.17

5.78% at room temperature and 7.47% at refrigerated temperature; S3 has decreased by 4.60% at room temperature and 4.18% at refrigerated temperature; and P1, at the end of the observation the median glucose decreased by 5.72% at room temperature and 8.42% at refrigerated temperature. Moreso, the overall glucose concentration from the four different tubes, differs significantly at 1% level of significance, $H(3)=25.3$, $p = <0.001$. Among the three serum tubes, S2-BD Vacutainer serum tube with clot activator has the least Wilcoxon rank sum test statistic of $W = 4.598$.

However, contrary to common notion, at 1% level of significance, glucose concentration did not differ significantly at either room or refrigerated temperature used as storage prior to testing. As recommended and suggested by the researcher, based on this study, glucose, whether in plasma and serum, is optimally stable only up to one hour. Additionally, the red top tube (S3) with a clot activator can be used as an alternative to gray top tube, as it can be centrifuged within 30 minutes and analyzed within an hour. This would optimally prevent significant glycolysis in the absence of a tube containing an antiglycolytic agent.

CONCLUSION

This study demonstrates that pre-analytical variables significantly influence glucose measurement outcomes. The results revealed a statistically significant difference in glucose concentration between plasma and serum, with plasma glucose consistently higher than serum glucose. While the median numerical differences are within the 6mg/dL (0.33 mmol/L) allowable total error defined by CLIA, this systematic negative bias in serum relative to plasma becomes clinically relevant near diagnostic cut-offs such as the ADA fasting glucose threshold of 126 mg/dL. Overall collection conditions, glucose concentrations measured using different blood collection tubes, stored at room or refrigerated temperature, and measured at varying time intervals were significantly different. These findings emphasize the critical role of pre-analytical standardization in ensuring reliable glucose measurement. The implementation of standardized blood collection protocols, including appropriate tube selection and timely processing, is essential to improve diagnostic accuracy and support optimal clinical decision-making for diabetes in the Philippines.

RECOMMENDATIONS

Based on these findings, timely specimen processing should be prioritized, with blood samples centrifuged within 20–30 minutes and analyzed within one hour of collection whenever possible. The use of blood collection tubes containing antiglycolytic agents is strongly recommended to minimize ongoing in vitro glycolysis. When serum tubes are used, those with clot activators should be preferred to shorten clotting time and reduce serum contact with blood cells. Clinical laboratories are encouraged to standardize the type of blood collection tubes used for glucose testing to reduce variability in results. Future studies including individuals with prediabetes, diabetes, and gestational diabetes mellitus are warranted to determine how these pre-analytical differences affect diagnosis across all glycemic categories. Finally, the development and implementation of local laboratory protocols defining acceptable pre-analytical conditions and reference ranges for glucose monitoring are essential to promote consistency, diagnostic accuracy, and improved patient care outcomes.

STATEMENT OF AUTHORSHIP

All authors certified fulfilment of ICMJE authorship criteria.

AUTHOR DISCLOSURE

The authors declared no conflict of interest.

DATA AVAILABILITY STATEMENT

The datasets generated and analyzed in this study are included in the published article.

FUNDING SOURCE

None.

REFERENCES

1. Bishop ML, Fody EP, Schoeff LE. Clinical Chemistry, 8th ed. Wolters Kluwer; 2018.
2. Yang C, Feng W, Li Y, Tian X, Zhou Z, Lu L, Nie Y. A promising method for diabetes early diagnosis via sensitive detection of urine glucose by Fe-Pd/rGO. Dyes Pigments. 2019;164:20-6. DOI: 10.1016/j.dyepig.2018.12.061
3. Ng JYS, Clement IJ, Jimeno C, et al. Estimating direct medical costs of type 2 diabetes mellitus in the Philippines: a protocol. BMJ Open. 2020;10(7):e025696. PMID: 32723733 PMCID: PMC7389482 DOI: 10.1136/bmjopen-2018-025696
4. Cando LFT, Quebral EPB, Ong EP, et al. Current status of diabetes mellitus care and management in the Philippines. Diabetes Metab Syndr. 2024;18(2):102951. PMID: 38382166 DOI: 10.1016/j.dsx.2024.102951
5. American Diabetes Association. Classification and diagnosis of diabetes: standards of medical care in diabetes-2021. Diabetes Care. 2021;44(Suppl 1):S15-33. PMID: 33298413 DOI: 10.2337/dc21-S002
6. McPherson RA, Pincus MR, eds. Henry's clinical diagnosis and management by laboratory methods. 24th ed. Elsevier; 2022. ISBN: 9780323673204
7. Kubihal S, Goyal A, Gupta Y, Khadgawat R. Glucose measurement in body fluids: a ready reckoner for clinicians. Diabetes Metab Syndr. 2021;15(1):45-54. PMID: 33310176 DOI: 10.1016/j.dsx.2020.11.021
8. Landgraf R, Nauck M, Freckmann G, et al. Pitfalls in the diagnosis of diabetes: are we too lax with laboratory parameters? Dtsch Med Wochenschr. 2018;143(21):1549-55. PMID: 30235490 DOI: 10.1055/a-0673-2156
9. Lee H, Hong YJ, Baik S, Hyeon T, Kim DH. Enzyme-based glucose sensor: from invasive to wearable device. Adv Healthc Mater. 2018;7(8):e1701150. PMID: 29334198 DOI: 10.1002/adhm.201701150

10. Lippi G, Nybo M, Cadamuro J, Guimaraes JT, van Dongen-Lases E, Simundic AM. Blood glucose determination: effect of tube additives. Adv Clin Chem. 2018;84:101-23. PMID: 29478513 DOI: 10.1016/bs.acc.2017.12.003
11. Bonetti G, Carta M, Lapolla A, Miccoli R, Testa R, Mosca A; SIBioC-SIPMeL Working Group on Diabetes and the Italian Diabetes Society (SID). Correct determination of glycemia in the diagnosis and management of diabetes: recommendations for the optimization of the pre-analytical phase. Nutr Metab Cardiovasc Dis. 2019;29(1):1-3. PMID: 30482424 DOI: 10.1016/j.numecd.2018.09.013
12. Winter T, Hannemann A, Suchsland J, Nauck M, Petersmann A. Long-term stability of glucose: glycolysis inhibitor vs gel barrier tubes. Clin Chem Lab Med. 2018;56(8):1251-8. PMID: 29525788 DOI: 10.1515/cclm-2017-0860
13. Pan CT, Francisco MD, Yen CK, Wang SY, Shiue YL. Vein pattern locating technology for cannulation: a review of the low-cost vein finder prototypes utilizing near infrared (NIR) light to improve peripheral subcutaneous vein selection for phlebotomy. Sensors (Basel). 2019;19(16):3573. PMID: 31426370 PMCID: PMC6719195 DOI: 10.3390/s19163573
14. Francisco MD, Chen WF, Pan CT, et al. Competitive real-time near infrared vein finder imaging device to improve peripheral subcutaneous vein selection in venipuncture for clinical laboratory testing. Micromachines (Basel). 2021;12(4):373. PMID: 33808493 PMCID: PMC8067297 DOI: 10.3390/mi12040373
15. Leung GKW, Huggins CE, Ware RS, Bonham MP. Time of day difference in postprandial glucose and insulin responses: systematic review and meta-analysis of acute postprandial studies. Chronobiol Int. 2020;37(3):311-26. PMID: 31782659 DOI: 10.1080/07420528.2019.1683856
16. Pant V, Gautam K, Pradhan S, Pyakurel D, Shrestha A. Blood glucose concentration measured in EDTA/F plasma and serum in a referral clinical laboratory in Nepal. J Pathol Nepal. 2021;11(1):1837-41. DOI: 10.3126/jpn.v10i2.32351
17. Serin Y, Acar Tek N. Effect of circadian rhythm on metabolic processes and the regulation of energy balance. Ann Nutr Metab. 2019;74(4):322-30. PMID: 31013492 DOI: 10.1159/000500071
18. Bazzano G, Galazzi A, Giusti GD, Panigada M, Laquintana D. The order of draw during blood collection: a systematic literature review. Int J Environ Res Public Health. 2021;18(4):1568. PMID: 33562241 PMCID: PMC7915193 DOI: 10.3390/ijerph18041568
19. McCall RE. Phlebotomy essentials, 8th ed. Jones and Bartlett learning; 2021.
20. Keohane EM, Otto CN, Walenga JM. Rodak's Hematology: Clinical principles and applications. 6th ed. Elsevier; 2020.
21. Burtis CA, Ashwood ER, Tietz NW. Tietz fundamentals of clinical chemistry and molecular diagnostics, 7th ed. Elsevier; 2018.
22. Ayer T, Zhang C, Zeng C, White CC, Joseph VR. Analysis and improvement of blood collection operations. Manuf Serv Oper Manag. 2019;21(1):29-46. DOI:10.1287/msom.2017.0693
23. Chadwick K, Whitehead SJ, Ford C, Gama R. kEDTA sample contamination: a reappraisal. J Appl Lab Med. 2019;3(6):925-35. PMID: 31639684 DOI: 10.1373/jalm.2018.027920
24. Becton Dickinson and Company. BD vacutainer evacuated blood collection system; 2020. https://www.bd.com/documents/guides/directions-for-use/PAS_BC_BD-Vacutainer-Evacuated-Blood-Collection-System_SF_EN.pdf
25. Dickson LM, Buchmann EJ, Janse Van Rensburg C, Norris SA. The impact of differences in plasma glucose between glucose oxidase and hexokinase methods on estimated gestational diabetes mellitus prevalence. Sci Rep. 2019;9(1):7238. PMID: 31076622 PMCID: PMC6510785 DOI: 10.1038/s41598-019-43665-x
26. Loganathan P, Gasper SK, Afel FK, Kandaswamy S. Pre-analytical errors in glucose estimation results in query on diabetic management. Indian J Clin Biochem. 2020;35(1):32-42. PMID: 32071494 PMCID: PMC6995467 DOI: 10.1007/s12291-018-0782-6
27. Pleus S, Freckmann G, Baumstark A, Haug C. Stability of glucose concentrations in frozen plasma. J Diabetes Sci Technol. 2021;15(3):745-51. DOI: 10.1177/1932296820963657
28. Bhargava M, Singh NP, Gupta AK. Should we still collect blood glucose sampling in fluoride tubes? An evidence-based study. Int J Diabetes Dev Ctries. 2019;39(2):243-4. DOI: 10.1007/s13410-018-0688-0
29. Bhatt MP, Shrestha S. Rate of glucose utilization by blood cells in serum and plasma specimens with or without using preservative. Mod Med Lab J. 2022;17(5):1-9. DOI: 10.30699/mmlj17.5.1.1

OPEN ACCESS – REVIEW ARTICLE

Reassessing the Gold Standard: The Role of AI-Powered Urinalysis in Diagnosing Urinary Tract Infections

Mark Justine Bansil

Our Lady of Fatima University, Valenzuela City, Philippines

ABSTRACT

Urinary tract infections (UTIs) are among the most common bacterial infections worldwide, requiring timely and accurate diagnosis to guide appropriate therapy and reduce antimicrobial resistance. Although urine culture remains the diagnostic gold standard, its prolonged turnaround time and susceptibility to pre-analytical variability limit its clinical efficiency. Recent advances in artificial intelligence (AI) have positioned urinalysis as a promising alternative diagnostic approach, utilizing machine learning and deep learning algorithms for automated analysis and prediction. This review synthesizes current evidence on AI applications in urinalysis for UTI diagnosis, examining computational techniques, diagnostic performance, clinical integration, limitations, and future directions. The literature demonstrates that AI-powered urinalysis can achieve diagnostic accuracy comparable to urine culture, with high sensitivity and specificity while reducing diagnostic time. Integration of AI into clinical workflows has the potential to enhance decision-making, streamline laboratory processes, and support antimicrobial stewardship. However, challenges related to data heterogeneity, algorithm interpretability, validation, and regulatory requirements remain significant barriers to widespread adoption. Overall, AI-driven urinalysis represents a transformative opportunity to complement the existing diagnostic standard and advance more rapid, efficient, and personalized approaches to UTI management.

Key words: artificial intelligence, urinalysis, urinary tract infection, machine learning, deep learning, diagnostic accuracy

ISSN 2507-8364 (Online)
Printed in the Philippines.

Received: 8 February 2026.
Accepted: 18 February 2026.
Published online first: 11 June 2026.
https://doi.org/10.21141/PJP.2026.595

Corresponding author: Mark Justine Bansil, RMT
E-mail: mdbansil1232val@student.fatima.edu.ph
ORCiD: https://orcid.org/0009-0003-5527-3575

INTRODUCTION

Urinary tract infections (UTIs) remain one of the most common bacterial infections worldwide, particularly affecting women, older adults, and individuals with underlying health conditions.[1] Accurate and timely diagnosis is essential to reduce complications, guide targeted antimicrobial therapy and mitigate the rise of antimicrobial resistance. At present, urine culture is regarded as the gold standard for UTI diagnosis because it enables pathogen identification and antibiotic susceptibility testing.[2] However, culture-based techniques are inherently time-consuming—typically requiring 24 to 72 hours to generate results—and are susceptible to pre-analytical variations such as specimen handling, contamination, and prior antibiotic use.[3] These limitations often delay clinical decision-making and appropriate therapeutic intervention.

The emergence of artificial intelligence (AI) has opened new avenues for revolutionizing diagnostic microbiology, including urinalysis. AI-powered systems employ machine learning and image-recognition algorithms to analyze urinalysis data, predict culture outcomes, and even identify causative microorganisms without the inherent delays of conventional methods.[4,5] Several studies have demonstrated that AI-driven urinalysis can achieve diagnostic performance comparable to traditional culture, with notable improvements in sensitivity, specificity, and turnaround time.[6,7] Furthermore, systematic reviews have emphasized AI's potential to enhance diagnostic accuracy, streamline laboratory workflows, and support antimicrobial stewardship through early and reliable detection of infections.[2,8]

Despite this progress, challenges persist in translating AI diagnostics into routine clinical practice. Issues surrounding algorithm validation across diverse populations, data standardization, interpretability, and regulatory compliance continue to hinder widespread adoption.[1,3] Against this backdrop, this review reexamines the long-standing gold standard of urine culture in the context of emerging AI-powered urinalysis technologies. By consolidating current evidence, this work provides a critical analysis of their diagnostic capabilities, implementation barriers, and clinical implications. The novelty of this review lies in its focused reassessment of urine culture through the lens of AI innovation, highlighting not only how artificial intelligence may complement or replace conventional diagnostics but also how it can redefine the future of UTI detection and management.

METHODOLOGY

This narrative review synthesizes current literature on artificial intelligence (AI) applications in urinalysis for the diagnosis of urinary tract infections (UTIs). A structured search strategy was employed to identify relevant studies assessing AI-driven diagnostic performance, predictive accuracy, and clinical applicability compared to conventional urine culture.

Literature search strategy

A comprehensive search was conducted using PubMed, Google Scholar, ScienceDirect, and Web of Science. Sources included peer-reviewed journals, clinical reports, and white papers covering AI algorithms, machine learning, predictive modeling, and digital urinalysis technologies. Search terms included "AI in urinalysis," "machine learning in UTI diagnosis," "automated urine analysis," "urine culture prediction," and "smart diagnostics for UTIs."

Inclusion and exclusion criteria

- Inclusion: Studies reporting AI applications in urinalysis, diagnostic performance comparisons with urine culture, algorithm development for UTI detection, and workflow improvements in laboratory diagnostics.
- Exclusion: Studies unrelated to urinalysis or UTI diagnosis, general AI applications without clinical relevance, or publications lacking sufficient methodological rigor.

Data extraction and thematic analysis

Key themes extracted and analyzed included:

1. AI algorithms and computational techniques for urinalysis
2. Diagnostic performance metrics (sensitivity, specificity, predictive values)
3. Comparative effectiveness versus urine culture
4. Workflow and clinical integration
5. Challenges, limitations, and validation requirements
6. Future directions in AI-driven UTI diagnostics

A qualitative synthesis was performed to identify recurring patterns, evidence gaps, and insights into the potential for AI-powered urinalysis to complement or replace traditional urine culture.

Critical evaluation and discussion

The review evaluates the impact of AI on diagnostic speed, accuracy, and clinical decision-making. Barriers to implementation, ethical considerations, and strategies for integration into routine clinical practice are also examined, highlighting the evolving role of AI in UTI diagnosis.

RESULTS

The following section is a systematic integrative review, presenting the results, clustered according to discussion.

A structured literature search identified a total of 54 records across the selected databases. After removal of duplicates, 41 articles remained for title and abstract screening. Of these, 22 studies were considered potentially eligible and underwent full-text review. Following the application of inclusion and exclusion criteria, 14 studies were included in the final analysis. The included studies comprised systematic reviews, retrospective analyses, experimental investigations, and preprint studies examining the application of artificial intelligence in urinalysis for the diagnosis and prediction of urinary tract infections.

AI algorithms and computation techniques for urinalysis

Artificial intelligence (AI) has significantly transformed urinalysis, introducing advanced computational techniques that enhance diagnostic accuracy and efficiency. Machine learning algorithms, including logistic regression, random forests, and support vector machines, have been widely employed to predict urinary tract infections (UTIs) based on routine urinalysis parameters. Naik et al., demonstrated that machine learning models could reliably predict urine culture positivity and identify urinary bloodstream infections by integrating automated urinalysis data with clinical information, achieving high sensitivity and specificity. Such predictive models have the potential to support early diagnosis and guide antimicrobial stewardship, reducing unnecessary delays associated with traditional culture-based methods.[2]

Deep learning approaches, particularly convolutional neural networks (CNNs), have been applied to analyze urine sediment images with remarkable accuracy. Studies have shown that CNN-based models can automatically detect and classify various urine particles, including erythrocytes, leukocytes, and casts, significantly reducing the subjectivity and time demands of manual microscopy.[4] These models demonstrate robust pattern recognition capabilities, even in complex urine samples, and can be continuously improved with larger datasets, enhancing reliability across different patient populations. AI-driven prediction models have also been developed to forecast urine culture outcomes directly. Dedeene et al., introduced a multilayer perceptron-based tool incorporating parameters such as urine dipstick analysis, urine cytometry, and patient demographic features, achieving an area under the curve (AUC) of 0.88. Such tools allow clinicians to make rapid decisions regarding empiric therapy, particularly in acute care settings.[7]

The integration of AI with mobile and point-of-care (POC) devices represents another promising application in urinalysis. Choi et al., demonstrated that AI algorithms

could accurately interpret urine test strips using smartphone cameras, providing immediate diagnostic insights without the need for conventional laboratory infrastructure.[5] This approach offers substantial advantages in resource-limited settings and during high-demand periods, enabling rapid triage and monitoring of patients. Despite these advances, validation in real-world clinical settings remains essential. Goździkiewicz et al., and De Bruyne et al., emphasized that large-scale prospective studies are needed to confirm the reliability, generalizability, and clinical utility of AI-powered urinalysis.[3,4] Additionally, considerations related to data standardization, algorithm transparency, and integration with electronic health records are critical for safe and effective implementation.

Overall, AI algorithms and computational techniques are reshaping the landscape of urinalysis, offering faster, more accurate, and potentially cost-effective alternatives to traditional diagnostic methods. The growing body of evidence suggests that, with rigorous validation and thoughtful integration into clinical workflows, AI-powered urinalysis could significantly enhance the early detection and management of UTIs, complementing or in some cases reducing reliance on conventional urine culture.

Diagnostic performance metrics

The diagnostic performance of AI-powered urinalysis has been a major focus of recent research, emphasizing its potential to match or even surpass conventional urine culture in certain clinical contexts. Studies have consistently reported high sensitivity, specificity, and predictive values for AI algorithms when applied to automated urinalysis data. Choi et al., found that machine learning models could predict urine culture results with sensitivity exceeding 90% for common uropathogens, while maintaining specificity above 85%, demonstrating reliable discrimination between positive and negative cultures. Such performance metrics indicate that AI algorithms can effectively support early diagnosis, allowing clinicians to initiate timely treatment and reduce the unnecessary use of broad-spectrum antibiotics.[5]

Several studies have compared AI-based urinalysis to traditional culture in terms of overall accuracy and predictive performance. Naik et al., reported that AI models integrating urine dipstick results, urine sediment analysis, and patient clinical data achieved an overall accuracy of 87–92% in predicting culture outcomes.[2] Similarly, Dedeene et al., demonstrated that multilayer perceptron classifiers could generate area under the curve (AUC) values of 0.88–0.91, reflecting strong discriminative power. These findings suggest that AI-driven urinalysis can serve as a reliable triage tool, particularly in settings where immediate culture results are not available and may reduce laboratory workload without compromising diagnostic integrity.[7]

The positive and negative predictive values of AI models also support their clinical utility. Shen et al., highlighted that AI algorithms exhibited high positive predictive values for Enterobacteriaceae and Escherichia coli infections, the most common causative organisms in UTIs, while negative predictive values remained consistently high across different patient populations.[8] This balance of predictive accuracy allows for confident rule-in and rule-out decisions, potentially reducing unnecessary empirical antibiotic prescriptions. Additionally, De Bruyne et al., observed that performance metrics remained robust even when AI algorithms were applied to large and heterogeneous datasets, indicating potential generalizability across multiple clinical environments.[4]

Despite these promising results, some limitations persist. Variability in dataset quality, differences in laboratory equipment, and incomplete clinical metadata can affect model performance.[1,3] Prospective studies are needed to validate retrospective findings and evaluate real-world implementation. Nonetheless, the growing body of evidence demonstrates that AI-powered urinalysis consistently achieves diagnostic performance metrics comparable to, and in some cases exceeding, conventional urine culture, offering a rapid, reliable, and potentially transformative approach to UTI diagnosis.

Comparative effectiveness versus urine culture

Recent studies have increasingly focused on comparing the effectiveness of AI-powered urinalysis to the traditional gold standard of urine culture for diagnosing urinary tract infections (UTIs). While urine culture remains the definitive method for confirming infection and identifying causative organisms, it is time-consuming, often requiring 24–48 hours for results, and is susceptible to delays in clinical decision-making. AI-powered urinalysis offers the potential to bridge this gap by providing rapid, reliable predictions of culture outcomes, potentially guiding early intervention. Choi et al., reported that AI-driven models achieved predictive accuracy comparable to urine culture, correctly identifying the presence of common pathogens such as Escherichia coli and Enterococcus spp. in over 90% of cases, while reducing turnaround time.[5]

Several studies have demonstrated that AI algorithms can complement urine culture by serving as an effective triage tool. Dedeene et al., showed that AI predictions allowed clinicians to prioritize samples with a high probability of positivity, thereby optimizing laboratory workflows and reducing unnecessary cultures. This approach not only improves efficiency but also has significant cost-saving implications, particularly in high-volume clinical settings.[7] Naik et al., further highlighted that AI-powered urinalysis could identify cases with a high likelihood of negative culture results, allowing clinicians to withhold unnecessary antibiotic therapy and limit antimicrobial resistance. Such stratification demonstrates that AI may function not only as a diagnostic aid but also as a decision-support tool for more targeted patient management.[2]

Comparative analyses have also examined the concordance between AI predictions and culture-confirmed results. De Bruyne et al., found that while AI models rarely misclassified true positives, minor discrepancies arose in cases involving mixed or atypical infections, underscoring the importance of continued validation and integration with confirmatory culture.[4] Similarly, Taylor et al., reported that AI algorithms performed exceptionally well for single-pathogen infections but exhibited slightly lower accuracy for polymicrobial samples.[9] Despite these limitations, the overall concordance with culture results remains high,

suggesting that AI-powered urinalysis can serve as a reliable first-line diagnostic approach, particularly when rapid decision-making is essential.

Beyond diagnostic accuracy, AI-based urinalysis offers significant advantages in speed, scalability, and accessibility. Mobile and point-of-care applications have demonstrated that AI algorithms can deliver near-instant results at the bedside or in outpatient settings, which is particularly valuable in resource-limited environments where culture facilities may be unavailable.[10] Sen et al., also emphasized that combining AI-based urine sediment analysis with automated flow microimaging significantly enhanced pathogen detection while maintaining strong agreement with culture-based methods.[11] Collectively, these studies indicate that AI-powered urinalysis is not intended to replace urine culture entirely but can act as a highly effective adjunct, improving diagnostic workflows, patient outcomes, and antimicrobial stewardship efforts.

Workflow and clinical integration

The integration of AI-powered urinalysis into clinical workflows has shown considerable promise in enhancing efficiency, reducing diagnostic delays, and improving patient management. Traditional urine culture workflows often involve multiple steps, including specimen collection, transportation, incubation, and manual interpretation, which can take 24–72 hours and contribute to bottlenecks in patient care. AI algorithms offer an opportunity to streamline these processes by rapidly analyzing urine samples and predicting culture outcomes, thereby enabling more timely clinical decisions. Naik et al., demonstrated that AI-based predictive models could reduce the time to preliminary diagnosis from days to mere hours, allowing clinicians to initiate empiric therapy or prioritize further testing without waiting for full culture results.[2]

The practical application of AI in clinical settings has been facilitated by automated urine analyzers, smartphone-based urinalysis tools, and integration with electronic health record (EHR) systems. Choi et al., showed that AI-assisted urinalysis, when coupled with automated dipstick readers and sediment analysis, could provide real-time diagnostic insights while maintaining compatibility with existing laboratory information systems.[5] This integration allows for seamless incorporation of AI predictions into routine clinical decision-making, enabling clinicians to rapidly identify patients at risk of urinary tract infections and optimize care pathways. Demirci et al., emphasized that AI-driven platforms not only accelerate analysis but also minimize human error associated with manual microscopy, improving consistency and reproducibility of results.[12]

Point-of-care (POC) applications represent another critical aspect of workflow enhancement. Althowaimer et al., highlighted that AI-enabled POC devices could be deployed in outpatient clinics, emergency departments, and resource-limited settings, offering immediate feedback to healthcare providers.[1] This capability reduces reliance on centralized laboratories, shortens patient wait times, and supports timely antimicrobial stewardship decisions. Additionally, Dedeene et al., reported that AI integration could help laboratories triage specimens more effectively, focusing culture resources on samples most likely to yield positive results and thereby optimizing laboratory throughput and resource allocation.[7]

Despite these advantages, successful clinical integration requires careful consideration of validation, standardization, and staff training. Dai et al., noted that variability in sample preparation, laboratory equipment, and data quality could influence AI performance, underscoring the need for protocol harmonization.[13] Furthermore, clinicians must be trained to interpret AI-generated predictions appropriately, balancing rapid results with confirmatory testing when necessary. Shen et al., emphasized that workflow integration should also address ethical and regulatory concerns, including data privacy, algorithm transparency, and accountability in clinical decision-making.[8]

Overall, the evidence suggests that AI-powered urinalysis can improve workflow efficiency, reduce turnaround times, and enhance patient care when thoughtfully integrated into clinical practice. By complementing existing laboratory processes and supporting rapid decision-making at both central and point-of-care settings, AI has the potential to

Table 1. Comparison of diagnostic characteristics between conventional urine culture and AI-powered urinalysis

Parameter	Conventional urine culture	AI-powered urinalysis	Key insights
Diagnostic turnaround time	24–72 hours to obtain definitive results	Produces preliminary or predictive results within minutes	AI significantly reduces diagnostic delay, enabling earlier treatment initiation.
Pathogen identification	Provides confirmed pathogen identification and antimicrobial susceptibility	Utilizes algorithmic prediction based on image and data analysis	AI models can predict likely pathogens before culture confirmation.
Diagnostic accuracy (sensitivity/specificity)	Considered the reference standard with high accuracy	Comparable accuracy in many studies, improving with larger and diverse datasets	Continued training and validation enhance AI reliability.
Data requirements	Relies on biological culture media and manual processing	Requires large, annotated datasets, digital images, and computational resources	AI depends on data quality and diversity for robust performance.
Interpretability	Results are transparent and easily interpretable by clinicians	May lack interpretability due to algorithmic complexity	Explainable AI is essential to increase clinical trust and adoption.
Cost and Labor	Labor-intensive and resource-demanding with recurring costs	Higher initial setup cost but lower long-term operational costs	AI systems offer long-term efficiency and scalability once implemented.
Clinical Utility	Confirms infection and guides antibiotic therapy	Provides rapid screening and decision support for suspected infections	AI serves as a complementary tool, reducing unnecessary cultures and improving workflow efficiency.

Table 2. Workflow and clinical integration of AI-powered urinalysis compared with conventional diagnostic processes

Workflow component	Conventional urine analysis and culture	Ai-powered urinalysis workflow	Impact on clinical integration
Sample Collection	Manual urine collection and labeling; prone to handling errors	Similar process but can be linked to digital sample tracking systems	Enhanced traceability and reduced labeling errors through automation.
Laboratory Processing	Manual microscopy and culture incubation requiring skilled personnel	Automated imaging and data acquisition using AI-enabled analyzers	Reduces manual workload and laboratory turnaround time.
Data Interpretation	Microbiologist interpretation of microscopic findings and culture results	Algorithm-based interpretation and pattern recognition for pathogen prediction	Provides faster, standardized, and reproducible diagnostic insights.
Reporting and Documentation	Manual entry into laboratory information systems	Seamless integration with electronic health records (EHR) and automated report generation	Streamlines reporting, minimizes transcription errors, and supports real-time updates.
Clinical Decision Support	Dependent on culture confirmation and clinician judgment	AI-generated risk scores and predictive outcomes assist early decision-making	Enables early empirical therapy and supports antimicrobial stewardship.
Quality Control	Periodic manual calibration and review of test performance	Continuous algorithmic self-learning and performance monitoring	Ensures consistent diagnostic quality and adaptive system improvement.
Interdisciplinary Communication	Relies on verbal or written communication between lab and clinicians	Integrated dashboards facilitate real-time collaboration	Improves coordination between laboratory staff and clinicians, expediting care delivery.

transform the diagnostic management of urinary tract infections while maintaining high standards of accuracy and reliability.

Challenges, limitations, and validation requirements

Despite the promising advances of AI-powered urinalysis, multiple challenges and limitations must be addressed before widespread clinical adoption can occur. One major concern is the variability in dataset quality, which can significantly impact algorithm performance. Li et al., highlighted that many studies rely on retrospective datasets that may not fully capture the heterogeneity of patient populations, specimen collection methods, and laboratory conditions.[14] Inconsistent pre-analytical procedures, such as variations in urine collection, storage, and handling, can introduce noise into AI models, potentially reducing predictive accuracy. Similarly, differences in laboratory equipment, including automated analyzers and flow imaging systems, may limit generalizability across institutions.[6]

Another significant challenge is the interpretability of AI algorithms. While machine learning and deep learning models offer high predictive performance, their "black-box" nature can limit clinician trust and acceptance. Naik et al., emphasized that transparent, explainable AI systems are critical to ensure that clinicians can understand the rationale behind predictions and integrate them safely into decision-making.[2] Furthermore, ethical, and regulatory considerations present additional hurdles. Issues related to patient data privacy, algorithm accountability, and adherence to local and international diagnostic standards must be addressed to avoid misuse and ensure patient safety.[1]

Validation requirements represent another key area of focus. Many studies report high diagnostic accuracy under controlled research settings, but real-world implementation may reveal performance gaps. De Bruyne et al., and Shen et al., highlighted the need for prospective, multicenter trials to assess AI algorithms under diverse clinical conditions and patient populations.[4,8] These studies are necessary to evaluate robustness, reproducibility, and reliability before AI can be considered a true adjunct or replacement for urine culture. Additionally, continuous monitoring and periodic recalibration of AI models are essential to maintain accuracy over time, especially as microbial patterns and resistance profiles evolve.

Limitations also extend to specific infection scenarios. Choi et al. and Dedeene et al., observed that AI algorithms perform slightly less effectively in cases involving polymicrobial infections, rare pathogens, or atypical presentations, underscoring that culture remains necessary in complex or ambiguous cases.[5,7] Similarly, AI predictions may be influenced by comorbidities or medications that alter urine composition, highlighting the need for clinical context and judgment alongside algorithmic recommendations. Integration challenges, including interoperability with electronic health records and laboratory information systems, further complicate deployment, requiring robust IT infrastructure and staff training.

In summary, while AI-powered urinalysis demonstrates considerable promise, its adoption is contingent upon addressing key limitations and validation requirements. High-quality, diverse datasets, explainable algorithms, rigorous prospective testing, and careful integration into clinical workflows are essential to ensure that AI can safely and effectively complement or enhance traditional urine culture diagnostics. Addressing these challenges will enable AI to achieve its potential as a transformative tool in urinary tract infection management while maintaining patient safety, diagnostic reliability, and clinical trust.

Future directions in AI-driven in UTI diagnostics

The evolving landscape of AI-powered urinalysis presents numerous opportunities for future development and integration into urinary tract infection (UTI) diagnostics. One key direction is the refinement of AI algorithms to enhance diagnostic accuracy, particularly in complex cases involving polymicrobial infections or atypical pathogens. Shen et al., emphasized the potential of hybrid models that combine multiple AI techniques, including deep learning, machine learning, and ensemble approaches, to improve sensitivity and specificity across diverse patient populations.[8] By leveraging larger, multicenter datasets, AI models can become more robust and generalizable, addressing current limitations in dataset heterogeneity and algorithm performance.[3]

Table 3. Summary of included studies on AI applications in urinalysis for UTI diagnosis

Author (Year)	Study design	AI Technique/model	Data source	Key findings
Althowaimer et al. (2024)	Review	AI-based diagnostic systems	Laboratory diagnostic data	Highlighted AI's role in improving diagnostic accuracy and workflow efficiency
Naik et al. (2024)	Review	Machine learning models	Multi-source clinical data	Emphasized AI in rapid diagnosis and clinical decision support
Goździkiewicz et al. (2022)	Literature review	Machine learning algorithms	Various datasets	Identified benefits and limitations of AI in UTI diagnosis
De Bruyne et al. (2023)	Review	ML and deep learning	Clinical urinalysis datasets	Demonstrated broad applicability of AI in urinalysis
Choi et al. (2024)	Retrospective analysis	AI-integrated predictive modeling	Urine samples with culture results	High accuracy in predicting urine culture outcomes
Dong et al. (2022)	Experimental study	AI with flow microimaging	Suspected UTI patients	High diagnostic performance in rapid urinalysis
Dedeene et al. (2024)	Retrospective study	Neural networks	Clinical urinalysis + demographics	Effective prediction of urine culture results
Shen et al. (2024)	Systematic review and meta-analysis	ML and DL models	Multicenter datasets	Reported high pooled diagnostic accuracy of AI models
Taylor et al. (2018)	Retrospective study	Machine learning models	Emergency department data	Accurate prediction of UTI in clinical settings
Del Ben et al. (2023)	Observational study	Interpretable machine learning	Urine screening datasets	Improved effectiveness of urine culture screening
Şen et al. (2024)	Experimental study	Machine learning algorithms	Clinical datasets	Demonstrated reliable prediction of UTIs using ML
Demirci et al. (2025)	Retrospective cohort	Machine learning models	Urinalysis and hemogram data	Accurate prediction of positive urine cultures
Dai et al. (2024)	Preprint study	Explainable AI models	EHR and laboratory datasets	Enabled classification of UTI risk groups using AI
Li et al. (2021)	Preprint study	Attention-based AI model	Clinical datasets	Demonstrated AI potential in infection risk prediction

Integration with point-of-care (POC) testing represents another promising avenue. Althowaimer et al., highlighted the development of portable, AI-enabled urinalysis devices that provide near-instant results, enabling rapid triage in outpatient clinics, emergency departments, and resource-limited settings.[1] Such devices can facilitate timely clinical decision-making, reduce unnecessary urine cultures, and support antimicrobial stewardship by guiding empiric therapy more precisely. Coupling these devices with telemedicine platforms could further extend access to diagnostic services, particularly in underserved or rural populations.

The incorporation of multi-omics data into AI-driven models is also anticipated to enhance predictive capabilities. Naik et al., suggested that integrating genomic, proteomic, and metabolomic profiles from urine samples could allow AI algorithms to not only detect infections but also predict pathogen resistance patterns and disease severity. This approach could transform UTI management from a reactive to a proactive strategy, enabling personalized treatment plans based on individual patient risk profiles and microbial characteristics.[2]

Another significant future direction involves the standardization and regulatory approval of AI-assisted urinalysis platforms. De Bruyne et al., stressed the importance of developing universally accepted performance benchmarks, validation protocols, and reporting guidelines to ensure safety, reliability, and interoperability across different healthcare systems.[4] Continuous post-market surveillance and algorithm recalibration will be essential to maintain performance in real-world clinical environments, particularly as microbial patterns evolve over time.

Ethical and educational considerations will also shape the future of AI in UTI diagnostics. Clinicians must be trained to interpret AI-generated results effectively, balancing algorithmic predictions with clinical judgment.[7] Transparent and explainable AI systems will be critical to building trust among healthcare providers and patients alike, ensuring that technology complements rather than replaces human expertise. Choi et al., further emphasized the importance of integrating AI within broader diagnostic workflows, creating a synergistic approach that combines rapid AI-driven assessments with confirmatory urine cultures where necessary.[5]

Overall, the future of AI-driven UTI diagnostics lies in the convergence of advanced algorithms, point-of-care accessibility, multi-omics integration, regulatory standardization, and ethical implementation. By addressing current limitations and embracing these innovations, AI has the potential to transform UTI management, offering faster, more accurate, and personalized diagnostic solutions while maintaining high standards of patient safety and clinical reliability.

DISCUSSION

AI algorithms and computation techniques for urinalysis

The proliferation of AI algorithms and computational techniques in urinalysis demonstrates the field's rapid evolution toward precision diagnostics. Machine learning and deep learning models have shown strong capability in pattern recognition and predictive analytics, with ensemble and hybrid approaches further enhancing accuracy. The diversity of algorithms allows for tailored solutions for different laboratory setups and patient populations. How-

ever, performance variability due to dataset size, quality, and heterogeneity underscores the need for standardized training datasets and robust validation frameworks. Optimizing these algorithms will be critical for translating technical capability into consistent clinical outcomes.

Diagnostic performance metrics

AI-powered urinalysis has demonstrated high diagnostic performance across sensitivity, specificity, and predictive values, often approaching or surpassing conventional urine culture benchmarks. These metrics indicate potential for early detection and rapid clinical decision-making. However, variations in algorithm design, microbial complexity, and pre-analytical factors can influence performance, highlighting the importance of rigorous prospective validation. While impressive, these metrics alone are insufficient; clinical context and interpretability remain crucial for safe implementation.

Comparative effectiveness versus urine culture

Comparisons between AI-based urinalysis and traditional culture methods reveal promising concordance, particularly for common uropathogens. AI demonstrates potential to reduce reliance on time-consuming cultures, allowing earlier clinical intervention. Nevertheless, culture remains indispensable for complex or polymicrobial infections, antimicrobial susceptibility testing, and confirmatory diagnosis. Integrating AI as a complementary tool rather than a replacement may offer the most pragmatic path forward while maintaining diagnostic reliability.

Workflow and clinical integration

The integration of AI into laboratory and point-of-care workflows enhances efficiency and reduces turnaround times, potentially improving patient outcomes. Automated analyzers and EHR integration allow real-time clinical decision support, facilitating triage and antimicrobial stewardship. Despite these advantages, successful adoption requires careful attention to staff training, interoperability, and system validation. Workflow improvements alone are insufficient unless coupled with consistent quality assurance and clinician engagement.

Challenges, limitations, and validation requirements

Despite technological advancements, several challenges limit the clinical deployment of AI urinalysis. Dataset heterogeneity, algorithm interpretability, and variability in pre-analytical factors can reduce reliability. Ethical, regulatory, and infrastructural considerations further complicate adoption. Rigorous prospective validation, multicenter studies, and continuous recalibration are essential to ensure reproducibility and patient safety. Addressing these barriers is pivotal for AI to achieve its full potential.

Future directions in AI-driven UTI diagnostics

The future of AI in UTI diagnostics lies in hybrid algorithm development, integration with point-of-care devices, multi-omics incorporation, and regulatory standardization. Transparent and explainable AI, combined with clinician education, will be essential for trust and adoption. Emerging technologies could transform management from reactive to proactive, personalized interventions, while complementing traditional culture methods. By addressing current limitations and leveraging innovation, AI promises to redefine the diagnostic landscape of urinary tract infections.

CONCLUSION

Artificial intelligence has demonstrated significant potential to transform urinalysis and the diagnosis of urinary tract infections. Advances in machine learning, deep learning, and hybrid computational approaches have improved the accuracy and speed of detecting pathogens in urine samples, offering an alternative or complementary tool to traditional culture methods. These technologies provide rapid results, support early clinical decision-making, and hold promise for integration into point-of-care settings, which could enhance patient outcomes and optimize healthcare workflows.

Despite these promising developments, several challenges remain. Variability in dataset quality, algorithm interpretability, and pre-analytical factors can limit the reliability of AI-powered urinalysis. Ethical considerations, regulatory requirements, and the need for standardized validation protocols are crucial to ensure safe and consistent implementation across diverse clinical settings. Additionally, while AI can enhance diagnostic efficiency, conventional urine culture remains indispensable for complex infections, antimicrobial susceptibility testing, and confirmatory diagnoses. Therefore, AI is most effectively applied as a complementary tool rather than a full replacement of traditional methods.

Looking ahead, the future of AI-driven UTI diagnostics is likely to involve the integration of multi-omics data, advanced hybrid algorithms, and portable point-of-care devices. Transparent and explainable AI, coupled with clinician training, will be essential to foster trust and maximize clinical utility. By addressing current limitations and embracing innovative approaches, AI has the potential to redefine UTI management, providing faster, more accurate, and personalized diagnostics while maintaining patient safety and clinical reliability. The incorporation of AI into routine urinalysis represents a significant step toward a more precise and efficient future in UTI diagnosis.

ACKNOWLEDGMENTS

The author acknowledges the use of artificial intelligence–assisted tools, specifically *ChatGPT (GPT-5.3, OpenAI)*, in the preparation of this manuscript for purposes of language refinement, organization of content, and overall clarity. The application of these tools was limited to editorial support, and all scholarly interpretations, analyses, and conclusions presented in this paper remain the sole responsibility of the author.

STATEMENT OF AUTHORSHIP

All authors certified fulfillment of ICMJE authorship criteria.

AUTHOR DISCLOSURE

No conflicts of interest were declared by the author.

DATA AVAILABILITY STATEMENT

Datasets generated are included in the published article.

FUNDING SOURCE

None.

REFERENCES

1. Althowaimer MA, et al. Urinary tract infections (UTIs): laboratory diagnosis—the role of artificial intelligence and smart diagnosis. Int J Health Sci. 2024;8(S1): 1484-93. DOI: 10.53730/ijhs.v8nS1.15294
2. Naik N, Talyshinskii A, Shetty DK, et al. Smart diagnosis of urinary tract infections: is artificial intelligence the fast-lane solution? Curr Urol Rep. 2024;25(1):37-47. PMID: 38112900 PMCID: PMC10787904 DOI: 10.1007/s11934-023-01192-3
3. Goździkiewicz N, Zwolińska D, Polak-Jonkisz D. The use of artificial intelligence algorithms in the diagnosis of urinary tract infections—a literature review. J Clin Med. 2022;11(10):2734. PMID: 35628861 PMCID: PMC9146683 DOI: 10.3390/jcm11102734
4. De Bruyne S, De Kesel P, Oyaert M. Applications of artificial intelligence in urinalysis: is the future already here? Clin Chem. 2023;69(12):1348-60. PMID: 37708293 DOI: 10.1093/clinchem/hvad136
5. Choi MH, Kim D, Bae HG, et al. Predictive performance of urinalysis for urine culture results according to causative microorganisms: an integrated analysis with artificial intelligence. J Clin Microbiol. 2024;62(10):e01175-24. PMID: 39264202 PMCID: PMC11481504 DOI: 10.1128/jcm.01175-24
6. Dong F, Yao Y, Chen Y, Guo Y, Jing C, Wu J. Diagnostic performance of urine analysis based on flow microimaging and artificial intelligence recognition technology in suspected urinary tract infection patients. Scand J Clin Lab Invest. 2022;82(5):385-90. PMID: 35852133 DOI: 10.1080/00365513.2022.2100273
7. Dedeene L, Van Elslande J, Dewitte J, Martens G, De Laere E, De Jaeger P, De Smet D. An artificial intelligence-driven support tool for prediction of urine culture test results. Clin Chim Acta. 2024;562:119854. PMID: 38977169 DOI: 10.1016/j.cca.2024.119854
8. Shen L, An J, Wang N, Wu J, Yao J, Gao Y. Artificial intelligence and machine learning applications in urinary tract infections identification and prediction: a systematic review and meta-analysis. World J Urol. 2024;42(1):464. PMID: 39088072 DOI: 10.1007/s00345-024-05145-4
9. Taylor RA, Moore CL, Cheung KH, Brandt C. Predicting urinary tract infections in the emergency department with machine learning. PLoS One. 2018;13(3):e0194085. PMID: 29513742 PMCID: PMC5841824 DOI: 10.1371/journal.pone.0194085
10. Del Ben F, Da Col G, Cobârzan D, et al. A fully interpretable machine learning model for increasing the effectiveness of urine culture screening. Am J Clin Pathol. 2023;160(6):620-31. PMID: 37658807 PMCID: PMC10691191 DOI: 10.1093/ajcp/aqad099
11. Farashi S, Momtaz HE. Prediction of urinary tract infection using machine learning methods: a study for finding the most-informative variables. BMC Med Inform Decis Mak. 2025;13:47. DOI:10.1186/s12911-024-02819-2
12. Demirci F, Arıkan Y, Akbulut İ, Topçu Dİ. Machine learning-assisted prediction of positive urine cultures using urinalysis and hemogram data: a retrospective cohort study. Int J Med Biochem. 2025;8(3):222-32. DOI: 10.3390/ijmb.2025.222
13. Dai Y, Sullivan B, Montout A, et al. Explainable AI for classifying UTI risk groups using a real-world linked EHR and pathology lab dataset. Preprint. arXiv. 2024. DOI: 10.48550/arXiv.2411.17645
14. Li H, Rezvani R, Kolanko MA, Sharp DJ, Wairagkar M, Vaidyanathan R, Barnaghi P. An attention model to analyse the risk of agitation and urinary tract infections in people with dementia. Preprint. arXiv. 2021. DOI: 10.48550/arXiv.2101.07007

OPEN ACCESS – CASE REPORT

Angiomyolipoma with Epithelial Cysts: A Case Report and Review of Literature

Pia Nenita Duque, Jeffrey So, Jose Gabriel Gonzales, Josefino Castillo, Joseph Vincent Songco

Institute of Pathology, St. Luke's Medical Center, Quezon City, Philippines

ABSTRACT

Angiomyolipoma with epithelial cysts (AMLEC) is a rare subtype of angiomyolipoma that may closely mimic both malignant and benign neoplasms. We report a case of AMLEC in an 18-year-old female presenting with acute flank pain and radiologic suspicion for malignancy. This case highlights the diagnostic challenges posed by AMLEC, emphasizes its characteristic histopathologic and immunohistochemical features, and reviews current concepts regarding its pathogenesis. This case represents the first documented case of AMLEC in the Philippines.

Key words: angiomyolipoma, angiomyolipoma with epithelial cysts, kidney neoplasms, histopathology, immunohistochemistry, case report

ISSN 2507-8364 (Online)
Printed in the Philippines.

Received: 17 March 2026.
Accepted: 5 April 2026.
Published online first: 11 June 2026.
https://doi.org/10.21141/PJP.2026.613

Corresponding author: Pia Nenita A. Duque, MD
E-mail: piaduque04@gmail.com
ORCiD: https://orcid.org/0000-0002-4407-2108

INTRODUCTION

Angiomyolipoma with epithelial cysts (AMLEC) is recognized as a rare subtype of renal angiomyolipoma (AML) by the World Health Organization (WHO) Classification of Tumors.[1] Unlike classic AML, AMLEC is characterized by a complex admixture of solid and cystic components, a feature that may pose a diagnostic challenge due to its ability to closely mimic both benign and malignant renal neoplasms on imaging and histopathologic examination. Since its initial description in 2006,[2,3] only a limited number of cases have been reported in the literature, and its pathogenesis remains incompletely understood. This case report aims to describe the clinicopathologic features of AMLEC, highlight the diagnostic utility of immunohistochemistry in distinguishing it from its benign and malignant mimics, and discuss current theories regarding its pathogenesis. To the authors' knowledge, this represents the first reported case of AMLEC in the Philippines, and one of the youngest patients described in literature.

CASE

We present the case of a previously healthy 18-year-old female who was brought to the emergency department due to sudden onset left flank pain. Patient had no comorbid diseases, and no family history of tuberous sclerosis complex. Magnetic resonance imaging (MRI) revealed a heterogeneous mass in the anterior interpolar to inferior pole of the left kidney with an exophytic component measuring 3.9 x 4.3 x 3.6 cm (Figure 1). Also noted was a heterogeneous fluid collection representing hyperacute to acute subcapsular renal hemorrhage. The primary radiologic consideration at this time was a renal cell carcinoma associated with hemorrhage secondary to spontaneous rupture. The patient subsequently underwent left open radical nephrectomy. On gross examination, there was note of a cream tan to brown, firm to rubbery solid mass with irregular contour measuring 4 x 3.5 x 2.5 cm in single widest dimension, located predominantly within the perinephric fat of the middle to inferior pole of the kidney, with involvement of the renal cortex on sectioning.

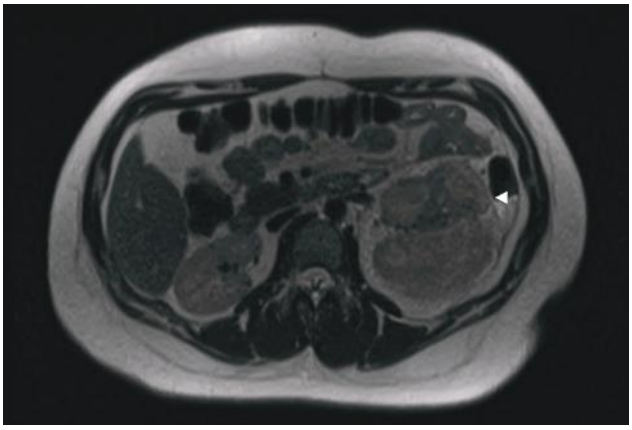

Figure 1. MRI of the upper abdomen showing a heterogeneous mass in the left kidney *(arrowhead)*.

Microsections of the mass disclosed plump spindle cells arranged in solid sheets, associated with thick-walled, dysmorphic blood vessels, and focal areas of mature adipose tissue, morphologically consistent with classic AML. Interspersed between these areas were multiple varisized cysts lined by bland-appearing cuboidal to columnar cells, with some exhibiting hobnailed appearance. These cystic structures were embedded in a cellular, cambium-like stroma composed of small, compact round to spindle cells with scant cytoplasm, associated with lymphocytic infiltrates (Figure 2).

Immunohistochemical studies (Table 1) were performed for a more definite diagnosis and to rule out benign and malignant differentials. The solid, spindled areas showed positive, patchy expression for melanocytic markers human melanoma black (HMB45) and Melan A, while smooth muscle actin (SMA) showed diffused positivity, consistent with a smooth muscle-predominant AML (Figure 3). The cambium-like stroma exhibited positive staining for melanocytic markers, with particularly strong staining for HMB45 relative to the smooth muscle-predominant area (Figure 4A). In addition, the cambium-like layer strongly expressed estrogen receptor (ER), progesterone receptor (PR), and cluster of differentiation 10 (CD10) (Figure 4B to 4D). The cyst-lining cells stained positive for cytokeratin, demonstrating their epithelial origin (Figure 5A). Additionally, these cells showed positive staining for paired box 8 transcription factor (PAX8) (Figure 5B) and negative staining for melanocytic markers, ER, and PR (Figure 4A to 4C). Based on these findings, a diagnosis of AMLEC was rendered.

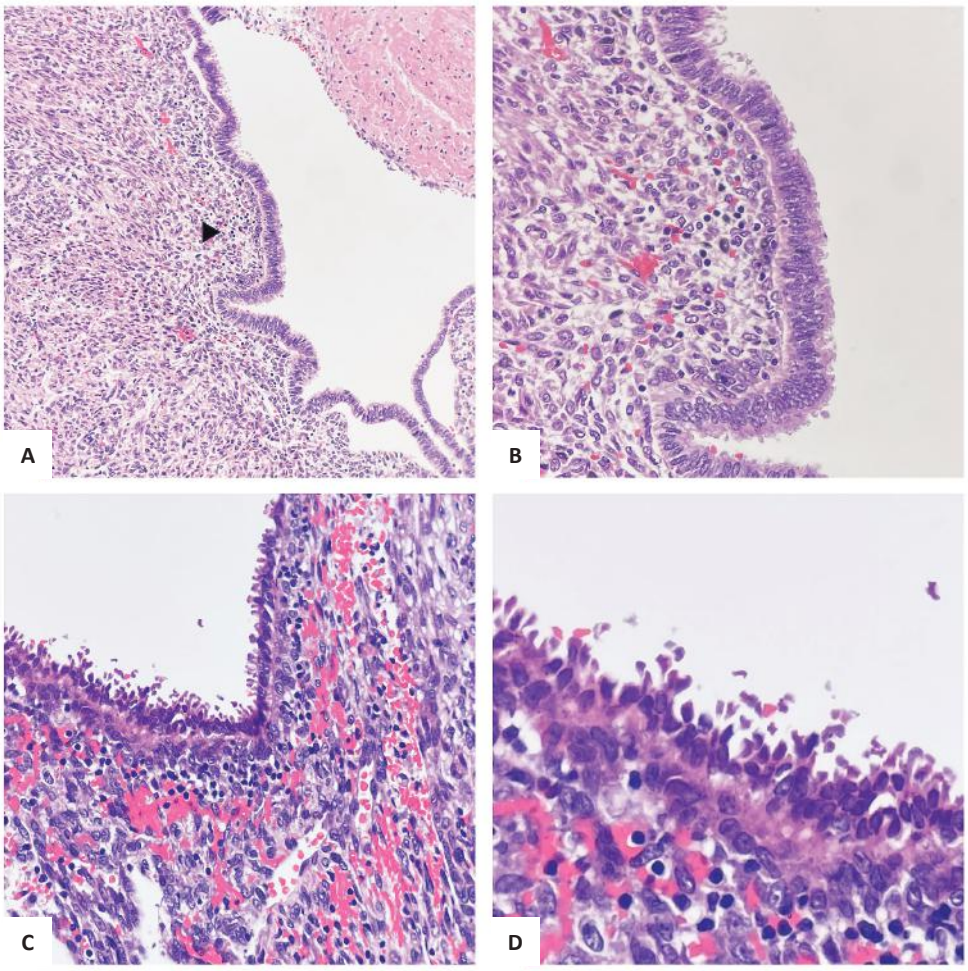

Figure 2. Cysts lined by columnar to cuboidal cells embedded in a cambium-like stroma *(arrowhead)* **(A)** H&E, 100x **(B)** H&E, 200x. Cyst-lining cells exhibiting hobnailed appearance **(C)** H&E, 200x **(D)** H&E, 400x.

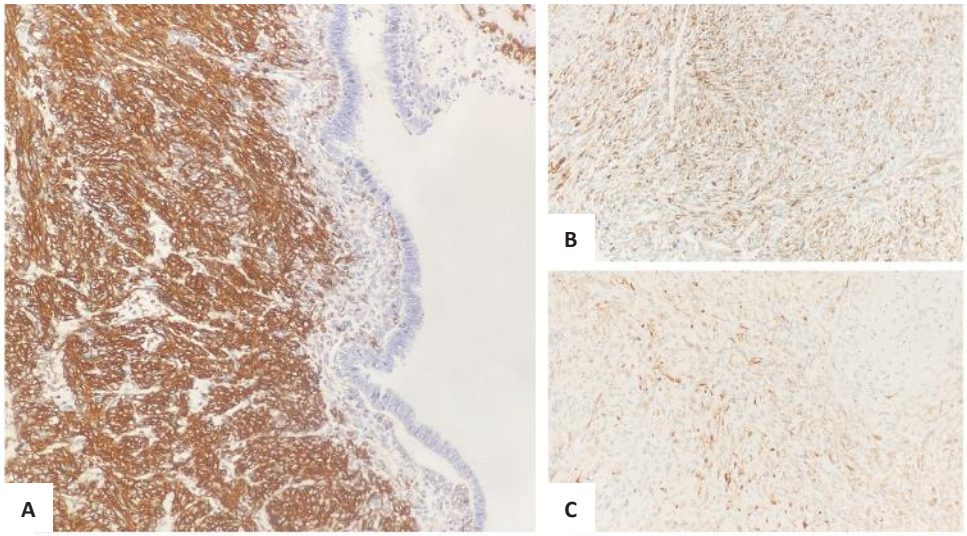

Figure 3. Spindle cell component of tumor with positive staining for **(A)** SMA, 200x, **(B)** HMB45, 200x, and **(C)** Melan A, 200x, with note of negative expression of SMA in the subepithelial stroma **(A)**.

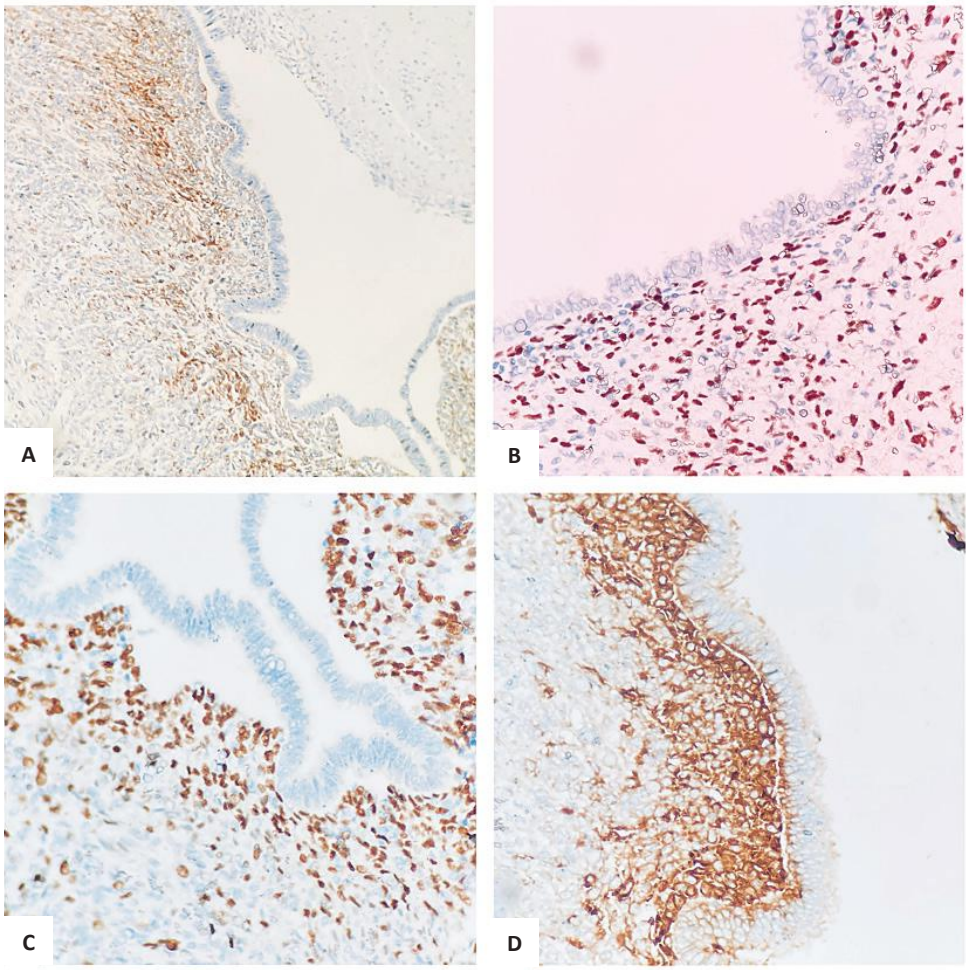

Figure 4. Cambium-like subepithelial stroma with positive staining for **(A)** HMB45, 200x, **(B)** ER, 200x, **(C)** PR, 200x, **(D)** CD10, 200x, and negative staining in cyst-lining cells.

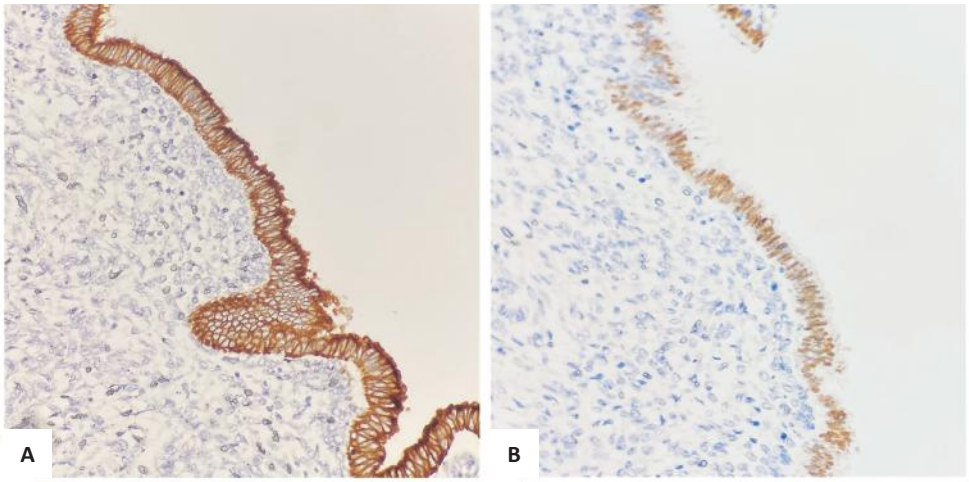

Figure 5. Cyst-lining cells showing positive staining for **(A)** CK, 200x and **(B)** PAX8, 200x.

Table 1. Summary of immunohistochemical stain results

Immunohistochemical Stain	Spindle cell-predominant area	Cyst-lining cells	Cambium-like stroma
CK	Negative	Positive	Negative
PAX8	Negative	Positive	Negative
SMA	Positive, strong, diffuse	Negative	Negative
HMB45	Positive	Negative	Positive, strong
Melan A	Positive	Negative	Positive
ER	Negative	Negative	Positive
PR	Negative	Negative	Positive
CD10	Negative	Positive, weak, focal	Positive

CD10, cluster of differentiation 10; CK, cytokeratin; ER, estrogen receptor; HMB45, human melanoma black; PAX8, paired box 8 transcription factor; PR, progesterone receptor; SMA, smooth muscle actin

Table 2. Comparison of clinical and demographic features of present and previously reported cases

Feature	Previously reported cases[2-3,5-18] (36 patients)	Present case
Age (years)	17-76 (Median 41.5)	18
Sex	Female predominance (67%)	Female
Clinical presentation	Incidental findings (52%) Others: Flank pain, hematuria, dysuria	Flank pain
Laterality	Unilateral (Right = Left) Bilateral in one case[3]	Left
Size (cm.)	1.3-11 (Median 3)	4
Tuberous sclerosis complex	Three cases: 17/Male[5], 37/Female[3], 46/Female[6]	No personal or family history
Outcome	Alive with no disease recurrence	Alive with no evidence of disease at most recent follow-up

Following surgery, the patient had an unremarkable postoperative course and was discharged stable. At the most recent follow-up, patient was clinically well with no evidence of disease.

DISCUSSION

AMLEC is a rare subtype of renal AML exhibiting cystic and solid architecture, in which epithelial-lined cysts surrounded by a cambium-like stromal layer are admixed with a predominantly smooth muscle-rich angiomyolipomatous component.[1-4] The characteristic histopathologic features of this entity were first described in 2006 by Davis et al.,[2] in a series of 11 cases, while in the same year, Fine et al.,[3] formally designated the lesion as angiomyolipoma with epithelial cysts, or AMLEC.

Based on a review of published literature[2,3,5-18] (Table 2), fewer than 40 histopathologically well-documented cases of AMLEC have been reported, with additional isolated cases described in clinically or radiologically focused publications. Reported cases of AMLEC span a wide age range, from 17 to 76 years, with a median age of 41.5 years among the cases reviewed. A female predominance was observed, and tumors most commonly arose unilaterally, with no clear predilection for the right or left kidney. One case demonstrated bilaterality;[3] however, histopathologic confirmation was done for only one kidney. Tuberous sclerosis complex was identified in only three patients,[3,5,6] diagnosed at 17, 37, and 46 years of age, with all tumors occurring unilaterally. Notably, one patient with tuberous sclerosis complex was found to have an associated eosinophilic solid and cystic renal cell carcinoma and epithelioid AML in the same kidney.[6] Consistent with

literature, our patient is female with a unilateral tumor; however, at 18 years of age, she represents one of the youngest reported cases, and the youngest case with no personal or family history of tuberous sclerosis complex. AMLEC has most commonly been reported as an asymptomatic incidental finding on imaging performed during routine medical examinations or evaluation for unrelated conditions,[2-4] in contrast to our patient who presented with sudden onset flank pain. When symptomatic, presenting features have included flank pain,[2,3,7,8] hematuria,[2,3,9] dysuria,[3,7] and less commonly, groin pain,[3] chronic renal insufficiency,[3] and acute abdomen from retroperitoneal hemorrhage.[2] Radiologically, AMLEC typically appears as a solid or complex cystic mass,[4] as opposed to most classic AMLs which exhibit high fat content on ultrasonography and computed tomography.[1] Owing to its nonspecific imaging characteristics, AMLEC has been reported to mimic renal cell carcinoma,[3,7,10-13] resulting in radical surgical management. In the present case, although renal cell carcinoma was similarly the primary clinical and radiologic consideration, the presence of acute subcapsular hemorrhage was a factor that influenced the decision to proceed with radical surgical intervention in the context of tumor-associated bleeding. Following resection, AMLEC was grossly described in literature as a well-circumscribed, yellow to gray, solid to cystic mass, with sizes ranging from 1.3 cm. to 11 cm,[2,3,5-18] the largest of which was reported by Varshney et al.[7] In this patient, the tumor was predominantly solid on gross examination, and fell within the reported size range.

Microscopically, AMLEC is characterized by three distinct features, namely, a smooth muscle-predominant angiomyolipomatous component, epithelial-lined cysts, and a compact, subepithelial cambium-like stromal layer.[1-3]

The smooth-muscle predominant AML accounts for the solid areas of the tumor, and is composed of sheets or fascicles of plump spindle cells arising from thick-walled vessels, and scant to absent adipose tissue.[2-4] These typically stain positive for SMA and the melanocytic markers HMB45 and Melan A, consistent with the immunohistochemical profile of a smooth muscle-predominant AML.[2-4]

The subepithelial layer immediately beneath the epithelial-lined cysts is composed of small, compact spindle cells with scant cytoplasm, forming a cambium-like pattern that is sharply demarcated from the surrounding smooth muscle component.[2-4] Immunohistochemically, this cambium-like stromal layer shows strong expression of melanocytic markers, compared to the adjacent smooth muscle stroma where staining is less intense. It also typically expresses ER, PR, and CD10. Together with its morphologic resemblance to endometrial stroma and distinct immunoprofile, this stromal component has been interpreted as exhibiting features of both Müllerian and melanocytic differentiation.[3,4,10] In the literature, Müllerian differentiation in renal neoplasms has been attributed to the shared embryologic origin of the urinary and genital systems from the urogenital ridge, resulting in overlapping epithelial and mesenchymal differentiation between the two systems.[3-4,10] This cambium-like layer is considered a defining feature of AMLEC that distinguishes it from other cystic renal neoplasms.[2-4]

The epithelial cysts are described as variably sized and lined by bland-appearing cuboidal to columnar cells with eosinophilic to clear cytoplasm.[2-4] Some exhibit hobnail morphology, with nuclei protruding into the cystic lumen.[2-4] These cyst-lining cells typically stain positive for pancytokeratins, thereby supporting their epithelial nature, and are negative for melanocytic markers, as well as ER, PR, and CD10.[2-4] The origin of these epithelial cells, however, is a subject of contention, with two possible theories discussed in literature. One was proposed by Fine et al.,[3] who theorized that the cysts come from dilated entrapped native tubules because of their morphologic resemblance to collecting duct epithelium. Obstruction of these tubules by the AML is said to result in dilatation and cyst formation.[3] This mechanism is favored by a number of subsequent case reports.[13,14] Notably, a study by Karafin et al.,[5] further supported this theory by demonstrating similar PAX2 and PAX8 positivity between epithelial cysts of AMLEC and renal tubules of benign kidney tissue. In contrast, Davis et al.,[2] argued against entrapment of renal tubules as the origin, stressing that entrapped tubules are typically confined to the periphery of AMLs, which they did not observe in their case series. They further noted the presence of epithelial cysts located completely outside the kidney, which is incompatible with entrapment of native renal parenchyma.[2] On the basis of these observations, Mikami et al.,[9] speculated that the epithelial cysts may represent a component of the neoplastic process. In support of this, Filho et al.,[15] demonstrated expression of melanocytic markers in the epithelial lining of the cysts, suggesting neoplastic differentiation from AML. However, this finding is documented only in a single case and has not been reproduced in other published reports. Several authors have acknowledged that either mechanism may be possible.[7,10,16,17] More recently, Li et al.,[13] made use of the immunohistochemical stains glycoprotein non-metastatic melanoma protein B (GPNMB) and tuberous sclerosis 2 (TSC2) to demonstrate aberrant expression in the stromal component of AMLEC cases, while a normal immunoprofile was observed in the epithelial cysts and adjacent renal parenchyma, suggesting that these cysts represent entrapped tubules. In the present case, positive expression for PAX8 and lack of expression for melanocytic markers of the epithelial lining is more in keeping with renal tubular derivation, though conclusions regarding cyst origin cannot be definitively drawn.

Due to its complex histomorphology, AMLEC may be confused with a variety of benign and malignant renal tumors. Renal cell carcinoma is the most commonly cited malignant mimic of AMLEC in published cases, both radiologically and histopathologically.[3,7,10-13,18] In particular, clear cell renal cell carcinoma with cystic architecture in which neoplastic cells line cystic spaces, may closely resemble AMLEC, which has also been shown to exhibit clear cell change within the epithelial lining.[3-4,9] In the present case, a renal cell carcinoma with a sarcomatoid component was also considered due to the presence of a prominent spindle cell stroma. Another malignant entity entertained in the differential diagnosis of this case is synovial sarcoma. Similar to AMLEC, biphasic synovial sarcoma is composed of both spindle cell and epithelial components, with the latter forming glandular spaces lined by cuboidal to columnar cells.[19] Among the benign

mimics, mixed epithelial and stromal tumor (MEST) is regarded as one of the prime differentials owing to its substantial morphologic overlaps with AMLEC.[19] Like AMLEC, MEST exhibits a biphasic architecture composed of epithelial cysts lined by cuboidal or hobnail-shaped cells embedded in a spindle cell stroma that also expresses ER, PR, and CD10.[1] By immunohistochemistry, positivity for HMB45 and Melan A in the subepithelial cambium-like layer and spindle cell component can reliably distinguish AMLEC from its benign and malignant mimics, which lack melanocytic expression.[4]

Recent case reports have identified alterations in TSC1 and TSC2 in sporadic cases of AMLEC. Song et al.,[8] reported a case with a TSC2 nonsense mutation, while Xu et al.,[18] described a fat-poor AMLEC harboring a TSC1 splice-site mutation. In addition to lending support to the discussion on the origin of epithelial cysts, GPNMB and TSC2 immunostains were utilized by Li et al.,[13] to demonstrate underlying TSC2 pathway alterations in a number of AMLEC cases.

AMLEC is considered a benign renal neoplasm, and to date, there have been no reported cases of recurrence, metastasis, or malignant transformation. Most patients described in the literature underwent surgery in the form of partial or radical nephrectomy, commonly because of preoperative radiologic suspicion for renal cell carcinoma.[2-4] When follow-up information is available, reported outcomes have been favorable, with patients remaining alive and without evidence of disease following resection.[3,4,6-10,16-18]

CONCLUSION

Angiomyolipoma with epithelial cysts is a rare renal neoplasm with a limited number of reported cases in the literature. Owing to its tendency to mimic malignancy on imaging and its close morphologic overlap with several benign and malignant renal tumors, AMLEC should be considered in the differential diagnosis of solid to cystic renal neoplasms. Careful histopathologic evaluation, supplemented by immunohistochemistry, is essential for accurate diagnosis.

ACKNOWLEDGMENTS

The authors acknowledge Dr. Rodelio D. Lim, Chairman of the Institute of Pathology at St. Luke's Medical Center-Quezon City for his support and guidance. ChatGPT (OpenAI) was used for proofreading assistance, minor sentence restructuring, and reference list organization. The authors have duly overseen, reviewed, edited, and finalized the content.

ETHICAL CONSIDERATIONS

All efforts to secure patient's consent have been exhausted. The patient's anonymity is ensured. No other identifiers were included.

STATEMENT OF AUTHORSHIP

All authors certified fulfillment of ICMJE authorship criteria.

AUTHOR DISCLOSURE

The authors declared no conflict of interest.

DATA AVAILABILITY STATEMENT

No datasets were generated or analyzed for this study.

FUNDING SOURCE

None.

REFERENCES

1. WHO Classification of Tumours Editorial Board. WHO Classification of tumours of the urinary system and male genital organs, 5th ed. Lyon: International Agency for Research on Cancer; 2022.
2. Davis CJ, Barton JH, Sesterhenn IA. Cystic angiomyolipoma of the kidney: a clinicopathologic description of 11 cases. Mod Pathol. 2006;19(5):669-74. PMID: 16528375 DOI: 10.1038/modpathol.3800572
3. Fine SW, Reuter VE, Epstein JI, Argani P. Angiomyolipoma with epithelial cysts (AMLEC): a distinct cystic variant of angiomyolipoma. Am J Surg Pathol. 2006;30(5):593-9. PMID: 16699313 DOI: 10.1097/01.pas.0000194298.19839.b4
4. LeRoy MA, Rao P. Angiomyolipoma with epithelial cysts. Arch Pathol Lab Med. 2016;140(6):594-7. PMID: 27232352 DOI: 10.5858/arpa.2015-0170-RS
5. Karafin M, Parwani AV, Netto GJ, et al. Diffuse expression of PAX2 and PAX8 in the cystic epithelium of mixed epithelial stromal tumor, angiomyolipoma with epithelial cysts, and primary renal synovial sarcoma: evidence supporting renal tubular differentiation. Am J Surg Pathol. 2011;35(9):1264-73. PMID: 21836481 DOI: 10.1097/PAS.0b013e31822539a1
6. Cho WC, Collins K, Mnayer L, Cartun RW, Earle JS. Concurrent eosinophilic solid and cystic renal cell carcinoma and angiomyolipoma with epithelial cysts in the setting of tuberous sclerosis complex. Int J Surg Pathol. 2019;27(7):804-11. PMID: 31142207 DOI: 10.1177/1066896919849679
7. Varshney B, Vishwajeet V, Madduri V, Chaudhary GR, Elhence PA. Renal angiomyolipoma with epithelial cyst. Autops Case Rep. 2021;11:e2021308. PMID: 34458176 PMCID: PMC8387069 DOI: 10.4322/acr.2021.308
8. Song H, Mao G, Jiao N, et al. TSC2 nonsense mutation in angiomyolipoma with epithelial cysts: a case report and literature review. Front Oncol. 2024;14:1274953. PMID: 38590655 PMCID: PMC10999537 DOI: 10.3389/fonc.2024.1274953
9. Mikami S, Oya M, Mukai M. Angiomyolipoma with epithelial cysts of the kidney in a man. Pathol Int. 2008;58(10):664-7. PMID: 18801088 DOI: 10.1111/j.1440-1827.2008.02287.x
10. Armah HB, Yin M, Rao UN, Parwani AV. Angiomyolipoma with epithelial cysts (AMLEC): a rare but distinct variant of angiomyolipoma. Diagn Pathol. 2007;2:11. PMID: 17376246 PMCID: PMC1845137 DOI: 10.1186/1746-1596-2-11

11. Rosenkrantz AB, Hecht EM, Taneja SS, Melamed J. Angiomyolipoma with epithelial cysts: mimic of renal cell carcinoma. Clin Imaging. 2010;34(1):65-8. PMID: 20122523 DOI: 10.1016/j.clinimag.2009.04.026
12. Wood A, Young F, O'Donnell M. Angiomyolipoma with epithelial cysts masquerading as a cystic renal cell carcinoma. Curr Urol. 2017;9(4):209-11. PMID: 28413382 PMCID: PMC5385450 DOI: 10.1159/000447142
13. Li H, Dairo O, Lotan T, Argani P, Matoso A. Examination of the histogenesis of epithelial cysts in angiomyolipoma with epithelial cysts using GPNMB and TSC2 immunostains. Hum Pathol. 2025;157:105764. PMID: 40180055 DOI: 10.1016/j.humpath.2025.105764
14. Tajima S, Yamada Y. Cysts in angiomyolipoma with epithelial cysts may consist of entrapped and dilated renal tubules. Int J Clin Exp Pathol. 2015;8(9):11729-34. PMID: 26617918 PMCID: PMC4637734
15. Filho JDE, Meneses de Amorim D, Sweet GM, Rodrigues de Freitas LA, Athanazio PR, Athanazio DA. Renal epithelioid angiomyolipoma with epithelial cysts: demonstration of Melan A and HMB45 positivity in the cystic epithelial lining. Ann Diagn Pathol. 2012;16(5):397-401. PMID: 21676635 DOI: 10.1016/j.anndiagpath.2011.03.004
16. Wei J, Li Y, Wen Y, Li L, Zhang R. Renal angiomyolipoma with epithelial cysts: a rare entity and review of the literature. Int J Clin Exp Pathol. 2015;8(9):11760-5. PMID: 26617923 PMCID: PMC4637739
17. Mtshali NZ, Shandu N, Mukendi AM. Angiomyolipoma with epithelial cysts: an unexpected discovery in a gunshot abdomen. Afr J Urol. 2023;29:8. DOI:10.1186/s12301-023-00340-y
18. Xu Q, Yin L, Tao J, Peng F. TSC1 splicing mutation in renal angiomyolipoma with epithelial cysts without fat: a very rare case report and literature review. Heliyon. 2024;10(14):e34191. PMID: 39100442 PMCID: PMC11295956 DOI: 10.1016/j.heliyon.2024.e34191
19. WHO Classification of Tumours Editorial Board. WHO classification of tumours of soft tissue and bone, 5th ed. Lyon: International Agency for Research on Cancer; 2020.

OPEN ACCESS – CASE REPORT

Monomorphic Epitheliotropic Intestinal T-cell Lymphoma with Alveolar and Maxillary Metastases: A Case Report

Clarisse Anne Nuqui,[1] Waldemar Siy,[1] Karen Damian[2]

[1]*Department of Laboratories, University of the Philippines – Philippine General Hospital*
[2]*Department of Pathology, University of the Philippines Manila College of Medicine*

ABSTRACT

This is a case of monomorphic epitheliotropic intestinal T cell lymphoma presenting as ruptured viscous in a 64-year-old male. Monotonous cells were seen to infiltrate the full thickness of the bowel with immunoreactivity for CD3, CD8, CD56, CD68 and Granzyme B. The patient subsequently presented with maxillary and alveolar mass with similar immunohistomorphologic findings, suggesting metastasis. This rare disease has poor prognosis thus further reports should be conducted to profile this type of tumor.

Key words: monomorphic epitheliotropic intestinal T-cell lymphoma; intestinal perforation; enteropathy-associated T-cell lymphoma type II; case report

ISSN 2507-8364 (Online)
Printed in the Philippines.

Received: 10 February 2026.
Accepted: 9 April 2026.
Published online first: 11 June 2026.
https://doi.org/10.21141/PJP.2026.483

Corresponding author: Clarisse Anne D. Nuqui, MD
E-mail: cdnuqui@up.edu.ph
ORCiD: https://orcid.org/0009-0006-1129-6849

INTRODUCTION

Monomorphic epitheliotropic intestinal T-cell lymphoma (MEITL) is a rare and aggressive type of tumor derived from intraepithelial T lymphocytes. This entity was previously grouped under Type II Enteropathy associated T-cell lymphoma but was re-classified as a distinct entity due to its lack of association with celiac disease.[1] The disease has a worldwide distribution, however, most reports are seen in the Asian population, with most cases occurring in East Asia.[2-5] MEITL and EATL comprise 2% of known cases of peripheral T-cell lymphomas in Asia. In the Philippines, cases of primary intestinal T-cell lymphoma are underreported. As of writing, there is no known case of MEITL reported in recent literature locally.

CASE

We report a case of a 64-year-old male who presented in the emergency room with a 3-day history of sharp periumbilical pain which eventually worsened and became associated with fever. Patient has no known comorbidities, or history of celiac disease. He is a 20-pack year smoker, with a family history of emphysema. Physical examination findings showed stable vital signs but with distended abdomen, direct and rebound tenderness on all quadrants with guarding. Chest X-ray revealed pneumoperitoneum thus a ruptured viscus was considered.

The patient was subsequently admitted and underwent an exploratory laparotomy where intraoperative findings showed a necrotic segment of jejunum 10 to 20 cm from the Ligament of Treitz (LOT), thick walled and perforated ileum located 200 cm from LOT, and multiple palpable mesenteric lymph nodes. Ileal resection, gastrojejunostomy, and double barrel ileostomy was done, and the specimen submitted for histopathology.

The patient was discharged well. Three weeks after the initial presentation, the patient noted enlarging right maxillary and left alveolar mass, warranting consultation in the outpatient department. Biopsy done revealed similar

microscopic and immunohistochemical findings with the intestinal specimen. One month after initial admission, the patient was readmitted for generalized abdominal pain, vomiting with noted hypotension, guarding and abdominal distention on physical examination. Patient was managed as a case of ruptured viscous and underwent re-exploratory laparotomy and partial duodenojejunectomy. During his hospital stay, the patient had episodes of hypotension, desaturation, and melena. The patient was referred to hospice and palliative care but eventually opted discharge and was lost to follow up.

Segments of ileum and jejunum were sent for histopathologic examination. Both ileal and jejunal resection specimens showed multiple, dark green, ill-defined masses which constrict but do not obstruct the lumen. The mass was also seen to grossly perforate the jejunum (Figure 1). On microscopy, monotonous small to medium round cells are seen to densely infiltrate the mucosa. The intestinal villi appear to be attenuated and are entirely lost in other areas (Figure 2). No glandular spacing or dropout is seen (Figure 3A). On high power view, the cells have vesicular nuclei and conspicuous nucleoli with scant cytoplasm (Figure 3B). Other areas of the intestine adjacent to the tumor show necrosis and ulceration (Figure 4A). Areas uninvolved by the tumor also show lymphoid infiltration, similar to lymphocytic colitis. (Figure 4B). The same microscopic features were also seen in the maxillary, alveolar and second resection specimens (Figure 5).

Immunohistochemistry studies showed positive expression for LCA, CD3, CD8, CD56, CD68 and Granzyme B (Figure 5). The tumor has negative staining for Pancytokeratin, CD20, CD30, CD4 and CD5 (Figure 6). Given the clinical and immunohistomorphologic findings, the diagnosis of Monomorphic Epitheliotrophic Intestinal T-cell Lymphoma was established.

DISCUSSION

MEITL is a primary intestinal T-cell lymphoma that is known to have a worldwide distribution but is mostly reported among the Asian and Hispanic population. Most reported cases are in the East Asian Region, but cases have also been reported in western countries, which share the same clinical course and histomorphologic findings.[6] Historically, MEITL was grouped under Enteropathy-type-T-cell lymphoma and designated as Type 2 Enteropathy associated T-cell lymphoma (EATL). In 2016, it was reclassified as a separate entity due to its lack of association

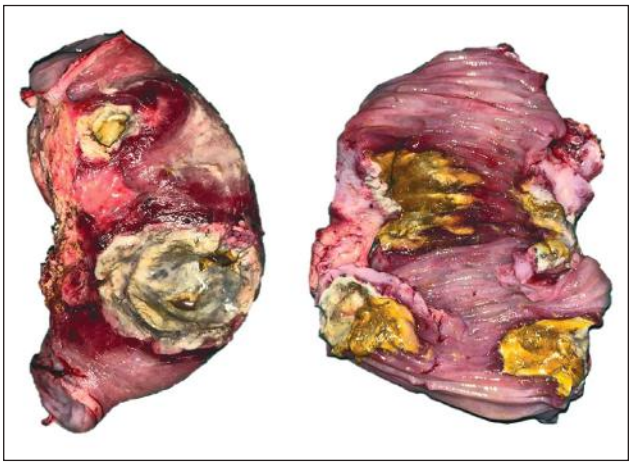

Figure 1. Resected segment of the ileum shows multiple ill-defined cream white to yellow necrotic lesions which perforate the full thickness of the intestinal wall

Photos courtesy of Dr. Darwin Del Rosario from the Surgery Department.

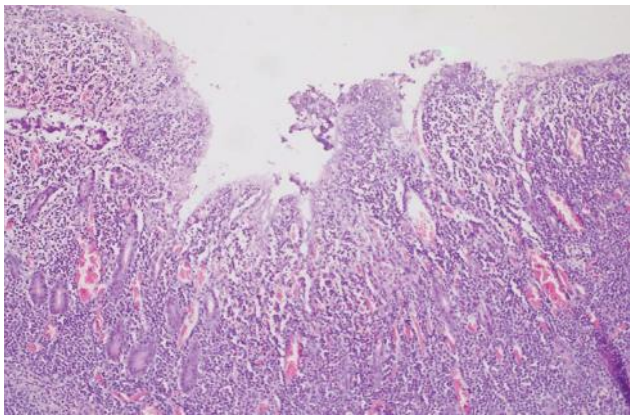

Figure 2. ***Intestinal Mass.*** Dense sheets of round blue cells are seen to infiltrate the mucosa, with attenuation of the small intestinal villi, and ulceration of the surface epithelium (H&E, 20x).

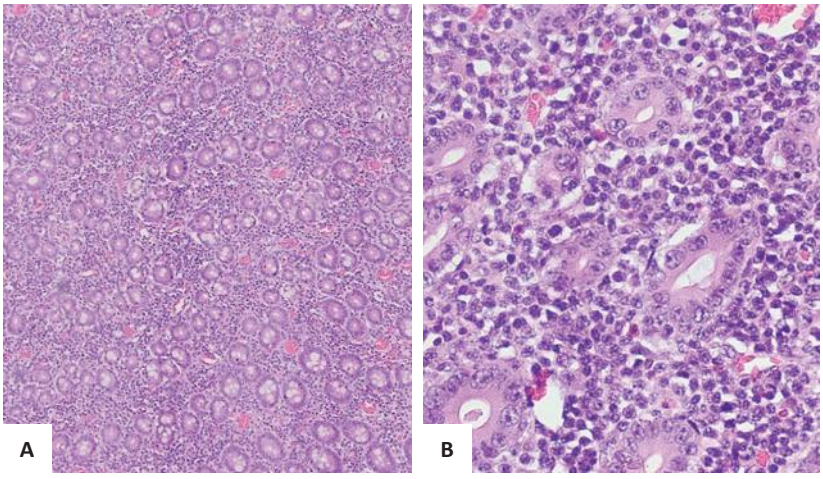

Figure 3. ***Intestinal Mass.*** Monomorphic round blue cells are seen to surround glands. **(A)** No increased glandular spacing or loss of glands are seen (H&E, 20x). **(B)** The cells are monomorphic with round to irregular vesicular nuclei, conspicuous nucleoli, and dense chromatin (H&E, 100x).

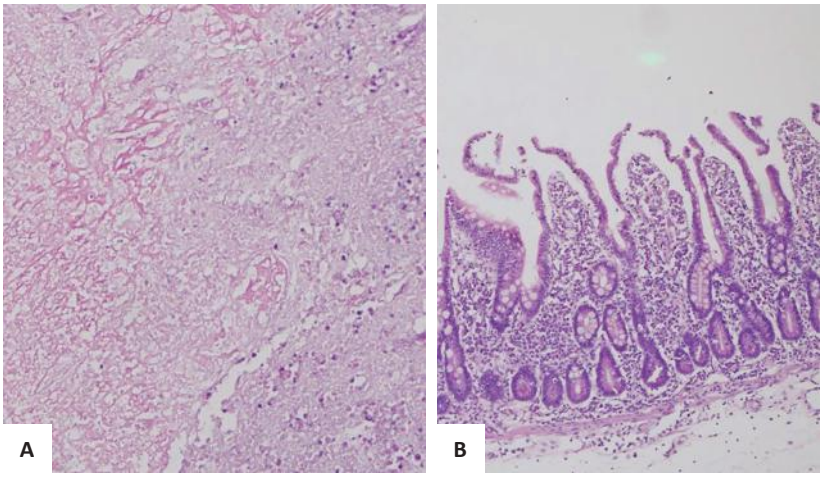

Figure 4. ***Intestinal Mass.*** **(A)** Other areas of the small intestine show necrosis (H&E, 20x). **(B)** Areas uninvolved by the tumor show normal architecture with intraepithelial lymphocytes (H&E, 20x).

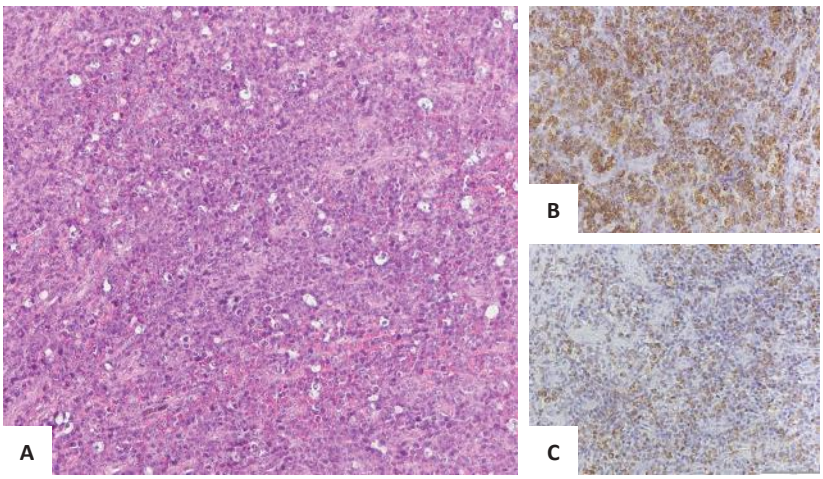

Figure 5. ***Alveolar Mass.*** **(A)** Morphologically similar monomorphic cells are also seen to infiltrate the alveolar mass, showing a "starry sky" appearance (H&E, 20x). **(B)** Tumor cells stained positive for CD3, confirming their T-cell lineage (HRP, 20x). C. CD20 only stained positively in the admixed non-neoplastic B cells (HRP, 20x).

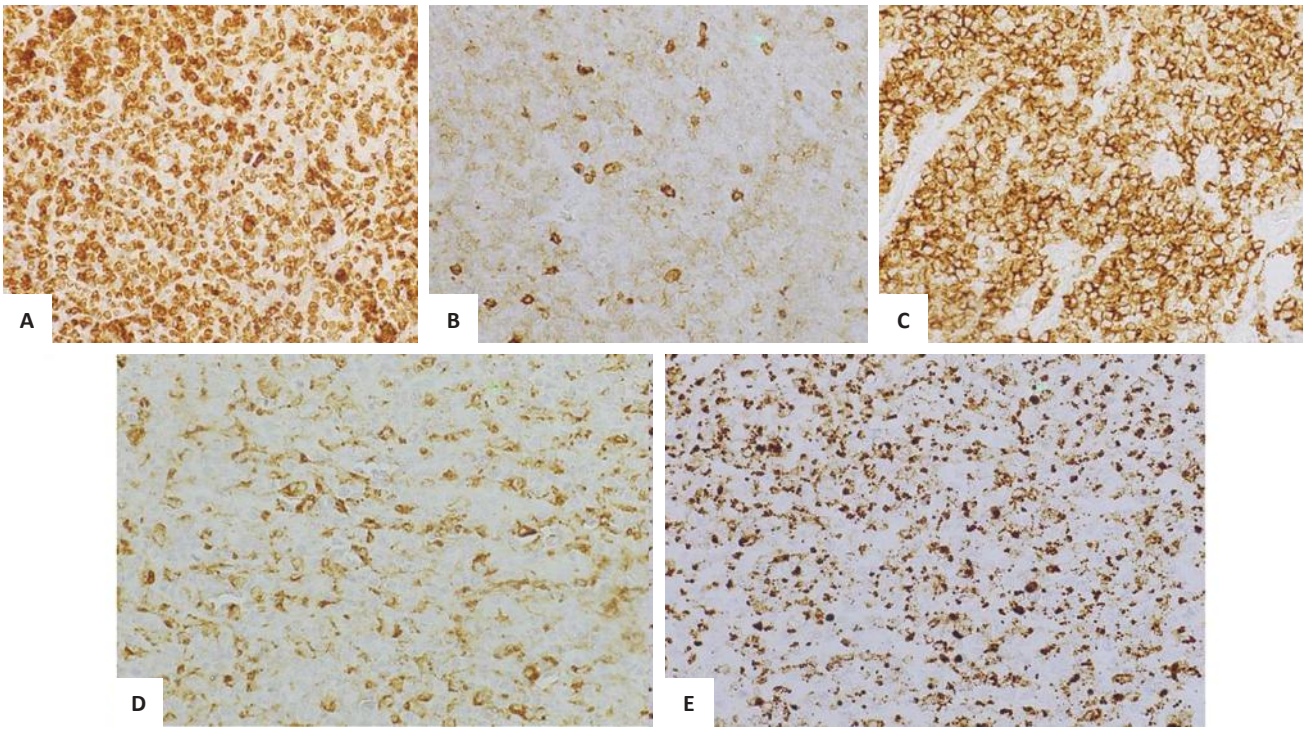

Figure 6. ***Immunohistochemistry profile of the intestinal mass.*** The mass showed: **(A)** Strong, diffuse positivity for CD3 (HRP, 40x); **(B)** Patchy positivity for CD8 (HRP, 40x); **(C)** Diffuse positivity for CD56 (HRP, 40x); **(D)** Diffuse positivity for CD68 (HRP, 40x); **(E)** Diffuse positivity for Granzyme B (HRP, 40x).

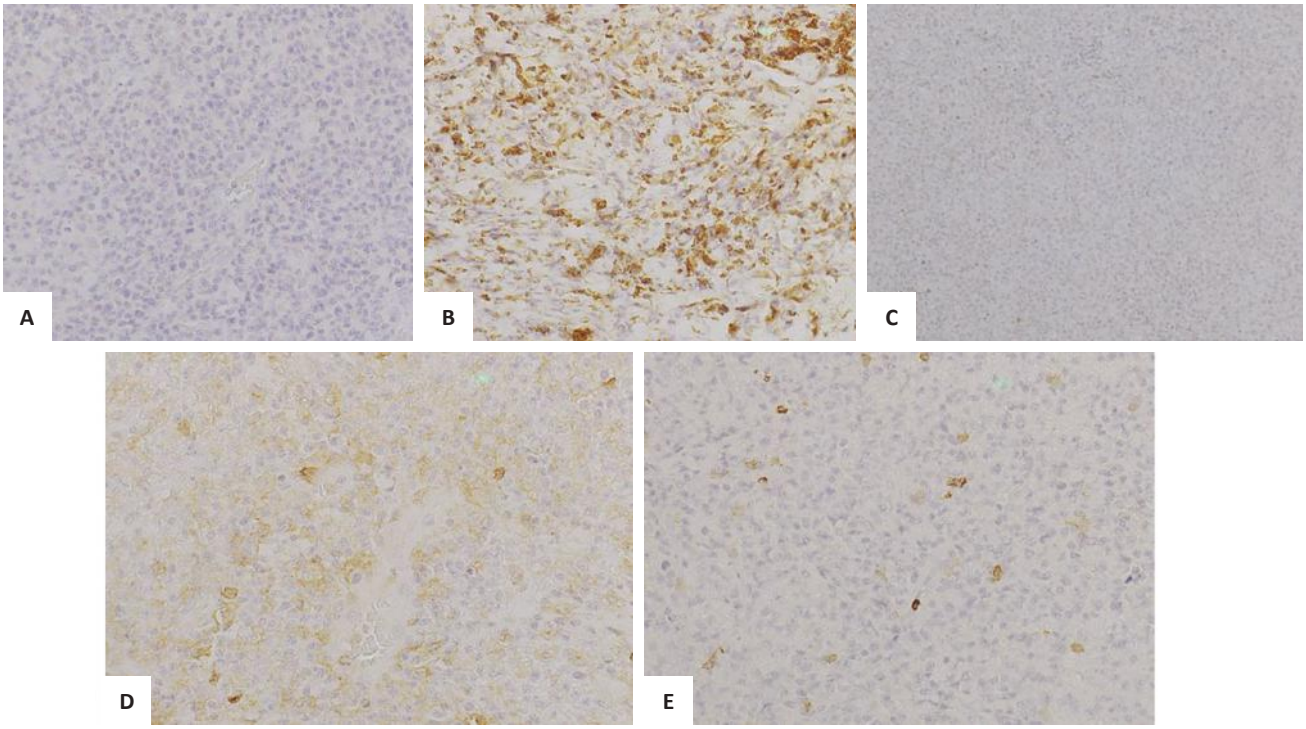

Figure 7. ***Immunohistochemistry profile of the intestinal mass.*** **(A-E)** The mass showed negativity for **(A)** Pancytokeratin, **(B)** CD20, **(C)** CD30, **(D)** CD4, and **(E)** CD5 (HRP, 40x).

with celiac disease, and its pathogenesis is less dependent on its presence. Genetic differences between the two entities supported this change in classification. MEITL showed MYC oncogene locus gain, and rare gains of chromosome 1q and 5q.[7] On the other hand, Type 1 Enteropathy associated T-cell lymphoma showed gains of chromosome 1q and 5q and HLA-DQB1 genotype patterns with celiac disease.

MEITL is reported to affect mostly adults, with an age range of 54-67 years old, with male predominance.[2] The disease usually presents with vague symptoms including abdominal pain, weight loss, and intestinal obstruction or perforation. MEITL most commonly affects the small intestine, with some cases being reported to affect the colon, stomach, and duodenum. The disease is known to disseminate to mesenteric lymph nodes, and in rare cases, in the lung, liver, and brain.[8-10] In the patient's case, the disease was noted to have metastasized to the bone, particularly in the right maxilla.

Because symptoms can be non-specific, patients tend to be diagnosed late and may not be able to start treatment early. The disease carries a poor prognosis, with only a median survival rate of 7 months, coupled with a low chemotherapy response rate on CHOP-like polychemotherapy. Despite this, cases with recurrence free survival for five years have been previously reported and those with complete surgical resection carry a better prognosis.[2,11]

Grossly, the tumor presents as an ulcerated mass and is indistinguishable from other hematolymphoid tumors. Microscopic examination shows monomorphic small round blue cells invading the intestinal mucosa, expanding the and distorting the villi. The affinity of the T-cells to the intestinal mucosa is the basis for their epitheliotropism. However, neoplastic cells may also invade the entirety of the gastrointestinal wall causing perforation. Typical immunophenotypic profile of MEITL shows CD2+, CD3+, CD4−, CD5−, CD7+, CD8+, and CD56+. Granzyme expression is less consistent.[12] Differential diagnoses are listed below (Table 1). The closest differential diagnosis with the case presented is EATL, which shares similar cytotoxic T-cell immunophenotype. However, for EATL, tumor cells are more polymorphic, and CD8 and CD56 are negative. Intestinal T-cell lymphoma, NOS, should also be considered which can also show atypical lymphoid infiltration and epitheliotropism. However, this can be excluded with its CD4 positivity and CD56 negativity.

Another entity that should be excluded is Extranodal NK/T-cell lymphoma (ENKTL). These tumors are composed of medium-sized lymphoid cells, with positivity for CD3, Granzyme B, and variably express CD56, similar to our case. However, no angiocentric or angioinvasive pattern was seen, which is characteristic of ENKTL.[13] Epstein Barr Virus positivity for this case is still in question, however, since the patient was lost to follow up, further testing cannot be done. It is therefore recommended that EBER-In Situ Hybridization be performed to complete rule out this entity, as there may be a modification in the chemotherapy regimen. Addition of L-Asparaginase to the traditional CHOP regimen is recommended in some studies.[14] Other studies recommend a different treatment altogether, without the use of anthracycline-based drugs, using asparaginase-gemcitabine based regimens.[15]

Etiology of MEITL remains unknown. Neoplastic T-cells are implicated to arise from intestinal intraepithelial lymphocytes with CD8+ and CD56+. Whole genome

Table 1. Differential diagnoses

	Patient	Monomorphic Epitheliotropic Intestinal T-cell Lymphoma	Enteropathy-Associated T-cell Lymphoma	Intestinal T-cell Lymphoma, NOS	Extranodal NK/T-cell Lymphoma
CD3	+	+	+	+	+
CD4	-	-	-	+/-	-
CD5	-	-	-	+	-
CD8	+	+	-	+	-
CD56	+	+	-	-	+/-
CD68	+	+			
CD30	-	-		-	
CD20	-	-	-	-	-
Granzyme B	+	+	+	+	+
LCA	+	+	+	+	+
CK	-	-	-	-	-

sequencing showed characteristic activating mutations of the JAK-STAT pathway, with mutations of *STAT5B* being the most common.[16] In one small study using Next Generation Sequencing, mutations in STAT5B, SETD2, NRAS, KRAS, and JAK3 were identified.[17] Fluorescence in-situ hybridization studies have also demonstrated SETD2 deletions and MYC gene locus alterations. Expression of MYC was associated with less monomorphic morphology on histology, p53 mutations, and poorer overall survival in one study.[6]

Although diagnosis rests mostly on the morphology and immunophenotypic profile, molecular studies can help in detecting more mutations which can be future drug targets. Reporting should be intensified to characterize this type of tumor and increase the index of suspicion for its occurrence before patients deteriorate. More knowledge on MEITL can help in the search for better therapeutic regimen for these patients and alter their clinical course.

CONCLUSION

This is a case of a 64-year-old male presenting with abdominal pain and ruptured viscous at the emergency room. On histopathologic examination, dense sheets of small to medium sized mononuclear cells were seen to infiltrate and perforate the bowel wall. The tumor was immunoreactive for CD3, CD8, CD56, CD68 and Granzyme B, confirming its diagnosis as Monomorphic Epitheliotropic Intestinal T-cell Lymphoma. Although this entity is commonly seen in the Asian population, no case has been reported yet in the Philippines. Reporting should be intensified to characterize this type of rare tumor to help future researchers in their search for a cure.

ETHICAL CONSIDERATION

Multiple attempts were made to obtain informed consent from the patient. However, the patient was lost to follow-up, and no responses to these communications were received.

STATEMENT OF AUTHORSHIP

The authors certified fulfillment of ICMJE authorship criteria.

AUTHOR DISCLOSURE

The authors declared no conflicts of interest.

DATA AVAILABILITY STATEMENT

No datasets were generated or analyzed for this study.

FUNDING SOURCE

No funding was received for this research.

REFERENCES

1. Swerdlow SH, Campo E, Pileri SA, et al. The 2016 revision of the World Health Organization classification of lymphoid neoplasms. Blood. 2016;127(20):2375-90. PMID: 26980727 PMCID: PMC4874220 DOI: 10.1182/blood-2016-01-643569
2. Chan JKC, Tan SY, de Leval L. Monomorphic epitheliotropic intestinal T-cell lymphoma. In: WHO Classification of Tumours Editorial Board, ed. Digestive System Tumours. 5th ed. Vol. 1. Lyon, France: International Agency for Research on Cancer; 2019.
3. Fei F, Reddy V, Patel CR, et al. Monomorphic epitheliotropic intestinal T-cell lymphoma: a study of four cases and review of literature. Ann Clin Lab Sci. 2020;50(6):806-12. PMID: 33334797
4. Zhong H, Zheng Y, Zhang F. Monomorphic epitheliotropic intestinal T-cell lymphomas: a case report. Diagn Pathol. 2021;16(1):80. PMID: 34461952 PMCID: PMC8407069 DOI: 10.1186/s13000-021-01143-x
5. Shin SY. A rare case of intestinal T-cell lymphoma with multiple complications. J Diagn Case Rep. 2023; 11(2):114-8. DOI: 10.52927/jdcr.2023.11.2.114
6. Veloza L, Cavalieri D, Missiaglia E, et al. Monomorphic epitheliotropic intestinal T-cell lymphoma comprises morphologic and genomic heterogeneity impacting outcome. Haematologica. 2023;108(1):181-95. PMID: 35708139 PMCID: PMC9827163 DOI: 10.3324/haematol.2022.281226
7. Deleeuw RJ, Zettl A, Klinker E, et al. Whole-genome analysis and HLA genotyping of enteropathy-type T-cell lymphoma reveals 2 distinct lymphoma subtypes. Gastroenterology. 2007;132(5):1902-11. PMID: 17484883 DOI: 10.1053/j.gastro.2007.03.036
8. Bhatlapenumarthi V, Patwari A, Siddiqui AD. An unusual case of enteropathy-associated T-cell lymphoma type 2 with pulmonary metastasis. Cureus. 2019;11(9):e5714. PMID: 31720182 PMCID: PMC6823092 DOI: 10.7759/cureus.5714

9. Suzuki Y, Minemura H, Tomita H, et al. Monomorphic epitheliotropic intestinal T-cell lymphoma involving the lung and brain: a rare case study. Intern Med. 2020;59(20):2559-63. PMID: 32641648 PMCID: PMC7662048 DOI: 10.2169/internalmedicine.4710-20
10. Muramoto K, Kaida S, Miyake T, et al. Rare monomorphic epithelial intestinal T-cell lymphoma of the stomach with a giant gastric perforation rescued by liver-covering sutures followed by a total gastrectomy and lateral hepatectomy: a case report. Surg Case Rep. 2022;8(1):27. PMID: 35129729 PMCID: PMC8821748 DOI: 10.1186/s40792-022-01381-1
11. Ozaka S, Inoue K, Okajima T, et al. Monomorphic epitheliotropic intestinal T-cell lymphoma presenting as melena with long-term survival: a case report and review of literature. World J Gastroenterol. 2021;27(38):6501-10. PMID: 34720538 PMCID: PMC8517785 DOI: 10.3748/wjg.v27.i38.6501
12. Huang D, Lim JQ, Cheah DMZ, et al. Whole-genome sequencing reveals potent therapeutic strategy for monomorphic epitheliotropic intestinal T-cell lymphoma. Blood Adv. 2020;4(19):4769-74. PMID: 33017466 PMCID: PMC7556141 DOI: 10.1182/bloodadvances.2020001782
13. Chan JKC, Hyeh Y, Li GD, Takeuchi K. Extranodal NK/T-cell lymphoma. In: WHO Classification of Tumours Editorial Board, ed. Digestive System Tumours. 5th ed. Vol 1. Lyons, France: International Agency for Research on Cancer; 2019.
14. Zheng W, Gao Y, Ke X, et al. PEG-L-CHOP treatment is safe and effective in adult extranodal NK/T-cell lymphoma with a low rate of clinical hypersensitivity. BMC Cancer. 2018;18(1):910. PMID: 30241515 PMCID: PMC6151061 DOI: 10.1186/s12885-018-4782-y
15. Luo F, Wang JN, Liu X, Wang X, Qi SN, Li YX. Efficacy of frontline chemotherapy for extranodal natural killer/T-cell lymphoma: a systematic review and network meta-analysis. J Hematol. 2023;12(5):215-26. PMID: 37936976 PMCID: PMC10627360 DOI: 10.14740/jh1169
16. Alburqueque-Melgarejo J, Gárate BB, De la Cruz-Vargas JA. Epitheliotropic monomorphic intestinal T-cell lymphoma: case report and literature review. Curr Probl Cancer Case Rep. 2024;15(1):100313. DOI: 10.1016/j.cpccr.2024.100313.
17. Roberti A, Dobay MP, Bisig B, et al. Type II enteropathy-associated T-cell lymphoma features a unique genomic profile with highly recurrent SETD2 alterations. Nat Commun. 2016;7:12602. PMID: 27600764 PMCID: PMC5023950 DOI: 10.1038/ncomms12602

OPEN ACCESS – CASE REPORT

DEK::AFF2 Squamous Cell Carcinoma is a Deceptive Mimic of Inverted Sinonasal Papilloma: A Case Report

Karen Cybelle Sotalbo, Jonathan Rivera, Clarisse Anne Nuqui

Department of Laboratories, Philippine General Hospital

ABSTRACT

An elderly Filipino female presented with a 5-year enlarging left nasolacrimal mass initially diagnosed as Inverted Papilloma of the Lacrimal Sac. Repeat biopsy revealed a papillomatous neoplasm with thick and thin papillae, solid invaginating lobules, and anastomosing trabeculae of monomorphic squamotransitional cells, briskly infiltrated by neutrophils. Mucocytes, respiratory epithelium, and microcysts, typical of Inverting Sinonasal Papilloma, are absent. Immunohistochemistry, including a validated AFF2 IHC, confirmed the diagnosis of *DEK::AFF2* sinonasal carcinoma. Awareness of this emerging entity is essential to prevent misdiagnosis and prompt surgical management.

Key words: DEK, AFF2, squamous cell carcinoma, case report, Philippines

ISSN 2507-8364 (Online)
Printed in the Philippines.

Received: 21 March 2026.
Accepted: 19 April 2026.
Published online first: 11 June 2026.
https://doi.org/10.21141/PJP.2026.615

Corresponding author: Jonathan P. Rivera, MD
E-mail: jonathanpriveraMD@gmail.com
ORCiD: https://orcid.org/0000-0003-0268-4664

INTRODUCTION

DEK::AFF2 sinonasal carcinoma is an emerging entity in the sinonasal tract and skull base classified as a subtype of Non-keratinizing Squamous Cell Carcinoma. However, it is likely an under-recognized neoplasm often misdiagnosed as a benign inverted sinonasal papilloma (ISP) due to its frequent papillomatous growth and strikingly bland monomorphic cytology.[1-5] Alternatively, due to its banal appearance, some cases of *DEK::AFF2* sinonasal carcinoma have been previously classified as "low-grade papillary Schneiderian carcinoma."[2-6] A subset of cases may also display overt carcinomatous features similar to non-keratinizing squamous cell carcinoma or adenosquamous carcinoma of the sinonasal tract and skull base.[2,3,5] The diagnosis is made upon evaluation of key histologic and immunophenotypic features followed by confirmatory molecular testing for the *DEK::AFF2* fusion or a validated immunohistochemical (IHC) assay for the AFF2 protein, as a confirmatory surrogate.[3] Increasing awareness is important as this tumor can have frequent local recurrences, occasional lymph node and distant metastases, and rare tumor-related deaths.[3,5] Here, we report the first diagnosed case of *DEK::AFF2* sinonasal carcinoma in an elderly Filipino patient.

CASE

A 76-year-old female presented with a 5-year history of an enlarging left nasolacrimal mass. The mass began at the medial aspect of the left eye, with associated tearing and discharge. Eye drops were initially prescribed but afforded no relief from symptoms. She then sought consultation from another institution, where she was diagnosed with Chronic Dacryocystitis and Nasolacrimal Duct Obstruction, and subsequently underwent laser dacryocystorhinostomy. The patient reported slight relief of symptoms. However, in the interim, there was a gradual enlargement of the mass with an increase in tearing and discharge. Two months before the consult, a biopsy was done in another institution, where she was diagnosed with papilloma of the lacrimal duct, inverted type. Antibiotics

were prescribed, but the mass continued to increase in size, now with a left nasal extension. The patient eventually sought a consultation at the outpatient department.

On physical examination, there was a 4.0 x 4.0 x 2.0 cm firm, non-tender, fixed nodular mass on the left maxilla involving the left orbit and medial canthus. There was noted tearing and crusting of the left eye. On rhinoscopy, there was a fleshy mass completely obstructing the left nasal cavity. The rest of the physical examination, family history, and previous medical history are unremarkable.

Imaging showed that the mass arose from the left lacrimal sac with extension to the pre- and post-septal cavity, abutting the medial rectus muscle. The mass also extends to the inferomedial aspect of the globe, left frontal sinus, left anterior ethmoid sinus, and left nasal cavity, indenting the turbinates, and occupying the left nasolacrimal sac and duct. Mild septal deviation is seen (Figure 1A). No intracranial extension was noted. The right frontal, ethmoid, and sphenoid sinuses, as well as the right nasal cavity, are uninvolved. A repeat biopsy was done and sent for histopathologic examination.

The tissue sample consists of several tan-brown fleshy fragments with an aggregate dimension of 3.5 cm. Histologic examination shows a papillomatous neoplasm forming thin and thick papillae, solid endophytic lobules, and anastomosing trabeculae of epithelial tumor cells (Figure 1B). The endophytic lobules comprise a solid proliferation of squamotransitional cells reminiscent of inverting sinonasal papilloma (Figure 1C). However, in contrast to inverting sinonasal papilloma, the neoplastic epithelium does not contain mucocytes, intermediate or respiratory-type epithelial cells, and microcysts that contain microabscesses. Instead, the polygonal tumor cells display striking monomorphism, ovoid vesicular nuclei, conspicuous nucleoli, and ample eosinophilic cytoplasm. An accompanying brisk peritumoral and intratumoral neutrophilic infiltrate is seen (Figure 1D). Due to the aforementioned histologic findings, immunohistochemical work-up using Pancytokeratin (AE1/AE3), p63, NUT, INI-1, and AFF2 for the C-terminus were performed. The tumor showed strong and diffuse expression of pancytokeratin and p63 (Figure 1E), confirming an epithelial neoplasm with squamous differentiation, was negative for NUT *(image not included)*, ruling out a NUT carcinoma, and had retained expression of INI-1 *(image not included)*, excluding a SMARCB1-deficient sinonasal carcinoma. The tumor showed a strong diffuse nuclear expression of AFF2 in all tumor cells (Figure 1F), confirming the diagnosis of *DEK::AFF2* sinonasal carcinoma. The patient underwent complete resection of the tumor, including the orbital contents.

DISCUSSION

Epidemiology/Incidence

Sinonasal carcinomas are rare (1/100,000 population) and aggressive tumors that represent 3-5% of all head and neck cancers. Investigation of publicly available RNA data sets of sinonasal papillomas and squamous cell carcinomas and review of recurrent sinonasal papillomas over a two-decade period have suggested *DEK::AFF2* sinonasal carcinoma to occur in 4.7-10.7% of cases. A total of 49 cases has been published to date.[1-10] This is the first reported case of *DEK::AFF2* sinonasal carcinoma in the Philippines.

Clinicopathologic features, presentation, and anatomic involvement

DEK::AFF2 sinonasal carcinoma most frequently involves the nasal cavity. This is followed in decreasing order of frequency by the nasopharynx, skull base, paranasal sinuses, middle ear, orbit, temporal bone, and rarely, by the lacrimal sac, similar to the present case.[3,5] Interestingly, a case of *DEK::AFF2*-rearranged carcinoma has been reported in the lung with broncho-centric growth and co-expression of p40 and TTF-1, suggesting a potential origin from the basal cells of the respiratory epithelium.[7]

Morphologic features, differential diagnosis, and ancillary work-up

The histologic features of *DEK::AFF2* sinonasal carcinoma usually fit into three distinct morphologic patterns, which may guide pathologists to its recognition. The Low-grade Papillary Schneiderian Carcinoma subtype is the most common. From its namesake, prior cases with this morphologic pattern were previously classified as "Low-grade Papillary Schneiderian Carcinomas" but were later found to harbor the defining *DEK::AFF2* fusion, resulting in their reclassification.[2,6] In this subtype, the neoplastic epithelium forms endophytic lobules usually with rounded non-infiltrative contours and anastomosing trabeculae, resembling ISP, its closest differential. In contrast to ISP, the tumor usually displays a greater architectural complexity, with back-to-back invaginating lobules and trabeculae forming a maze-like or labyrinthine pattern. Furthermore, the cells are strikingly monomorphic and bland, without the usual admixture of squamous, mucocytes, and respiratory-type cells in the epithelium and abscess-containing microcysts, which are distinguishing features of ISP. Likewise, these cell components are required to be at least focally present in ISP with dysplasia or carcinoma-ex ISP. Conspicuous central acantholytic change in the lobules confers a dilapidated appearance, pseudopapillary pattern, or areas reminiscent of stellate reticulum, which could be mistaken for ameloblastic epithelium. Stromal neutrophilic infiltrates surround the lobules or infiltrate between tumor cells.[2,3,6] Less commonly, *DEK::AFF2* sinonasal carcinoma may display an infiltrative pattern with varying but often limited squamous and/or glandular differentiation, corresponding to the non-keratinizing squamous cell carcinoma and adenosquamous carcinoma morphologic subtypes. When encountering these 2 morphologic subtypes, a wide range of differential diagnoses is considered. Briefly, cases of non-keratinizing squamous cell carcinoma subtype should be distinguished from 1) Virus-related (EBV or HPV) carcinomas; 2) Squamous cell carcinoma arising from ISP with an underlying EGFR-mutation; 3) poorly-differentiated malignant neoplasms with squamous phenotype to include NUT carcinoma, SWI/SNF-related carcinoma, and adamantinoma-like ewing sarcoma; and 4) Carcinogen-driven squamous cell carcinomas. Cases with adenosquamous carcinoma should be distinguished from HPV-multiphenotypic sinonasal carcinoma, adenosquamous carcinoma, and from mucoepidermoid carcinoma. Thus, work-up to variably consist of p40, p16,

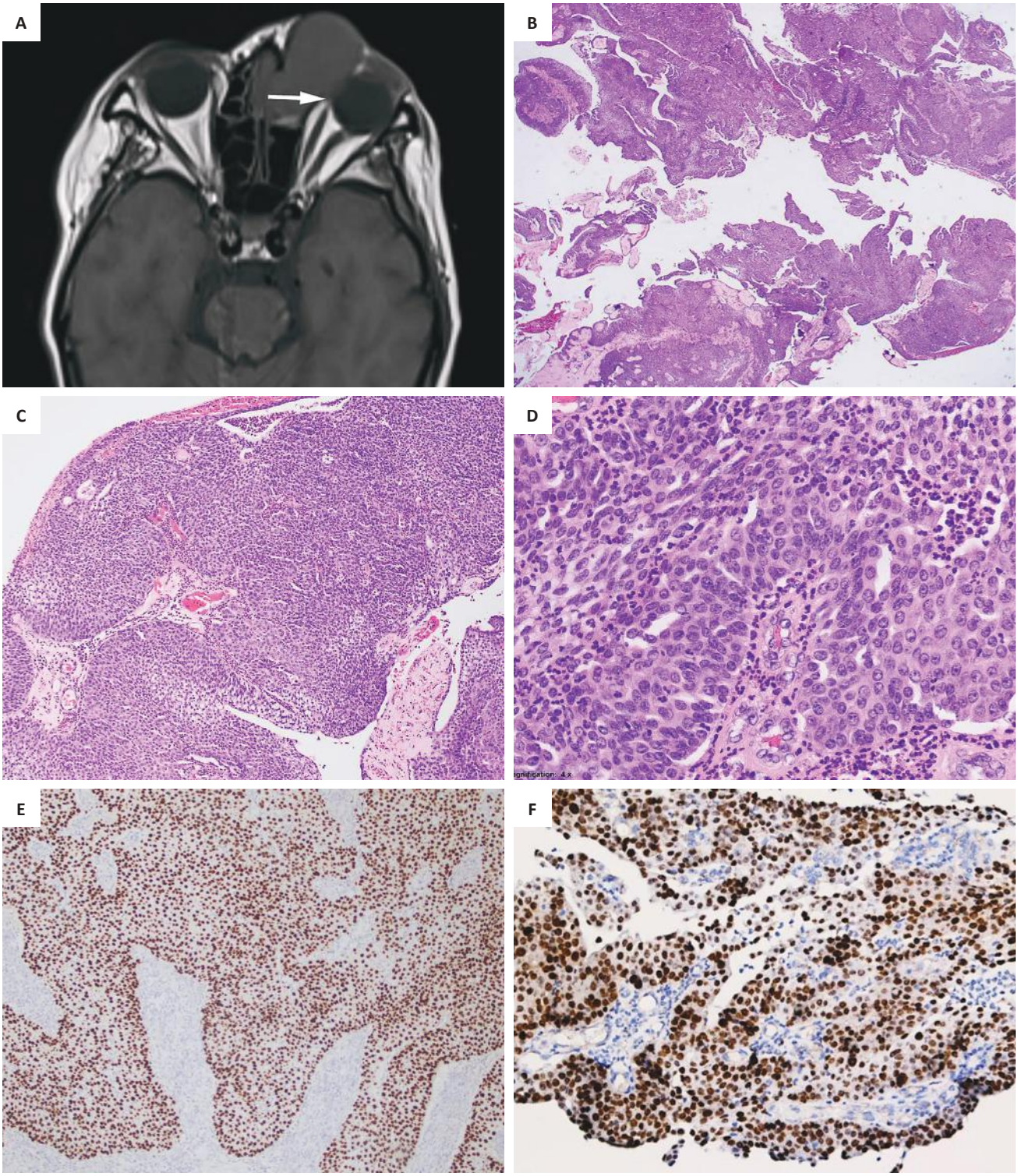

Figure 1. ***Imaging and histopathologic findings of the case.*** **(A)** Imaging shows the tumor in the ethmoid sinus and left nasal cavity. It abuts the medial rectus muscle and displaces the left globe *(white arrow)*. **(B)** Tumor fragments consist of papillae, solid endophytic lobules, and anastomosing thick trabeculae of tumor cells (H&E, 40x). **(C)** Solid endophytic lobules resemble those of inverting sinonasal papilloma but with greater cell crowding and solid growth (H&E, 100x). **(D)** Squamo-transitional tumor cells are monomorphic with ovoid vesicular nuclei and ample eosinophilic cytoplasm. Mucocytes, respiratory epithelium, and microcysts typical of ISP are not observed. Neutrophils surround the tumor cell clusters or infiltrate between tumor cells (H&E, 400x). **(E)** Tumor shows nuclear expression of p63 (IHC, 200x). **(F)** Tumor shows strong diffuse nuclear expression of AFF2 in all cells (IHC, 200x).

NUT, INI-1, BRG1, CD99, and NKX2.2 IHCs, EBERish and HPVish, and/or molecular testing for *MAML2* gene rearrangement, will select cases requiring further *DEK::AFF2* fusion confirmatory testing.[3,8,9]

Molecular testing and AFF2 IHC

The diagnosis of *DEK::AFF2* carcinoma is based on the presence of the defining *DEK::AFF2* gene fusion. The *DEK::AFF2* fusion has been identified using whole-genome sequencing,[10] whole transcriptome sequencing,[2] targeted RNA next-generation sequencing (NGS),[1,11,12] and/or fluorescent in situ hybridization (FISH) using *DEK* dual fusion or break-apart probes.[2,6,10,13,14] Furthermore, recognition of the breakpoints and fusion variants has led to the development of specific primers to identify the *DEK::AFF2* fusion via reverse transcription polymerase chain reaction (RT-PCR).[6] More recently, studies on the differential AFF2 protein expression in fusion-positive tumors have led to the development of an immunohistochemical assay targeting the C-terminus peptide of the AFF2 protein.[2] An adequately validated AFF2 IHC has demonstrated excellent sensitivity, specificity, positive predictive value, and negative predictive value as a surrogate marker for the *DEK::AFF2* fusion when at least 30% of tumor cells are observed to display moderate to strong nuclear expression.[2,5,14,15] Thus, in resource-limited settings, RT-PCR or a rigorously validated AFF2 IHC, combined with morphologic evaluation and an appropriate immunohistochemical panel to exclude other differentials, is an effective method to confirm the diagnosis of *DEK::AFF2* sinonasal carcinoma.

Prognosis/clinical behavior

DEK::AFF2 sinonasal carcinoma shows frequent local recurrences or progression (50-55.5%) with occasional lymph node (25.0-29.6%) and distant (17-25.9%) metastases. Tumor-related deaths are found to range from 5.9% to 25%, depending on the reported case series, with variable median follow-up (7-18 months).[3,5]

CONCLUSION

DEK::AFF2 sinonasal carcinoma is an under-recognized malignant neoplasm. Frequently, it shows papillomatous growth with banal and strikingly monomorphic tumor cells, easily misconstrued as an inverting sinonasal papilloma. In these cases, accurate diagnosis is facilitated by identifying architectural complexity, strikingly monomorphic tumor cells, absence of the typical cellular components of inverting sinonasal papilloma (mucocytes, respiratory-type epithelial cells, and microcysts), and peritumoral neutrophilic infiltrates. An appropriate IHC panel and molecular testing for the *DEK::AFF2* fusion or an AFF2 IHC targeting the C-terminus as a surrogate will confirm the diagnosis. Awareness of this emerging entity to distinguish from ISP is clinically relevant to prevent delay in surgical management, as it has been shown to behave aggressively with frequent local recurrence, occasional metastasis, and rare tumor-related deaths.

ACKNOWLEDGMENTS

The authors extend their special thanks to Dr. Jen Fan-Hang and Dr. Ying Ju-Kuo for their assistance in confirming the case using a validated AFF2 IHC stain in Taipei Veterans General Hospital, Department of Pathology and Laboratory Medicine.

STATEMENT OF AUTHORSHIP

All authors certified fulfillment of the ICMJE authorship criteria.

AUTHOR DISCLOSURE

The authors declared no conflict of interest.

DATA AVAILABILITY STATEMENT

No datasets were generated or analyzed for this research.

FUNDING SOURCE

None.

REFERENCES

1. Rooper LM, Agaimy A, Dickson BC, et al. DEK-AFF2 carcinoma of the sinonasal region and skull base: detailed clinicopathologic characterization of a distinctive entity. Am J Surg Pathol. 2021;45(12):1682-93. PMID: 34049316 DOI: 10.1097/PAS.0000000000001741
2. Kuo YJ, Lewis JS Jr, Truong T, et al. Nuclear expression of AFF2 C-terminus is a sensitive and specific ancillary marker for DEK::AFF2 carcinoma of the sinonasal tract. Mod Pathol. 2022;35(11):1587-95. PMID: 35701667 DOI: 10.1038/s41379-022-01117-4
3. Rivera JP, Kuo YJ, Hang JF. DEK::AFF2 carcinoma of the sinonasal tract and skull base: a comprehensive review. Surg Pathol Clin. 2024;17:587-97. PMID: 39489551 DOI: 10.1016/j.path.2024.07.008
4. Amin SE, Lewis JS Jr, Bridge JA, et al. DEK::AFF2 fusion-associated squamous cell carcinoma: a case series with literature review on an emerging and challenging entity. Head Neck Pathol. 2024;18(1):86. PMID: 39312022 PMCID: PMC11420419 DOI: 10.1007/s12105-024-01690-x
5. Trinquet A, Laé M, Lepine C, et al. Sinonasal squamous cell carcinoma with DEK::AFF2 rearrangement: an aggressive cancer with bland morphology. Am J Surg Pathol. 2024;48(11):1408-16. PMID: 39132684 DOI: 10.1097/PAS.0000000000002281
6. Kuo YJ, Lewis JS Jr, Zhai C, et al. DEK-AFF2 fusion-associated papillary squamous cell carcinoma of the sinonasal tract: clinicopathologic characterization of seven cases with deceptively bland morphology. Mod Pathol. 2021;34(10):1820-30. PMID: 34108636 DOI: 10.1038/s41379-021-00846-2
7. Savari O, Chang JC, Bishop JA, Sakthivel MK, Askin FB, Rekhtman N. First report of thoracic carcinoma with DEK::AFF2 rearrangement: a case report. J Thorac Oncol. 2022;17(8):1050-3. PMID: 35773081 PMCID: PMC9357138 DOI: 10.1016/j.jtho.2022.05.009

8. Taverna C, Agaimy A, Franchi A. Towards a molecular classification of sinonasal carcinomas: clinical implications and opportunities. Cancers (Basel). 2022;14(6):1463. PMID: 35326613 PMCID: PMC8946109 DOI: 10.3390/cancers14061463
9. Wartenberg M, Hool SL, Marrazzini A, Giger R, Rupp NJ. Differentiated papillary NUT carcinoma: an unexpected, deceptively bland presentation of a sinonasal carcinoma. Head Neck Pathol. 2023; 17(3):803-7. PMID: 37118352 PMCID: PMC10513967 DOI: 10.1007/s12105-023-01554-w
10. Yang W, Lee KW, Srivastava RM, et al. Immunogenic neoantigens derived from gene fusions stimulate T cell responses. Nat Med. 2019;25(5):767-75. PMID: 31011208 PMCID: PMC6558662 DOI: 10.1038/s41591-019-0434-2
11. Todorovic E, Truong T, Eskander A, et al. Middle ear and temporal bone nonkeratinizing squamous cell carcinomas with DEK-AFF2 fusion: an emerging entity. Am J Surg Pathol. 2020;44(9):1244-50. PMID: 32366754 DOI: 10.1097/PAS.0000000000001498
12. Bishop JA, Gagan J, Paterson C, McLellan D, Sandison A. Nonkeratinizing squamous cell carcinoma of the sinonasal tract with DEK-AFF2: Further Solidifying an Emerging Entity. Am J Surg Pathol. 2021;45(5):718-20. PMID: 33002918 DOI: 10.1097/PAS.0000000000001596
13. Tauziede-Espariat A, Chotard G, le Loarer F, et al. A novel LARGE1-AFF2 fusion expanding the molecular alterations associated with the methylation class of neuroepithelial tumors with PATZ1 fusions. Acta Neuropathol Commun. 2022;10(1):15. PMID: 35115049 PMCID: PMC8812055 DOI: 10.1186/s40478-022-01317-8
14. Ng JKM, Chow C, Tang CY, Chan AZ, Li JJX, Chan ABW. Prevalence and interpretation of AFF immunostain of DEK::AFF2 fusion-associated papillary squamous cell carcinoma in a retrospective cohort of recurrent sinonasal papillomas. Virchows Arch. 2024;484(1):119-25. PMID: 38063896 DOI: 10.1007/s00428-023-03717-0
15. Palsgrove D, Rooper L, Buresh C, Bishop J, Bridge J. AFF2 Immunohistochemistry: a promising surrogate marker for DEK::AFF2 fusion-associated carcinoma. Lab Invest. 2023;103(3):s1065. DOI: 10.1016/j.labinv.2023.100092

OPEN ACCESS – CASE REPORT

Recurrent Sporadic Parathyroid Carcinoma in a 29-Year-Old Filipino Female Presenting with Primary Hyperparathyroidism: A Case Report and Literature Review

Eldimson Bermudo, Jose Vicente Borja II, Al-Zamzam Abubakar

Department of Pathology and Laboratory Medicine, Zamboanga City Medical Center, Philippines

ABSTRACT

Parathyroid carcinoma is a rare endocrine malignancy with an indolent course but a high risk of recurrence. Diagnosis remains challenging, requiring integration of clinical, biochemical, radiologic, and histopathologic findings. We report a young patient presenting with primary hyperparathyroidism complicated by multiple pathologic fractures and chronic renal failure. Despite initial surgical and medical management, late aggressive recurrence occurred, resulting in significant systemic complications. This case highlights the need for vigilant long-term surveillance and improved diagnostic and therapeutic strategies.

Key words: parathyroid carcinoma, tumor recurrence, hyperparathyroidism, bone pains, pathologic fractures, case report, Philippines

ISSN 2507-8364 (Online)
Printed in the Philippines.

Received: 27 January 2026.
Accepted: 22 February 2026.
Published online first: 25 June 2026.
https://doi.org/10.21141/PJP.2026.583

Corresponding author: Eldimson E. Bermudo, MD, MPH
E-mail: eebermudo@up.edu.ph
ORCiD: https://orcid.org/0009-0000-5622-110X

INTRODUCTION

Parathyroid carcinoma is an exceptionally rare endocrine malignancy, typically characterized by indolent growth and a slow, progressive clinical course. The mean age at diagnosis reported in published studies is approximately 56 years, making occurrence in young adults distinctly uncommon. In this report, we present a recurrent sporadic parathyroid carcinoma in a 29-year-old Filipino female, who represents the second youngest patient documented in the literature to date.

While many published cases describe relatively favorable outcomes and prolonged survival following surgical management, parathyroid carcinoma is also recognized for its high propensity for recurrence, posing significant challenges in long-term treatment. Unlike typical cases, the index patient demonstrated an unusually long eight-year symptom-free interval prior to recurrence, followed by a more aggressive clinical course complicated by severe skeletal manifestations, multiple electrolyte imbalances and chronic renal failure. This case underscores the critical importance of early recognition, vigilant surveillance, and multidisciplinary management in patients with parathyroid carcinoma, even after apparent remission.

Due to the rarity of this malignancy, this case warrants thorough documentation, as it provides valuable insights into **diagnostic techniques**, treatment approaches, and the complexities associated with managing recurrent disease. Moreover, it underscores the necessity for further research to **standardize staging** systems and refine clinical protocols, ultimately aiming to improve diagnostic accuracy and long-term survival for similar future cases.

CASE

This is the case of a 29-year-old female who initially presented in 2014 with recurrent bone pain and multiple fractures and was diagnosed with primary hyperparathyroidism secondary to parathyroid carcinoma. She

underwent a 3 ½ parathyroidectomy with en bloc left thyroid lobectomy and isthmusectomy, with histopathology confirming the diagnosis. Postoperatively, the patient reported significant relief of symptoms following surgical and medical treatment. However, due to poor archiving in previous years, the original histopathology slides and previous biopsy reports were unavailable for retrospective review.

The patient experienced an eight-year period of symptomatic relief before bone pain recurred, accompanied by onset of chronic renal failure, prompting hospitalization. Physical examination revealed a palpable, firm, movable mass measuring 1.5 x 1.5 cm in the right paratracheal area. Neck ultrasonography revealed two well-defined hypoechoic solid lesions in the superior and inferior segments of the right thyroid lobe, measuring 2.1 x 1.7 cm and 3.4 x 1.7 cm, respectively (Figure 1). The left thyroid lobe was surgically absent.

The patient has no other significant comorbidities, and her family history is unremarkable. She presents with kyphoscoliotic chest deformity, exhibiting severe lower thoracolumbar dextroscoliosis (Figure 2A), along with multiple deformities in the right humerus and bilateral femurs. Radiologic examination of the humerus revealed

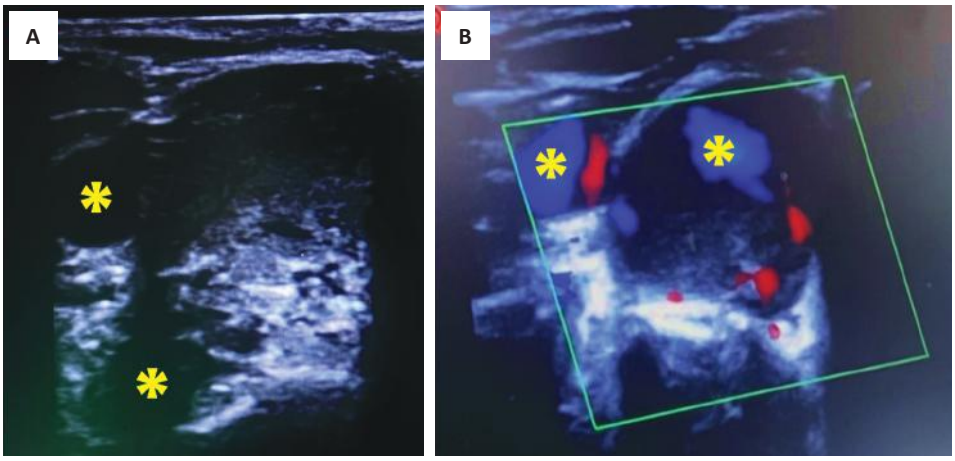

Figure 1. ***Ultrasound of the neck*** revealed hypoechoic solid lesions (*) in the superior and inferior segments of the right thyroid lobe with ill-defined margins **(A & B)**, and minimal perivascularity noted **(B)**.

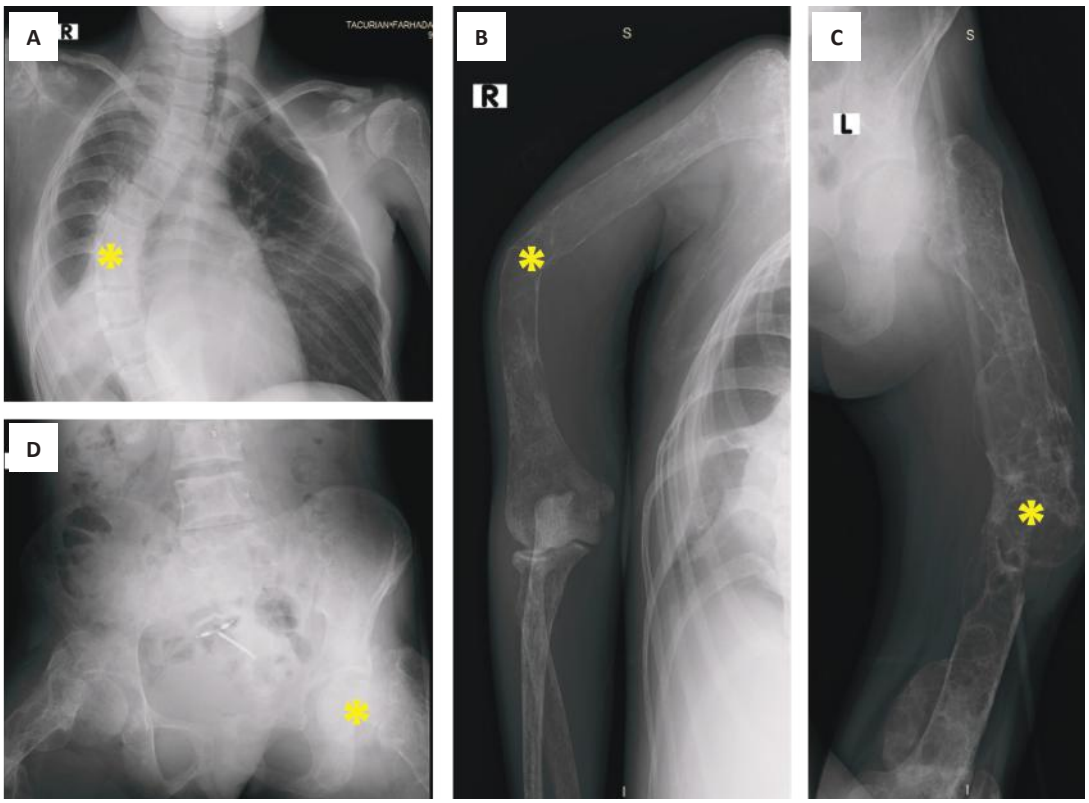

Figure 2. ***Multiple abnormal radiologic findings:*** **(A)** Chest radiography, postero-anterior view revealed severe lower thoraco-lumbar dextroscoliosis; **(B)** Humerus, antero-posterior view revealed pathologic fracture with angulation and impaction in the right humerus (*) with diffuse osteopenia; **(C)** Thigh, antero-posterior view showed pathologic fracture of the left femur with expansile osteolytic changes along the midshaft and distal posterior aspect; and **(D)** Pelvis radiography, anterior-posterior view revealed right femoral neck pathologic fracture (*) and mixed osteolytic-blastic changes.

a pathologic fracture with angulation and impaction in the right humerus, along with diffuse osteopenia and blastic changes in the proximal ulna. A pathologic fracture was also noted in the left femur, with expansile osteolytic changes along the midshaft and distal posterior aspect, accompanied by diffuse osteopenia. Additionally, mixed osteolytic-blastic changes were observed in the pelvis, which may suggest a metastatic process. A pathologic fracture was also noted in the right femoral neck. KUB ultrasound revealed bilateral nephrolithiasis. Additional diagnostic tests revealed multiple electrolyte imbalances (serum calcium: 14.03 mg/dL; serum potassium: 2.5 mmol/L; serum sodium: 135 mmol/L), anemia, elevated intact parathyroid hormone (546.96 pg/ml) level, hypothyroidism, and chronic renal failure (233 umol/L).

In the subsequent year, patient had undergone right inferior parathyroidectomy with en bloc total lobectomy, right frozen section biopsy and intraoperative iPTH for margin assessment and diagnosis. The specimen submitted for pathology consists of a single, intact, fresh, tan red to bright red, smooth and glistening parathyroid gland (3.1 x 2.3 x 1.6 cm) and left thyroid lobe (4.0 x 2.5 x 1.3 cm) Serial sections of the parathyroid gland show an encapsulated, tan gray to tan brown, slightly fleshy, homogenous, solid mass with lobulated appearance (Figure 3).

Histopathologic examination of the parathyroid gland revealed an encapsulated, well-delineated mass composed of tumor cells arranged in a solid growth pattern (Figures 4 and 6). The tumor cells exhibited distinct cytoplasmic membranes, moderately enlarged, irregularly round to ovoid vesicular nuclei, and inconspicuous to prominent nucleoli, with abundant eosinophilic cytoplasm. Broad fibrous bands were observed between tumor cells, and frequent mitotic figures were noted (Figures 5 and 9). Lymphovascular and capsular invasion were also present (Figures 7 and 8).

Along with the clinical and other diagnostic findings, the histomorphologic features are consistent with a diagnosis of parathyroid carcinoma. Immunohistochemical studies were performed to support the diagnosis, including GATA3, TTF-1, AE1/AE3, synaptophysin, chromogranin A, CEA, Ki-67, and PTH. The tumor cells showed strong nuclear reactivity with GATA3, a parathyroid-specific marker. Negative staining with TTF-1 further confirmed that the tumor is of parathyroid origin and excluded the differential diagnoses of well-differentiated or poorly differentiated thyroid carcinoma. Additionally, the negative staining with CEA ruled out medullary thyroid carcinoma.

Although strong cytoplasmic (granular) and nuclear expression of chromogranin A and GATA3, respectively, may suggest paraganglioma, the strong membranous expression of AE1/AE3 in this case ruled out this diagnosis. The immunoprofile, showing positive staining for GATA3, PTH, AE1/AE3, and chromogranin A, alongside negative staining for TTF-1, CEA, and synaptophysin, narrowed the differential diagnoses to parathyroid adenoma, atypical parathyroid adenoma, and parathyroid carcinoma.

However, the histomorphologic features, including moderate nuclear atypia, presence of macronucleoli,

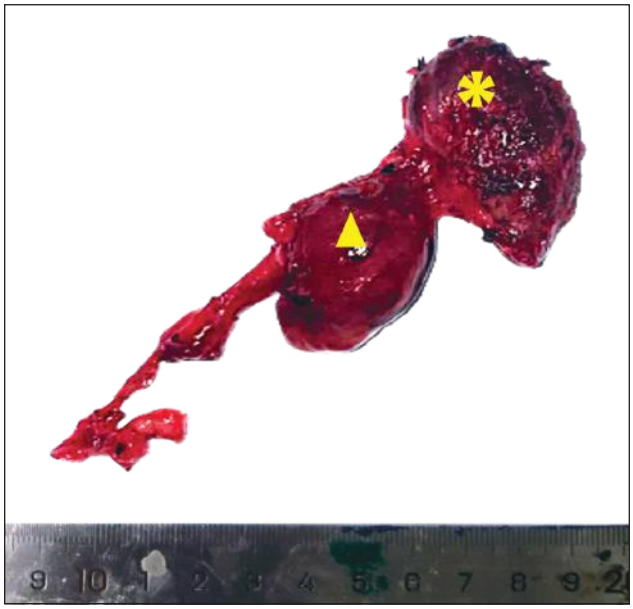

Figure 3. Gross appearance of the parathyroid gland (*) and left thyroid lobe (▲).

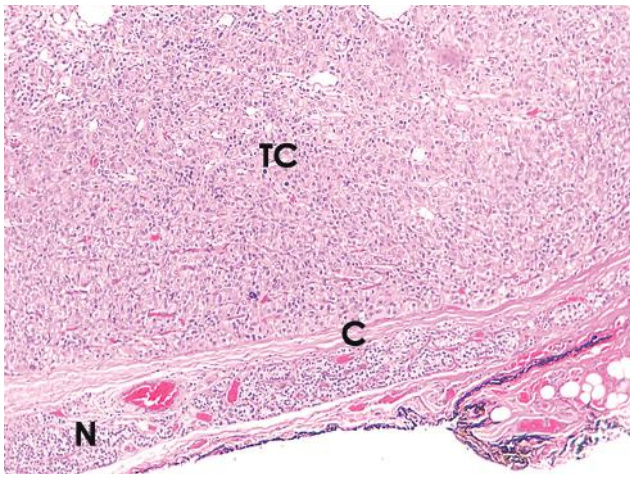

Figure 4. Encapsulated (C) mass showing uniform tumor cells (TC) in solid sheet growth pattern (H&E, 40x).

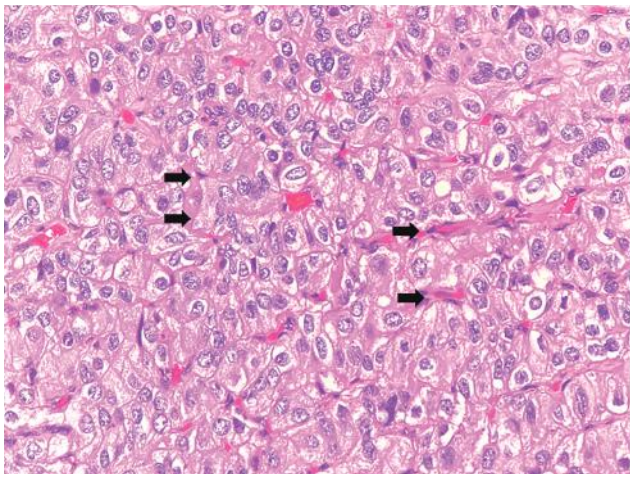

Figure 5. Uniform tumor cells with mild to moderate atypia. Seen also are dense fibrous bands (➡) between tumor cells (H&E, 100x).

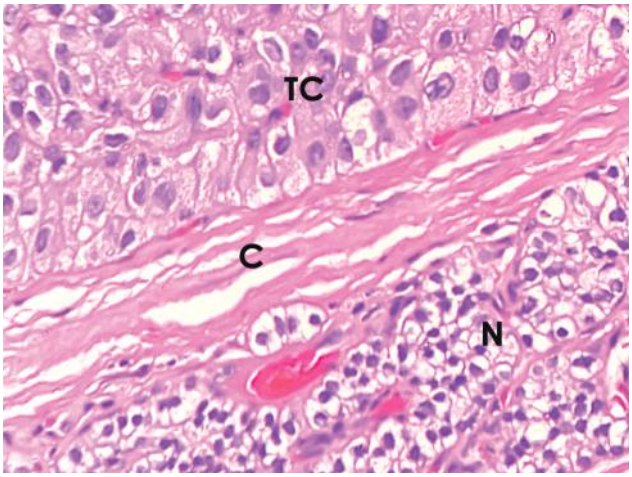

Figure 6. Transition between parathyroid tumor cells (TC) and remnant normal parathyroid tissue (N) (H&E, 40x).

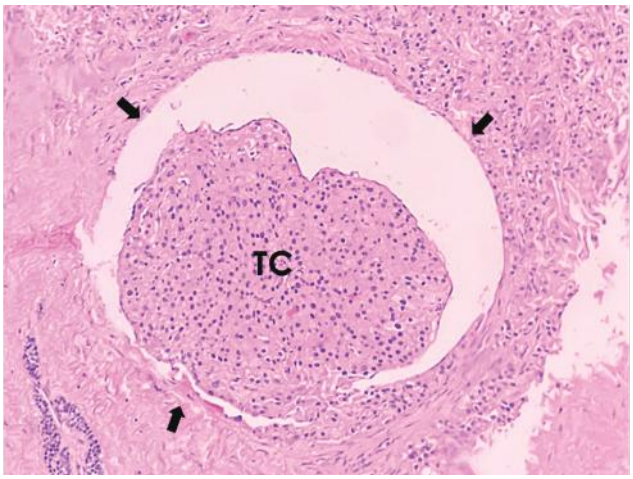

Figure 7. Lymphovascular invasion of tumor cells (H&E, 100x).

increased mitotic activity (>9/10 mm²), lymphovascular invasion (Figure 8F), and a high proliferative index (Ki-67: 10%), strongly support the diagnosis of parathyroid carcinoma.

Despite successful surgical intervention and multidisciplinary supportive management, the patient's clinical condition did not improve. Further treatment with radiation or systemic therapy was not pursued, as her condition became unstable several days after admission. She subsequently developed an acute myocardial infarction, which led to her demise.

DISCUSSION

Parathyroid carcinoma is an exceedingly rare endocrine malignancy, representing approximately 0.005% of all cancers and accounting for less than 1% of primary hyperparathyroidism cases.[1,2] While it can occasionally occur as part of genetic syndromes, it is more commonly sporadic.[3] Hereditary conditions linked to parathyroid carcinoma include hyperparathyroidism-jaw tumor (HPT-JT) syndrome, multiple endocrine neoplasia (MEN) syndromes, and non-syndromic familial isolated primary hyperparathyroidism (FIHP).[4] The mean age at diagnosis is 56 years (ranging from 15 to 89 years), with no significant sex predilection.[5,6] The youngest reported patient with parathyroid carcinoma was 13 years old. In the presented case, the patient was initially diagnosed with parathyroid carcinoma at the age of 19. Cases of parathyroid carcinoma are rarely documented, both in the Philippines and globally. Due to its rarity, there is no universally accepted standardized approach for diagnosis, prognosis, or treatment, and the TNM staging system is not consistently applied.[7,8]

Genomic alterations associated with parathyroid carcinoma (PC) are predominantly characterized by mutations in the **CDC73** germline gene, which encodes a loss-of-function protein known as parafibromin. Recent whole-exome sequencing studies of PC have revealed additional mutations in several other genes, including **mTOR, KMT2D, CDKN2C, THRAP3, PIK3CA,** and **EZH2**, as well as amplification of the **CCND1** gene. Notably, alterations in the **PI3K/AKT/mTOR** signaling pathway are frequently observed in the sporadic forms of parathyroid carcinoma.[9] In this case, the patient had no family history of hyperparathyroidism or parathyroid tumors.

It typically presents with severe symptomatic hypercalcemia, which is often associated with significant skeletal and renal complications. These may include multiple pathologic fractures, nephrolithiasis, and various electrolyte imbalances.[10] The extent of these complications can lead to substantial morbidity, highlighting the critical need for early recognition and intervention.

The diagnosis of parathyroid carcinoma remains challenging. Currently, histopathologic diagnosis is derived in parathyroid tumors that exhibit at least one of the following features: (1) angioinvasion (vascular invasion), (2) lymphatic invasion, (3) perineural invasion, (4) local malignant invasion into adjacent structures or organs, or (5) regional or distant metastasis.[11] In the present case, along with moderate nuclear atypia, the tumor exhibits macronucleoli, increased mitotic activity, a high Ki-67 index, and lymphovascular invasion. Clinical findings that may raise suspicion for malignancy include the presence of a palpable neck mass, a parathyroid gland larger than 3 cm, severe hypercalcemia (>12 mg/dL), markedly elevated parathyroid hormone (PTH) levels (more than three times the upper limit), and intraoperative adhesions.[12] If only some of these criteria are met, the tumor may be classified as an atypical parathyroid tumor.

Immunohistochemistry studies have been employed in the literature with variable diagnostic results, adding complexity to the diagnosis. Parathyroid carcinoma is typically characterized by the immunohistochemical loss of expression of markers such as parafibromin, APC, E-cadherin, p27, BCL2, MDM2, and 5-hydroxymethylcytosine. In contrast, positive expression of PGP9.5, galectin-3, and TERT is often observed. Parafibromin, encoded by the *CDC73/HRPT2* gene, is implicated in both hereditary hyperparathyroidism–jaw tumor syndrome and sporadic parathyroid carcinomas. Loss of parafibromin expression, typically resulting from *CDC73* mutations, has been associated with dysregulated cell proliferation, transcriptional control, and histone

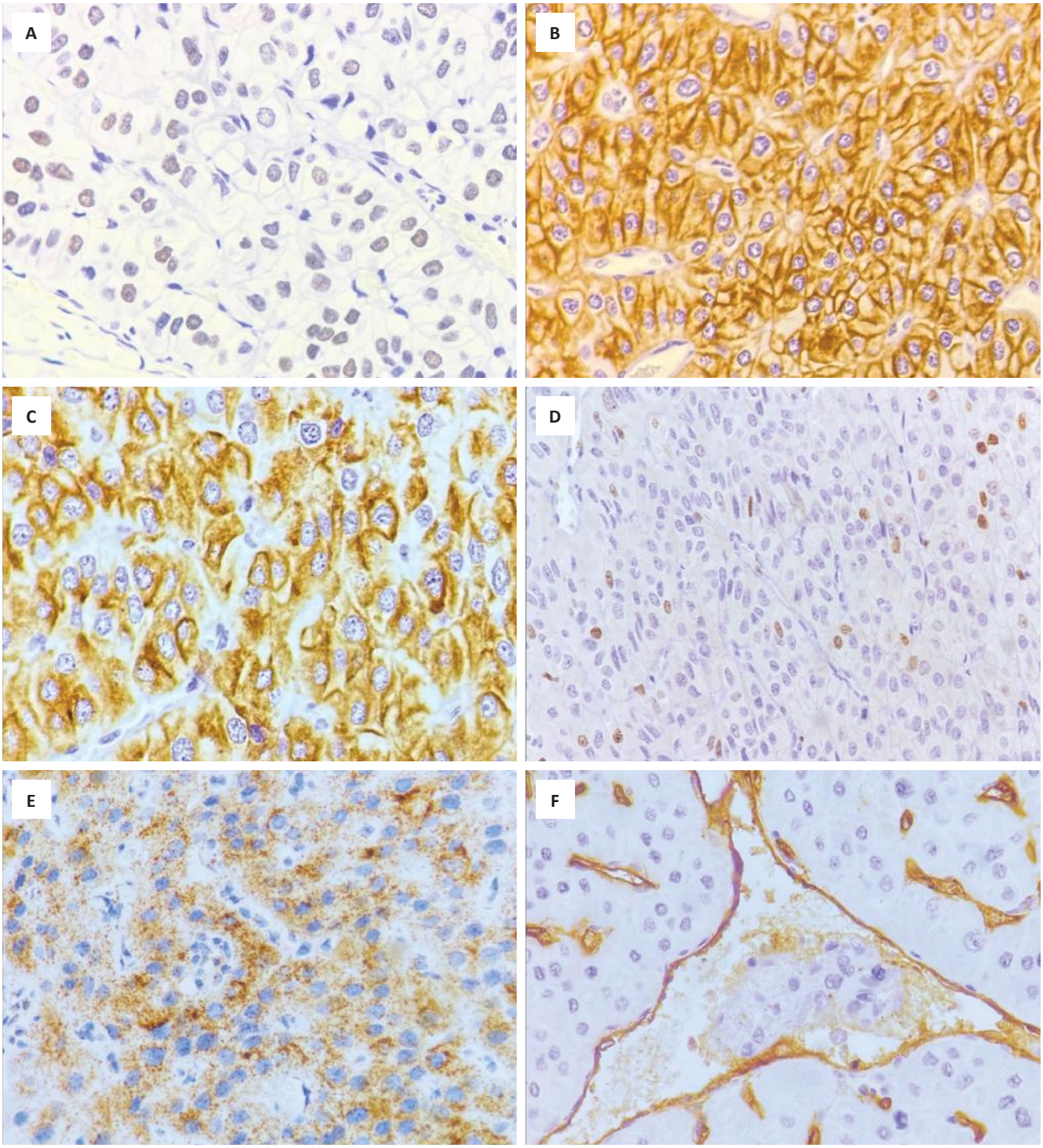

Figure 8. Immunohistochemical stains demonstrating weak and focal nuclear staining for GATA3 **(A)**; strong, diffuse membranous staining for pancytokeratin **(B)**; strong and diffuse cytoplasmic (granular) staining for chromogranin A **(C)**; nuclear staining for Ki-67 **(D)**; moderate, focal cytoplasmic granular staining for PTH **(E)**; and strong membranous staining for CD34, highlighting lymphovascular invasion **(F)** (all images at 400x magnification).

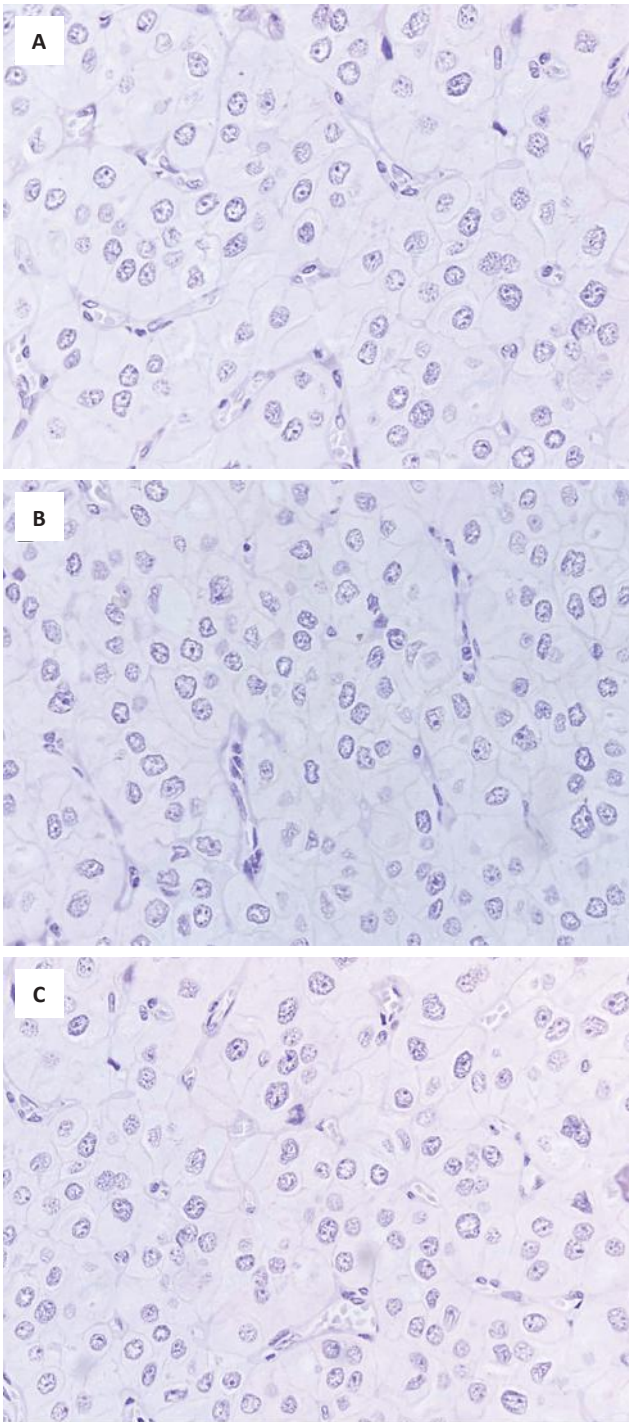

Figure 9. Immunohistochemical stains showing negative staining for TTF-1 **(A)**, synaptophysin **(B)**, and CEA **(C)** (all images at 400x magnification).

modification. However, the diagnostic utility of parafibromin immunohistochemistry (IHC) in parathyroid carcinoma remains variable.[13] Some studies reported loss of parafibromin expression in 29.1% of atypical parathyroid adenomas, a frequency intermediate between parathyroid carcinoma and parathyroid adenoma.[14] Thus, while parafibromin IHC is not definitive, it may serve as a supportive diagnostic adjunct in suspected parathyroid carcinoma. Additionally, there is frequently overexpression of p53 and an elevated Ki-67 labeling index, often exceeding 5%. While parathyroid hormone (PTH) is typically expressed in parathyroid carcinoma, its presence alone is not specific, as other neuroendocrine neoplasms can also demonstrate aberrant PTH staining. The co-expression of PTH and GATA3, however, can help confirm the parathyroid origin of the tumor. Similar to other epithelial neuroendocrine tumors, parathyroid carcinoma usually shows positive staining for cytokeratins and chromogranins.[11]

Parathyroid carcinoma typically exhibits an indolent and slowly progressive course, characterized by low rates of lymph node and systemic metastasis, but a higher incidence of local recurrence. Mortality is primarily attributed to complications arising from hypercalcemia, rather than the tumor burden itself.[2,15] According to the literature, the reported 5-year survival rate ranges from 76% to 85%, while the 10-year survival rate ranges from 49% to 77%.[6]

The primary treatment for parathyroid carcinoma is surgical excision of the tumor.[16] If there is a strong preoperative suspicion of parathyroid carcinoma, it is essential for the surgeon to consider more aggressive approaches, such as en bloc resection, to improve disease outcomes, as the prognosis is heavily influenced by the extent of surgical resection.[17,18] The surgical approach for parathyroid carcinoma consists of the en bloc resection of the primary tumor with negative margins, usually associated with the excision of ipsilateral thyroid lobes and adjacent involved structures.[19] For tumors that are not amenable to surgical removal, adjuvant treatments, including radiotherapy, chemotherapy, immunotherapy, and ablation, may be considered. Management of hypercalcemia often involves a combination of bisphosphonates, calcimimetic agents, and the osteoclast inhibitor denosumab.[15] Mortality from parathyroid carcinoma is typically linked to complications of hypercalcemia rather than the direct impact of tumor burden itself.

CONCLUSION

The diagnosis of parathyroid carcinoma continues to present significant challenges. Accurate diagnosis requires the integration of clinical, biochemical, radiologic, histomorphologic, and immunohistochemical findings. Parathyroid carcinoma is notably characterized by its tendency for recurrence and resistance to conventional treatment modalities. Despite its typically slow clinical progression, long-term surveillance and aggressive management strategies are often recommended to optimize patient outcomes. Given the rarity of parathyroid carcinoma, each case provides valuable insights that can help refine diagnostic approaches and treatment protocols. Documenting such cases is essential, as it contributes to the development of more effective strategies for managing future cases, ultimately improving patient care and survival outcomes.

ACKNOWLEDGMENTS

The authors would like to express their gratitude to all the pathologists and clinicians whose expertise contributed to this case.

ETHICAL CONSIDERATIONS

Patient consent was obtained before the submission of the manuscript.

STATEMENT OF AUTHORSHIP

All authors certified fulfilment of ICMJE authorship criteria.

AUTHOR DISCLOSURE

The authors declared no conflict of interest.

DATA AVAILABILITY STATEMENT

No datasets were generated or analyzed for this research.

FUNDING SOURCE

None.

REFERENCES

1. Lee PK, Jarosek SL, Virnig BA, Evasovich M, Tuttle TM. Trends in the incidence and treatment of parathyroid cancer in the United States. Cancer. 2007;109(9):1736-41. PMID: 17372919 DOI: 10.1002/cncr.22599
2. Ullah A, Khan J, Waheed A, et al. Parathyroid carcinoma: incidence, survival analysis, and management: a study from the SEER database and insights into future therapeutic perspectives. Cancers (Basel). 2022;14(6):1436. PMID: 35326576 PMCID: PMC8946517 DOI: 10.3390/cancers14061426
3. Zelano L, Locantore P, Rota CA, et al. Parathyroid carcinoma all-in-one, a rare life-threatening case with multiple systemic manifestations: case report and review of the literature. Front Endocrinol (Lausanne). 2022;13:881225. PMID: 35872978 PMCID: PMC9300921 DOI: 10.3389/fendo.2022.881225
4. Cardoso L, Stevenson M, Thakker RV. Molecular genetics of syndromic and non-syndromic forms of parathyroid carcinoma. Hum Mutat. 2017;38(12):1621-48. PMID: 28881068 PMCID: PMC5698716 DOI: 10.1002/humu.23337
5. Marcocci C, Cetani F, Rubin MR, Silverberg SJ, Pinchera A, Bilezikian JP. Parathyroid carcinoma. J Bone Miner Res. 2008;23(12):1869-80. PMID: 19016595 PMCID: PMC3276344 DOI: 10.1359/jbmr.081018
6. Shane E. Clinical review 122: parathyroid carcinoma. J Clin Endocrinol Metab. 2001;86(2):485-93. PMID: 11157996 DOI: 10.1210/jcem.86.2.7207
7. American Joint Committee on Cancer. AJCC cancer staging manual, 8th ed. Springer; 2017.
8. Fingeret AL. Contemporary evaluation and management of parathyroid carcinoma. JCO Oncol Pract. 2021;17(1):17-21. PMID: 32040373 DOI: 10.1200/JOP.19.00540
9. Hu Y, Liao Q, Cao S, Gao X, Zhao Y. Diagnostic performance of parafibromin immunohistochemical staining for sporadic parathyroid carcinoma: a meta-analysis. Endocrine. 2016;54(3):612-9. PMID: 27250989 DOI: 10.1007/s12020-016-0997-3
10. Perrier ND, Arnold A, Costa-Guda J, et al. Hereditary endocrine tumors: current state-of-the-art and research opportunities: new and future perspectives for parathyroid carcinoma. Endocr Relat Cancer. 2020;27(8):T53-63. PMID: 32449693 DOI: 10.1530/ERC-20-0018
11. World Health Organization. WHO classification of tumours: endocrine and neuroendocrine tumours, 5th ed. IARC Press; 2017.
12. Uljanovs R, Sinkarevs S, Strumfs B, Vidusa L, Merkurjeva K, Strumfa I. Immunohistochemical profile of parathyroid tumors: a comprehensive review. Int J Mol Sci. 2022;23(13):6981. PMID: 35805976 PMCID: PMC9266566 DOI: 10.3390/ijms23136981
13. Truran PP, Johnson SJ, Bliss RD, Lennard TW, Aspinall SR. Parafibromin, galectin-3, PGP9.5, Ki67, and cyclin D1: using an immunohistochemical panel to aid in the diagnosis of parathyroid cancer. World J Surg. 2014;38(11):2845-54. PMID: 25002250 DOI: 10.1007/s00268-014-2700-2
14. Pyo JS, Cho WJ. Diagnostic and prognostic implications of parafibromin immunohistochemistry in parathyroid carcinoma. Biosci Rep. 2019;39(4):BSR20181778. PMID: 30926677 PMCID: PMC6488858 DOI: 10.1042/BSR20181778
15. Machado NN, Wilhelm SM. Parathyroid cancer: a review. Cancers (Basel). 2019;11(11):1676. PMID: 31661917 PMCID: PMC6896123 DOI: 10.3390/cancers11111676
16. Cui M, Hu Y, Bi Y, et al. Preliminary exploration of potential molecular therapeutic targets in recurrent and metastatic parathyroid carcinomas. Int J Cancer. 2019;144(3):525-32. PMID: 30362515 DOI: 10.1002/ijc.31948
17. Ippolito G, Palazzo FF, Sebag F, De Micco C, Henry JF. Intraoperative diagnosis and treatment of parathyroid cancer and atypical parathyroid adenoma. Br J Surg. 2007;94(5):566-70. PMID: 17380564 DOI: 10.1002/bjs.5570
18. Long KL, Sippel RS. Current and future treatments for parathyroid carcinoma. Int J Endocr Oncol. 2018;5(1):IJE06. DOI: 10.2217/ije-2017-0011
19. Marini F, Giusti F, Palmini G, et al. Parathyroid carcinoma: update on pathogenesis and therapy. Endocrines. 2023;4(1):205-35. DOI: 10.3390/endocrines4010013

Cytogenetic Damage from E-cigarette Use: Buccal Micronucleus Frequencies and Policy Implications in the Philippines

Reality Araojo[1] and Norvie Jalani[2]

[1]*Ateneo De Zamboanga University-School of Medicine, Philippines*
[2]*Zamboanga City Medical Center, Philippines*

ABSTRACT

The rapid rise of e-cigarettes and vapes in the Philippines, especially after Republic Act No. 11900, has raised health concerns among youth. Though marketed as safer alternatives, their aerosols have been shown to cause harm. By measuring buccal micronucleus frequencies, this study found significantly higher counts in e-cigarette users compared to non-users, with secondhand smoke exposure independently associated with elevated genotoxic damage (adjusted OR 11.8; $p = 0.035$). The findings support stricter regulations and broader smoke-free policies to safeguard public health amid the growing use of electronic nicotine delivery systems.

Key words: e-cigarettes, buccal micronucleus, genotoxicity, youth vaping, tobacco regulation, Philippines

ISSN 2507-8364 (Online)
Printed in the Philippines.

Received: 21 April 2026.
Accepted: 16 May 2026.
Published online first: 25 June 2026.
https://doi.org/10.21141/PJP.2026.599

Corresponding author: Norvie T. Jalani, MD
E-mail: norviejalani@gmail.com
ORCiD: https://orcid.org/0000-0002-1642-4698

The human genome is constantly exposed to environmental and lifestyle-related genotoxins, making accessible biomarkers essential for early detection of chromosomal damage. The buccal mucosa, consisting of stratified squamous epithelial cells, is the first tissue to contact inhaled and ingested toxicants, making it a relevant site for monitoring aerodigestive exposures. The buccal micronucleus cytome (B-MNcyt) assay is a validated tool in molecular epidemiology for assessing chromosomal instability and early genotoxic damage. Micronuclei (MN) are formed from entire chromosomes or acentric fragments that do not incorporate into daughter nuclei during cell division. Their presence in exfoliated buccal cells indicates DNA damage in the basal epithelial layer that occurred 5-14 days prior to sampling. Although international research reports increased MN frequencies among e-cigarette users, there is limited local cytogenetic evidence in the Philippines. This study aimed to compare MN frequency between adult e-cigarette users and non-users in Southern Philippines and identify factors associated with elevated MN counts.

A study in the Southern Philippines, involving 62 adults (31 e-cigarette users and 31 non-smokers), examined buccal cells stained with Papanicolaou for micronuclei (MN). Micronuclei were identified and counted manually using a 5-headed electric light microscope by two independent raters blinded to group allocation, following the morphological criteria of Tolbert et al.[1] Inter-rater reliability was good (ICC = 0.770), and discrepancies were resolved through consensus review. Elevated MN was defined as ≥203 per 1,000 cells (Figure 1). This threshold was determined empirically as the 85th percentile of the combined cohort MN distribution (n = 62), since standard reference values were not suitable given the notably elevated baseline MN frequencies observed in both groups, likely reflecting shared environmental exposures in this urban population.[2] The dichotomized outcome (elevated vs not elevated) served as the dependent variable in the regression analyses. Binary logistic regression

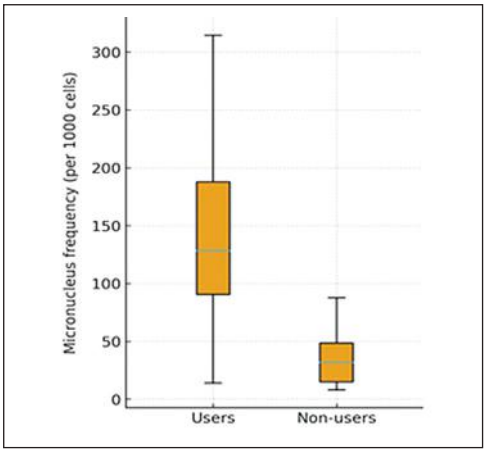

Figure 1. Boxplot of micronucleus frequencies among e-cigarette users and non-users.

Table 1. Regression analysis predictors of elevated micronucleus counts (≥203/1000 cells, n = 30)

Variable	Crude OR (95% CI)	*p*-value	Adjusted OR (95% CI)	*p*-value
Age (20-29)	3.3 (0.6-19.5)	0.551	1.2 (0.1-86.6)	0.934
Male sex	13.5 (1.4-128.3)	0.023*	8.5 (0.2-638.1)	0.178
Islamic faith	7.0 (1.3-37.9)	0.024*	1.7 (0.07-24.2)	0.704
Ethnicity	3.3 (0.6-19.5)	0.192	5.9 (0.2-221.8)	0.340
Socioeconomic status	0.5 (0.1-2.5)	0.402	3.9 (0.2-135.3)	0.432
Alcohol consumption	0.6 (0.1-3.3)	0.544	0.6 (0.003-10.7)	0.821
Secondhand smoke	16.0 (2.4-106.7)	0.004**	11.8 (2.2-72.0)	0.035*
Tooth brushing	0.7 (0.1-5.1)	0.730	0.6 (0.002-6219.8)	0.882
Daily flossing	0.6 (0.1-3.3)	0.544	0.7 (0.002-57.4)	0.877
Mouthwash use	1.9 (0.4-9.6)	0.432	2.5 (0.03-376.2)	0.695
Vegetable consumption	1.3 (0.2-6.4)	0.784	2.8 (0.07-21811)	0.655
Fruit consumption	2.7 (0.4-16.0)	0.283	0.8 (0.02-13.1)	0.865

*p <0.05; **p <0.01
Crude analysis: Binary logistic regression.
Adjusted analysis: Firth's bias-reduced logistic regression.

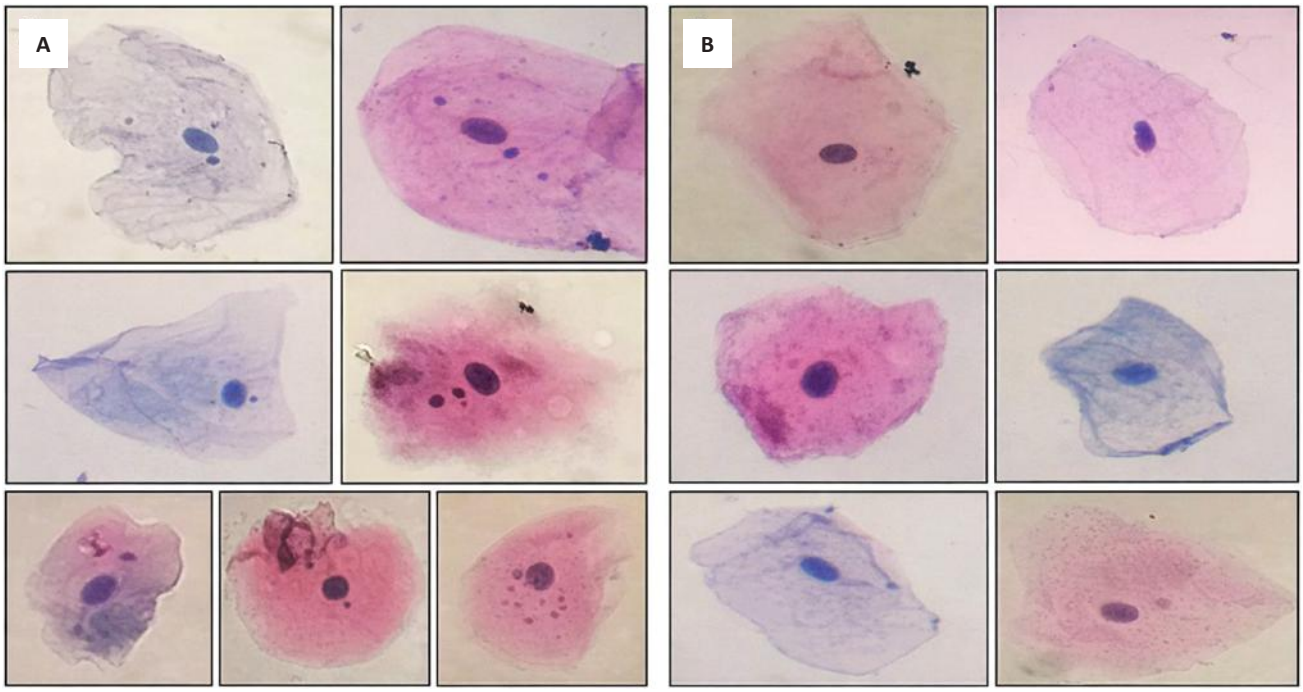

Figure 2. Buccal epithelial cells showing micronuclei among **(A)** e-cigarette users and **(B)** non-users (Papanicolaou stain, 400x).

was used for crude estimates, and Firth's bias-reduced logistic regression for adjusted estimates, selected to address potential complete or quasi-complete separation and ensure reliable parameter estimates given the small case-control subsample (n=30, 10 cases and 20 controls). Results indicated that e-cigarette users had significantly higher MN levels (152.3 ± 102.6 versus 34.9 ± 28.5; p <0.001). Regression analysis showed that secondhand smoke exposure was associated with elevated MN (adjusted OR 11.8; p = 0.035) (Table 1). Pearson's correlation found no significant relationships between continuous MN counts and vaping duration, frequency, device type, puff topography, or nicotine concentration among users (all p-values >0.05). These null findings should be interpreted cautiously, given the limited sample size (n = 31), which may have been insufficient to detect weak-to-moderate dose-response relationships. The possibility that genotoxic injury follows a threshold model warrants investigation in larger, adequately powered studies.[3,4]

A key finding was the independent association between secondhand smoke exposure and elevated MN counts. Vapers exposed to environmental tobacco smoke faced nearly twelve times the risk of higher MN counts compared to those without exposure. This association might be due to the inflamed state of the buccal mucosa in e-cigarette users, which reduces the cellular threshold for reacting to additional toxicants in combustible tobacco smoke. These findings have important public health implications, emphasizing that strict enforcement of smoke-free laws is necessary to protect individuals already experiencing baseline genotoxic stress from vaping.[5-7]

The rise of EVALI cases in the Philippines coincides with the surge in youth vaping, underscoring the urgent need for product safety monitoring. Data indicate a 110% increase in e-cigarette prevalence among Filipino youth between 2015 and 2019, and this trend has only accelerated with the recent legislative changes.[8] Experts from the Philippine Pediatric Society warn that 1 out of every 7 Filipino youths aged 13-15 is now using e-cigarettes.[7] Adolescents are particularly vulnerable to the genotoxic effects of aerosols because their tissues are still undergoing rapid growth and differentiation. Furthermore, the high prevalence of daily use among youth, often driven by fruit and candy flavors, prolongs exposure to carbonyls and metals during a critical window of biological development.[9]

The enactment of Republic Act No. 11900 in 2022 significantly reshaped the regulation of electronic nicotine delivery systems (ENDS) and heated tobacco products (HTPs) in the Philippines. A key feature of the law is the transfer of regulatory authority from the Food and Drug Administration (FDA) to the Department of Trade and Industry (DTI), shifting oversight from a health-based to a trade-oriented framework. This change has raised concerns regarding the adequacy of toxicological and genotoxic evaluation of vaping products.[10] RA 11900 also reduced the minimum age for purchase and use of vaping products from 21 to 18 years, expanding access to adolescents and young adults whose respiratory and neurological systems remain developmentally vulnerable. Although the law restricts youth-oriented flavor descriptors, it does not prohibit flavored products themselves, allowing the continued availability of fruit, dessert, and menthol variants, which are strongly associated with youth initiation. Local buffer-zone regulations around schools further face enforcement challenges, with retail proximity and point-of-sale marketing remaining common. Given emerging biological evidence of vaping-associated genotoxicity and compounded risk from secondhand smoke exposure, these regulatory gaps warrant reassessment. Incorpo-rating cost-effective biomarkers, such as the buccal micronucleus cytome assay, into community surveillance may provide early warning of harm.[11] The present findings support strengthening aerosol-free public space policies, reinforcing age protections, and aligning regulations with health-centered risk assessment.[12]

The study of buccal micronucleus levels among e-cigarette users and non-users in the Southern Philippines highlights the serious biological effects of vaping. Higher MN counts suggest that vapers' oral mucosa is experiencing early chromosomal instability, a known cancer precursor. The absence of a dose-response relationship raises the possibility that no level of vaping is entirely safe for genetic health, though this interpretation requires confirmation in larger, adequately powered studies. Secondhand smoke exposure adds to the risk, creating a double burden for those in shared environments. A limitation of this study is that the 203/1000 cells cut-off is population-specific, derived from local cohort data, and may not be applicable in other settings.

As the Philippines faces increasing EVALI cases and a significant surge in teen vaping, the current law, RA 11900, urgently calls for revision. Its focus on trade over toxicology and weaker protections for minors have contributed to an environment that may promote nicotine addiction and cellular damage. Replacing it with health-centered regulations, expanding aerosol-free policies, and adopting genomic monitoring tools like the B-MNcyt assay can foster a more science-driven public health approach. This strategy should prioritize the long-term biological health of Filipinos. The evidence of DNA damage in the buccal cells of young Filipinos highlights the urgent need for policymakers to treat health rights as a fundamental national priority.

STATEMENT OF AUTHORSHIP

Both authors certified fulfillment of ICMJE authorship criteria.

AUTHORSHIP DISCLOSURE

The authors declared no conflict of interest.

DATA AVAILABILITY STATEMENT

Datasets generated and analyzed are included in the published article.

FUNDING SOURCE

None.

REFERENCES

1. Tolbert PE, Shy CM, Allen JW. Micronuclei and other nuclear anomalies in buccal smears: methods development. Mutat Res. 1992;271(1):69-77. PMID: 1371831 DOI: 10.1016/0165-1161(92)90033-i
2. Ribeiro D. Evidence of genotoxicity and cytotoxicity of X-rays in the oral mucosa epithelium of adults subjected to cone beam computed tomography. Dentomaxillofac Radiol. 2019;48(6):20180299. PMID: 30285478 PMCID: PMC6747437 DOI: 10.1259/dmfr.20180299
3. Tadin A, Stazic V, Galic N, Zeljezic D. Evaluation of cytotoxic and genotoxic effects in buccal mucosal cells in non-smokers and users of traditional combustible tobacco products and non-combustible alternatives. J Xenobiot. 2024;14(1):154-65. PMID: 38249106 PMCID: PMC10801550 DOI: 10.3390/jox14010009
4. Toxicological Effects of Methylmercury. Toxicological effects of methylmercury. Washington, DC: National Academies Press; 2000. Chapter 5, Health effects of methylmercury. Bookshelf ID: NBK225765/
5. Salih MM, Tamr TA, Elmissbah TE, Hanafy SM, Dahlawi HA, Khalifa EH. Comparative analysis of cytological changes in the buccal mucosa among traditional cigarette and electronic cigarette users. Tob Induc Dis. 2025;23. PMID: 40552062 PMCID: PMC12184094 DOI: 10.18332/tid/203670
6. Szumilas P, Wilk A, Szumilas K, Karakiewicz B. The effects of e-cigarette aerosol on oral cavity cells and tissues: a narrative review. Toxics. 2022;10(2):74. PMID: 35202260 PMCID: PMC8878056 DOI: 10.3390/toxics10020074

7. Dai H. Exposure to secondhand aerosol from electronic cigarettes among US youth from 2015 to 2018. JAMA Pediatr. 2020;174(3):298-300. PMID: 31985771 PMCID: PMC6990747 DOI: 10.1001/jamapediatrics.2019.5665
8. Philippine News Agency. Experts warn youth lung injury crisis due to vaping. Published on April 12, 2024. Accessed January 27, 2026. https://www.pna.gov.ph/articles/1222493
9. Southeast Asia Tobacco Control Alliance (SEATCA). Philippines: 22-year-old's senseless death while denials on vape harms persist. TobaccoWatch. Published June 24, 2024. Accessed January 27, 2026. https://tobaccowatch.seatca.org/index.php/2024/06/25/philippines-22-year-olds-senseless-death-while-denials-on-vape-harms-persist/
10. House of Representatives of the Philippines. House Resolution No. 43: Resolution directing the appropriate committee to conduct an inquiry, in aid of legislation, on the effective implementation of Republic Act No. 11900, otherwise known as the Vaporized Nicotine and Non-Nicotine Products Regulation Act. Published 2025. Accessed January 27, 2026. https://docs.congress.hrep.online/legisdocs/basic_20/HR00043.pdf
11. Yadav AS, Jaggi S. Buccal micronucleus cytome assay - a biomarker of genotoxicity. J Mol Biomark Diagn. 2015;6(3):1-6. DOI: 10.4172/2155-9929.1000236
12. Republic of the Philippines. Republic Act No. 11900: Vaporized Nicotine and Non-Nicotine Products Regulation Act. Official Gazette of the Republic of the Philippines. Published July 25, 2022. Accessed January 27, 2026.

Nonmass Lesion on Breast Ultrasound: A Protean Finding

Ma. Theresa Buenaflor[1] and David Elijah Saguil[2]

[1]*Women's Health Department, Healthway Cancer Care Hospital, Taguig City, Philippines*
[2]*Department of Pathology, Healthway Cancer Care Hospital, Taguig City, Philippines*

Key words: nonmass lesion, breast ultrasound

ISSN 2507-8364 (Online)
Printed in the Philippines.

Received: 14 May 2026.
Accepted: 13 June 2026.
Published online first: 25 June 2026.
https://doi.org/10.21141/PJP.2026.643

Corresponding author: Ma. Theresa S. Buenaflor, MD
E-mail: buenates2@gmail.com
ORCiD: https://orcid.org/0000-0001-7257-1265

INTRODUCTION

The 2025 version of the Breast Imaging Reporting and Data System (BI-RADS) has undergone significant structural changes since 2013. Among the notable changes is the inclusion of Nonmass lesion (NML) on breast ultrasound. It is characterized as a discrete finding that is distinctly different from normal tissue but lacks the margins of a mass and cannot be assigned a specific shape.[1]

Nonmass lesion was first described in 2004 by the Japanese Association of Breast and Thyroid Sonology and has since undergone multiple classifications by different authors. A recent description by the Japan Society of Ultrasonics in Medicine encompasses the following findings: a hypoechoic area in the mammary gland, duct abnormalities, architectural distortion, multiple small cysts, and echogenic foci without a hypoechoic area.[2]

Nonmass lesions may be observed when ultrasound is used to further evaluate mammographic findings of asymmetries, suspicious calcifications, and findings of nonmass enhancement on MRI and contrast-enhanced mammogram (CEM).[3]

NML on ultrasound correlate with more than 50% of developing asymmetries on mammogram;[4] 21.4% of hypoechoic nonmass lesions or posterior shadowing correlated with architectural distortion.[5] About 39% of nonmass lesion correspond to nonmass enhancement on MRI.[6]

A nonmass lesion exhibits variable echogenicity and distribution. It may present as duct abnormalities involving single or multiple dilated ducts and may also have associated features such as echogenic foci, architectural distortion, posterior shadowing, or multiple cysts.[2]

The incidence of nonmass lesions ranges from 1-10%[2] and may signal malignancy in 6.3 – 54% of cases.[7]

The differential diagnoses of NMLs include benign processes such as fibrocystic changes, inflammation, postoperative scars, and biopsy scars.[8]

Ductal carcinoma in situ (DCIS) and invasive lobular cancer (ILC) comprise the most common malignancies presenting as nonmass lesions.[2] Twenty five to sixty one percent (25-61%) of DCIS present as NML on ultrasound.[9] High-grade DCIS comedo type is considered if there is posterior shadowing associated with clumped microcalcifications.[10] Nonmass findings of invasive lobular carcinoma may present as posterior shadowing only or

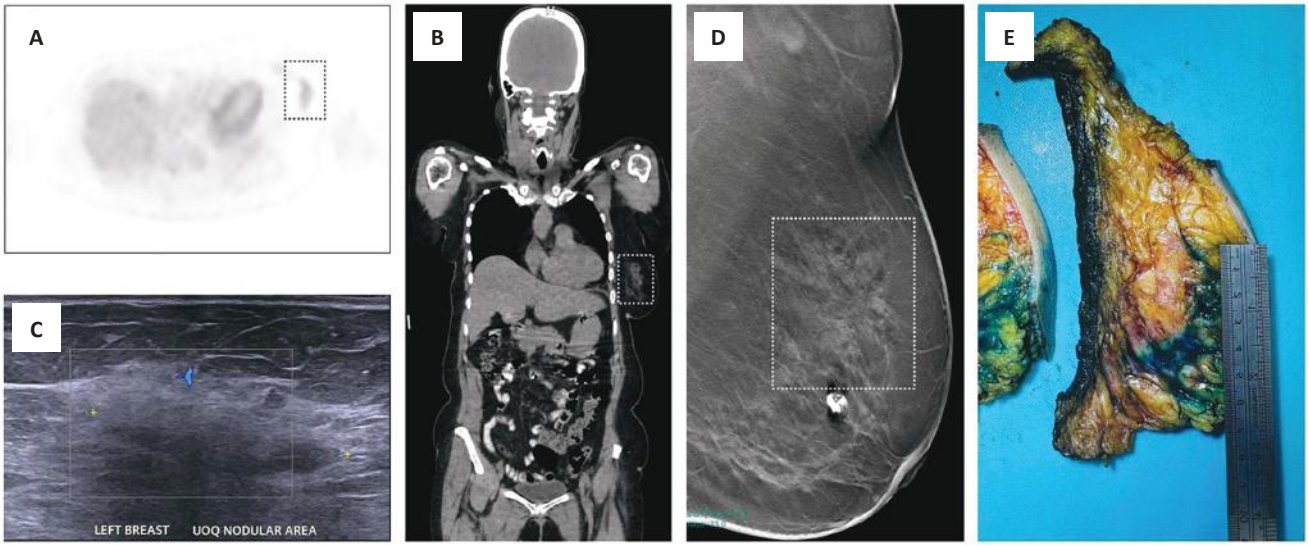

Figure 1. Selected images of her surveillance PET-CT images showed nonmass uptake in the upper outer quadrant of the left breast **(A, B)** corresponding to a hypoechoic nonmass lesion with shadowing on ultrasound **(C)**. MLO view of her digital breast tomosynthesis **(D)** demonstrated an architectural distortion *(box)* at the superior aspect of the left breast. Gross specimen **(E)** defined the lesion as the inked area.

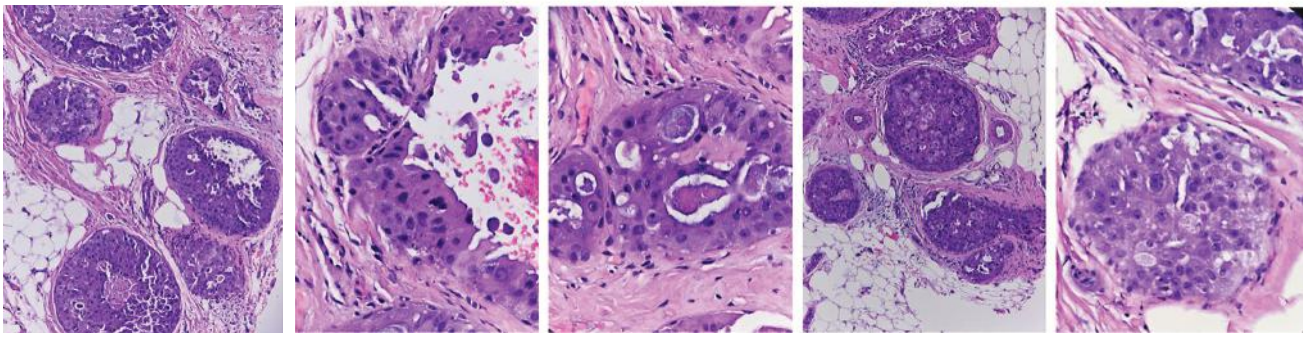

Figure 2. H & E of the needle core biopsy showing high-grade ductal carcinoma in situ (DCIS) on 100x magnification **(A)** showing comedo **(B)**, cribriform **(C)**, micropapillary **(D)** and solid **(E)** patterns.

manifest as hypoechoic inhomogeneous areas consistent with noncohesive and infiltrative growth pattern of ILC.[11]

LOCAL EXPERIENCE

The first case (Figure 1) demonstrates multimodality imaging findings of a 72-year-old female who is post-mastectomy of the right.

Post-cancer treatment changes and residual lesions after chemotherapy may also present as nonmass lesions (Figure 2).[2] This represents one of the challenging aspects of breast cancer care.

An example of this is the second case (Figure 3) of a 61-year-old female diagnosed with triple negative breast cancer in the left breast.

Radiologists use the Response Evaluation Criteria in Solid Tumor (RECIST 1.1) to document response to neo-adjuvant chemotherapy. Complete response (CR) is defined as the disappearance of all the target tumors while a partial response (PR) shows at least a 30% decrease in diameter of the tumor.[12]

In a study by Woo et al, radiologic complete response (breast rCR) is defined as disappearance of the breast tumor. If residual disease is observed on follow-up imaging, it is labelled as breast non-rCR.[13]

However, radiologic response is not equivalent to pathologic response. The latter remains as the gold standard in assessing residual tumor burden. In the 8th edition of the American Joint Committee on Cancer (AJCC), tumor size is based on the largest contiguous focus of residual tumor cells, excluding intervening treatment-related fibrosis.[14] It is not the extent of residual tumor foci spanning areas with treatment-related fibrosis.[15]

In a study involving one hundred female patients with breast cancer,[16] the prevalent morphological changes after chemotherapy are fibrosis and elastosis/collagenization

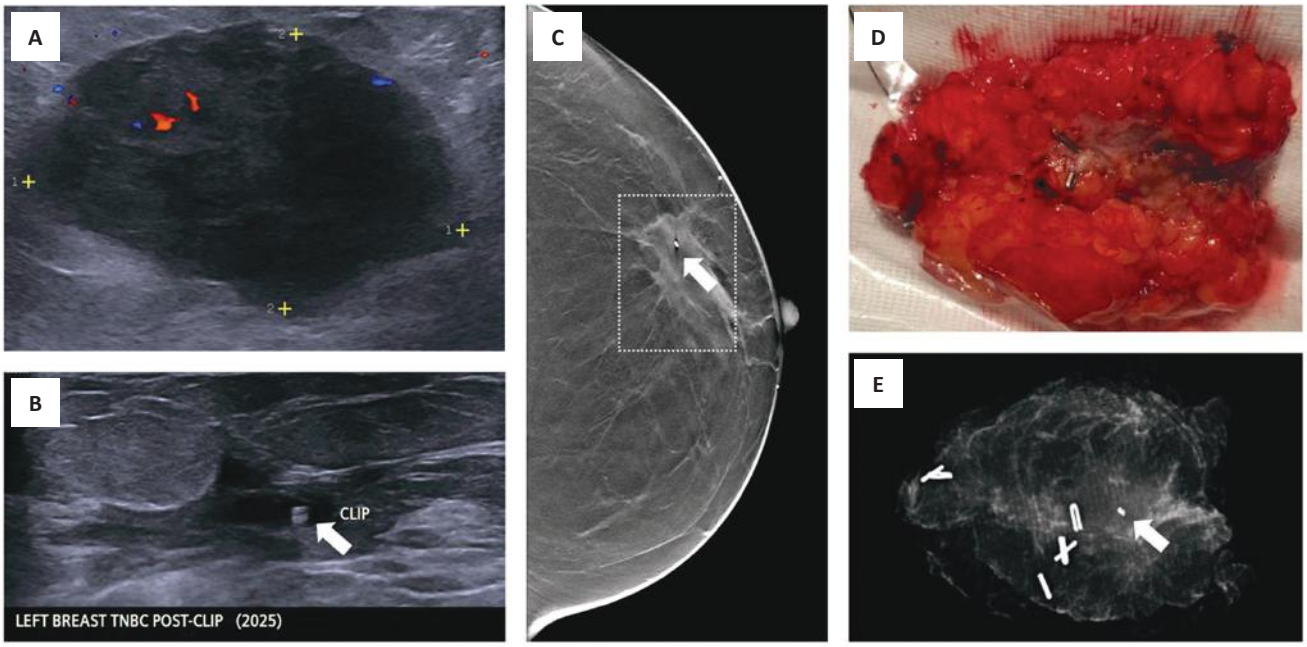

Figure 3. Initial breast ultrasound **(A)** showed an irregular hypoechoic solid mass prior to clip marking. She underwent neoadjuvant chemotherapy and on follow-up ultrasound **(B)**, a hypoechoic nonmass lesion was now noted with the clip visible *(arrow)*. CC view of her digital breast tomosynthesis **(C)** showed an asymmetry at the outer left breast. She then underwent partial mastectomy. Gross specimen **(D)** and the corresponding specimen mammogram **(E)** showing both the lesion and the metallic clip.

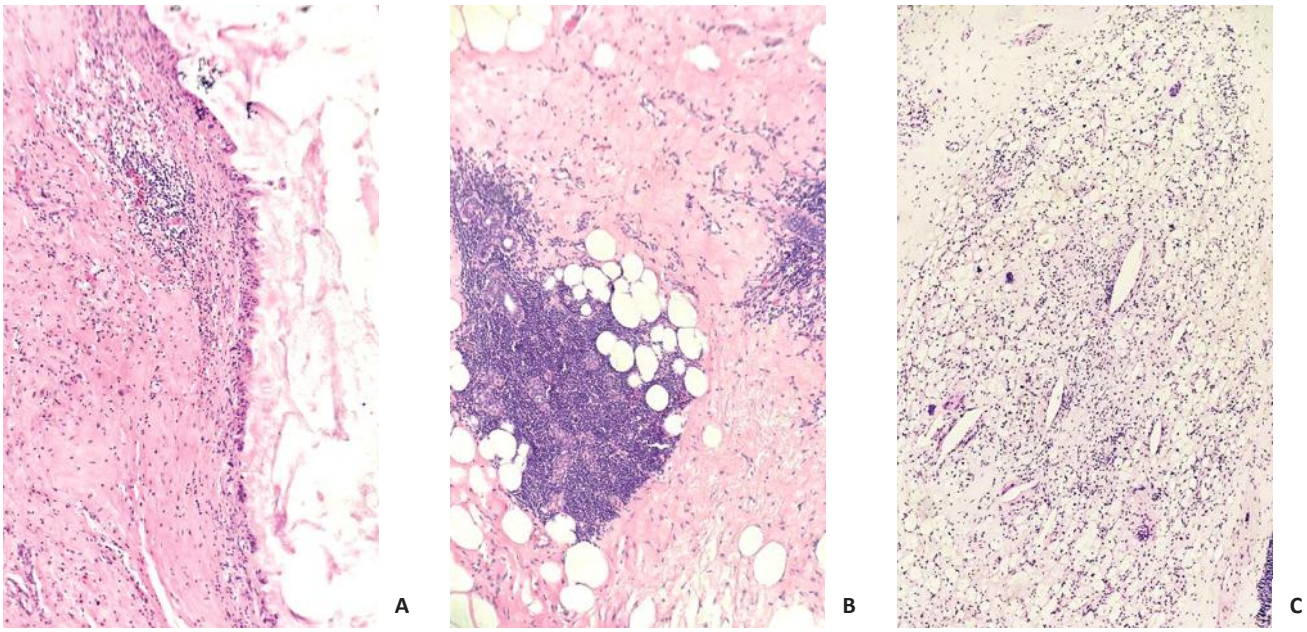

Figure 4. H & E 100x magnification showing **(A)** the area of the biopsy cavity with inflammation, fibrosis, and cystic contents; **(B)** shows intralobular stroma with dense lymphocytic infiltration while the interlobular stroma shows fibrosis. Other findings include **(C)** an area with aggregates of foamy histiocytes with scattered foreign-body type giant cells and cholesterol clefts.

in the stroma. Nuclear alterations are predominantly pyknosis and hyperchromasia.

In the second case, although a nonmass lesion was identified on ultrasound after chemotherapy, the final histopathology showed no residual carcinoma, and findings are illustrated in Figure 4.

DIAGNOSTIC INSIGHT

The management of breast cancer is continually evolving as evidenced by the evolution of its imaging and the emergence of new descriptors such as non-mass lesion on breast ultrasound. A team-based approach with close coordination among clinicians, radiologists and pathologists, is critically integral to optimizing patient care.

CONCLUSION

Cancer is a moving target, and we must not lose sight of it. Although a definitive mass or a protean nonmass lesion may appear at different points of care, as diagnosticians, our common goal remains the same: to identify and characterize it.

ACKNOWLEDGMENTS

The authors extend their thanks to the breast surgeon colleagues from the Women's Health Department, Healthway Cancer Care Hospital, Dr. Aldine Astrid A. Basa, MD, FPCS and Dr. Chris Evert R. Valdez, MD, FPCS.

STATEMENT OF AUTHORSHIP

All authors certified fulfillment of ICMJE authorship criteria.

AUTHOR DISCLOSURE

The authors have no conflict of interest.

DATA AVAILABILITY STATEMENT

Datasets generated and analyzed are included in the published article.

FUNDING SOURCE

None.

REFERENCES

1. American College of Radiology. Breast imaging reporting and data system. Accessed January 5, 2026. https://www.acr.org/Clinical-Resources/Clinical-Tools-and-Reference/Reporting-and-Data-Systems/BI-RADS
2. Mohan SL, Dhamija E, Gauba R. Approach to nonmass lesions on breast ultrasound. Indian J Radiol Imaging. 2024;34(4):677-87. PMID: 39318554 PMCID: PMC11419763 DOI: 10.1055/s-0044-1779589
3. Choi JS, Tsunoda H, Moon WK. Nonmass lesions on breast US: an international perspective on clinical use and outcomes. J Breast Imaging. 2024;6(1):86-98. PMID: 38243857 DOI: 10.1093/jbi/wbad077
4. Giess CS, Chesebro Al, Chikarmane SA. Ultrasound features of mammographic developing asymmetries and correlation with histopathologic findings. AJR Am J Roentgenol. 2018;210(1):W29-38. PMID: 29064753 DOI: 10.2214/AJR.17.18223
5. Bahl M, Baker JA, Kinsey EN, Ghate SV. Architectural distortion on mammography: correlation with pathologic outcomes and predictors of malignancy. AJR Am J Roentgenol. 2015;205(6):1339-45. PMID: 26587943 DOI: 10.2214/AJR.15.14628
6. Sotome K, Yamamoto Y, Hirano A, et al. The role of contrast enhanced MRI in the diagnosis of non-mass image-forming lesions on breast ultrasonography. Breast Cancer. 2007;14(4):371-80. PMID: 17986802 DOI: 10.2325/jbcs.14.371
7. Yamaguchi R, Watanabe H, Mihara Y, Yamaguchi M, Tanaka M. Histopathology of non-mass-like breast lesions on ultrasound. J Med Ultrason (2001). 2023;50(3):375-80. PMID: 36773105 PMCID: PMC10354136 DOI: 10.1007/s10396-023-01286-y
8. Hong S, Li W, Gao L, et al. Diagnostic performance of elastography for breast non-mass lesions: a systematic review and meta-analysis. Eur J Radiol. 2021;144:109991. PMID: 34638081 DOI: 10.1016/j.ejrad.2021.109991
9. Jin ZQ, Lin MY, Hao WQ, et al. Diagnostic evaluation of ductal carcinoma in situ of the breast: ultrasonographic, mammographic and histopathologic correlations. Ultrasound Med Biol. 2015;41(1):47-55. PMID: 25479813 DOI: 10.1016/j.ultrasmedbio.2014.09.023
10. Gunawardena DS, Burrows S, Taylor DB. Non-mass versus mass-like ultrasound patterns in ductal carcinoma in situ: is there an association with high-risk histology? Clin Radiol. 2020;75(2):140-7. PMID: 31739979 DOI: 10.1016/j.crad.2019.10.009
11. Selinko VL, Middleton LP, Dempsey PJ. Role of sonography in diagnosing and staging invasive lobular carcinoma. J Clin Ultrasound. 2004;32(7):323-32. PMID: 15293298 DOI: 10.1002/jcu.20052
12. Eisenhauer EA, Therasse P, Bogaerts J, et al. New response evaluation criteria in solid tumours: revised RECIST guideline (version 1.1). Eur J Cancer. 2009;45(2):228-47. PMID: 19097774 DOI: 10.1016/j.ejca.2008.10.026
13. Woo J, Ryu J, Jung SM, et al. Breast radiologic complete response is associated with favorable survival outcomes after neoadjuvant chemotherapy in breast cancer, Eur J Surg Oncol. 2021;47(2):232-9. PMID: 33213958 DOI: 10.1016/j.ejso.2020.08.023
14. Hortobagyi GN, Connolly JL, D'Orsi CJ, et al. Breast. In: Amin MB, Edge SB, Greene FL, et al, eds. AJCC Cancer Staging Manual, 8th ed. Springer; 2017.
15. Harter D, O'Connor SM, Hertel JD, Calhoun BC. Pathological measurement and staging of residual breast cancer after neoadjuvant chemotherapy. Histopathology. 2023;83(3):453-64. PMID: 37256703 PMCID: PMC10524558 DOI: 10.1111/his.14966
16. Ahuja S, Kiruthikasri G, Zaheer S. Evaluation of histomorphological changes in breast cancer post-neoadjuvant chemotherapy. Indian J Surg Oncol. 2024;15(2):236-40. PMID: 38741627 PMCID: PMC11088595 DOI: 10.1007/s13193-024-01876-3

Instructions to Authors

The **Philippine Journal of Pathology (PJP)** is an open-access, peer-reviewed, English language, medical and health science journal that is published continuously online and semi-annually in print by the Philippine Society of Pathologists, Inc. (PSP, Inc). All manuscripts must be submitted through the PJP Official Website (Open Journal Systems) (http://philippinejournalofpathology.org). All other correspondences and other editorial matters should be sent via electronic mail to philippinepathologyjournal@gmail.com.

Articles and any other material published in the PJP represent the work of the author(s) and do not reflect the opinions of the Editors or the Publisher. **Articles that do not subscribe to the Instructions to Authors shall be promptly returned.**

ARTICLE SECTIONS

The PJP welcomes manuscripts on all aspects of pathology and laboratory medicine, to include cytology, histopathology, autopsy, forensic pathology, clinical chemistry, clinical microscopy, medical microbiology, parasitology, immunology, hematology, blood banking, medical technology, laboratory diagnostics, laboratory biosafety and biosecurity, laboratory management, and quality assurance.

The PJP accepts original articles, review articles, case reports, feature articles, brief communications, autopsy cases, editorials, or letters to the Editor.

Original articles
The research must have received institutional review board approval that is explicitly stated in the methodology. The abstract should contain no more than 200 words with a structured format consisting of the objective/s, methodology, results and conclusion. A manuscript for original articles should not exceed 25 typewritten pages (including tables, figures, illustrations and maximum of 30 references) or 6000 words.

Reviews
Review articles, both solicited and unsolicited, provide information on the "state of the art." PJP reviews not only summarize current understanding of a particular topic but also critically appraise relevant literature and data sources, describe significant gaps in the research, and future directions. The abstract should be from 50 to 75 words and should not be structured. A manuscript for reviews should not exceed 15 typewritten pages (including tables, figures, illustrations and maximum of 50 references) or 4000 words.

Case Reports
This type of article pertains to single or multiple reports of well-characterized cases that are highly unusual, novel, or rare; or with a unique or variant presentation, evolution or course; or that represent an unexpected or uncommon association of two or more diseases or disorders that may represent a previously unsuspected causal relationship; or that are underreported in the literature. The abstract should be from 50 to 75 words and should not be structured. A manuscript for case reports should not exceed 10 typewritten pages (including tables, figures, illustrations and maximum of 15 references) or 3000 words.

Feature articles
The PJP may feature articles, either as part of an issue theme or a special topic on pathology by a local or international expert or authority. The abstract should be from 50 to 75 words and should not be structured. A manuscript for feature articles should not exceed 25 typewritten pages (including tables, figures, illustrations and maximum of 30 references) or 6000 words.

Autopsy Vault
The PJP highly welcomes articles on autopsy protocols of cases. The article must include a summary presentation of the history, evaluation and work-up, clinical course of a case, followed by the autopsy procedure performed, gross and microscopic findings, discussion, learning points and conclusion. The PJP recognizes the instructional and educational value of articles under this section. The abstract should be from 50 to 75 words and should not be structured. A manuscript for the Autopsy Vault should not exceed 25 typewritten pages (including tables, figures, illustrations and maximum of 30 references) or 6000 words.

Images in Pathology
Images of unique, interesting, or highly educational cases encountered in hematology, cytology, histopathology, or medical microbiology, may be submitted under this section, and may include photomicrographs, gross pictures, machine read-outs, among others. A brief history, the photograph(s) and short discussion of the case. No abstract is required. A manuscript for Images in Pathology should not exceed 500 words, with maximum of 10 references. This is distinct from the Case Report which is a full write up.

Brief Communications
Brief Communications are short reports intended to either extend or expound on previously published research or present new and significant findings which may have a major impact in current practice. If the former, authors must acknowledge and cite the research which they are building upon. The abstract should be from 50 to 75 words and should not be structured. A manuscript for brief communications should not exceed 5 typewritten pages (including tables, figures, illustrations and maximum of 10 references) or 1500 words.

Editorials
Recognized leaders in the field of pathology and laboratory medicine may be invited by the Editor-in-Chief/Editorial Board to present their scientific opinion and views of a particular topic within the context of an issue theme or issues on scholarly publication. No abstract or keywords necessary.

Letters to the Editor
PJP welcomes feedback and comments on previously published articles in the form of Letters to the Editor.
No abstract or keywords are necessary. A Letter to the Editor must not exceed 2 typewritten pages or 500 words.

Special Announcements
Special announcements may include upcoming conventions, seminars or conferences relevant to pathology. The Editors shall deliberate and decide on acceptance and publication of special announcements. Please coordinate with the Editorial Coordinator for any request for special announcements.

COVER LETTER

A cover letter must accompany each manuscript citing the complete title of the manuscript, the list of authors (complete names, position/designation and institutional affiliations), with one (1) author clearly designated as corresponding author, providing his/her complete institutional mailing address, institutional telephone/fax number, and work e-mail address. The **PJP Cover Letter Template** must be used.

PJP AUTHOR FORM

For submissions to the PJP to be accepted, all authors must read and sign this PJP Author Form consisting of (1) the Authorship Certification, (2) the Author Declaration, (3) the Author Publishing Agreement, and (4) the Statement of Disclosure of Conflicts of Interest. The completely accomplished PJP Author Form shall be scanned and submitted along with the manuscript. No manuscript shall be received without the PJP Author Form.

GENERAL FORMATTING GUIDELINES

- Authors must use the standard PJP templates for each type of manuscript. These templates are aligned with the most current versions of the EQuaToR Network guidelines and checklists (http://equatornetwork.org).
- The manuscript should be encoded on the template using Microsoft Word (2007 version or later version), single-spaced, 2.54 cm margins throughout, on A4 size paper. Preferred fonts may include Century Gothic (template default), Times New Roman, or Arial.
- The manuscript should be arranged in sequence as follows: (1) Title Page, (2) Abstract, (3) Text, (4) References, (5) Tables, and (6) Figures & Illustrations.
- All the sheets of the manuscript should be labelled with the page number (in Hindu-Arabic Numerals) printed on the upper right corner.
- References should pertain directly to the work being reported. Within the text, references should be indicated using Hindu-Arabic numerals in superscripts.

SPECIFIC FORMATTING GUIDELINES

Title and Authors

- The title should be as concise as possible.
- A running title (less than 50 characters) shall also be required. The running title is the abbreviated version of the title that will be placed in the header. The running title should capture the essence of the manuscript title.
- The full name of the author(s) directly affiliated with the work should be included (First name, Middle initial and Last name). The order of authorship shall be the prerogative of the author(s).
- There are 4 criteria for authorship (ICMJE recommendations). These are captured in the **PJP Author Form**.
  - **Substantial contributions to the conception or design of the work; or the acquisition, analysis, or interpretation of data for the work; AND**
  - **Drafting the work or revising it critically for important intellectual content; AND**
  - **Final approval of the version to be published; AND**
  - **Agreement to be accountable for all aspects of the work in ensuring that questions related to the accuracy or integrity of any part of the work are appropriately investigated and resolved.**
- The highest educational attainment or title of the authors should be included as an attachment whenever appropriate (MD, PhD, et cetera).
- Name and location of no more than one (1) institutional affiliation per author may be included.
- If the paper has been presented in a scientific forum or convention, a note should be provided indicating the name of the forum or convention, location (country), and date of its presentation.

Abstract

- **For manuscripts under the "Original Article" section:** the abstract should contain no more than 300 words with a structured format consisting of the following standard headings: objective/s, methodology, results and conclusion.
- **For manuscripts under the "Feature Article," "Review Article," "Case Report," "Brief Communications," and "Autopsy Vault" sections:** the abstract should be no more than 200 words and need not be structured.
- Letters to the Editor and editorials do not require an abstract.

Keywords

At least three (3) keywords but no more than six (6), preferably using terms from the **Medical Subject Headings (MeSH) list of Index Medicus,** should be listed horizontally under the abstract for cross-indexing of the article.

Text

- The text should be organized consecutively as follows: **Introduction, Methodology, Results and Discussion, Conclusion** (IMRaD format), followed by **Disclosures, Acknowledgments** and **References.**
- All references, tables, figures and illustrations should be cited in the text, in numerical order.
- All abbreviations should be spelled out once (the first time they are mentioned in the text) followed by the abbreviation enclosed in parentheses. The same abbreviation may then be used subsequently instead of the full names.
- All measurements and weights should be in System International (SI) units.
- Under **Methodology**, information should be provided on institutional review board/ethics committee approval or informed consent taking (if appropriate).
- **Acknowledgements** to individuals/groups of persons, or institution/s who have contributed to the manuscript but *did not qualify as authors* based on the ICMJE criteria, should be included at the end of the text just before the references. Grants and subsidies from government or private institutions should also be acknowledged.

References

- References in the text should be identified by Hindu-Arabic Numerals in superscript on the same line as the preceding sentence.
- References should be numbered consecutively in the order by which they are mentioned in the text. They should not be alphabetized.
- All references should provide inclusive page numbers.
- Journal abbreviations should conform to those used in PubMed.
- A maximum of six authors per article can be cited; beyond that, name the first three and add "et al."
- The style/punctuation approved by PJP conforms to that recommended by the International Committee of Medical Journal Editors (ICMJE) available at http://www.icmje.org. Examples are shown below:

One to Six Authors

Krause RM. The origin of plagues: old and new. *Science*. 1992;257:1073-1078.

Mokdad AH, Bowman BA, Ford ES, Vinicor F, Marks JS, Koplan JP. The continuing epidemics of obesity and diabetes in the US. JAMA. 2001;286(10):1195-1200.

More than Six Authors

Rhynes VK, McDonald JC, Gelder FB, et al. Soluble HLA class I in the serum of transplant recipients. Ann Surg. 1993; 217 (5): 485–9.

Authors Representing a Group

Moher D, Schulz KF, Altman D; for the CONSORT Group. The CONSORT statement: revised recommendations for improving the quality of reports of parallel-group randomized trials. JAMA. 2001;285(15):1987-1991.

Book

Byrne, DW. Publishing your medical research paper: What they don't teach in medical school. Baltimore: Williams & Wilkins, 1998.

World Wide Web

Barry JM. The site of origin of the 1918 influenza pandemic and its public health implications. [Commentary]. JTranslational Med. January 20, 2004;2(3):1-4. http://www.translational-medicine.com/content/2/1/3. Accessed November 18, 2005.

Tables

- Cite all tables consecutively in the text and number them accordingly.
- Create tables preferably using Microsoft Excel with one table per worksheet.
- Tables should not be saved as image files.
- The content of tables should include a table number (Hindu-Arabic) and title in capital letters above the table.
- Place explanatory notes and legends, as well as definitions of abbreviations used below the table. For legends, use small letters (i.e., a, b, c, d).
- Each table must be self-explanatory, being a supplement rather than a duplicate of information in the text.
- Up to a maximum of five (5) tables are allowed.

Figures and Graphs

- Figures or graphs should be identified by Hindu-Arabic Numeral/s with titles and explanations underneath.
- The numbers should correspond to the order in which the figures/graphs occur in the text.
- Figures & graphs should not be saved as image files. For illustrations and photographs, see next section.
- Provide a title and brief caption for each figure or graph. Caption should not be longer than 15-20 words.
- All identifying data of the subject/s or patient/s under study such as name or case numbers, should be removed.
- Up to a maximum of five (5) figures and graphs are allowed.

Illustrations and Photographs

- Where appropriate, all illustrations/photographic images should be at least 800 x 600 dpi and submitted as image files (preferably as .png, .jpeg, .tif, .psd or .pdf files).
- For photomicrographs, the stain used (e.g. H & E) and magnification (e.g. 400X) should be included in the description.
- Computer-generated illustrations which are not suited for reproduction should be professionally redrawn or printed on good quality laser printers. Photocopies are not acceptable.
- All letterings for illustration should be of adequate size to be readable even after size reduction.
- Place explanatory notes and legends, as well as definitions of abbreviations used below the illustration/photograph.
- Up to a maximum of five (5) illustrations/ photographs are allowed.

N.B.: For tables, figures, graphs, illustrations and photographs that have been previously published in another journal or book, a note must be placed under the specific item stating that such has been adapted or lifted from the original publication. This should also be referenced in the **References** portion.

EDITORIAL PROCESS (Figure 1)

- The Editorial Coordinator shall review each submission to check if it has met aforementioned criteria and provide feedback to the author within 24 hours.
- Once complete submission is acknowledged, the manuscript undergoes Editorial Board Deliberation to decide whether it shall be considered or not for publication in the journal. Within five (5) working days, authors shall be notified through e-mail that their manuscript either (a) has been sent to referees for peer-review or (b) has been declined without review.
- The PJP implements a strict double blind peer review policy. For manuscripts that are reviewed, authors can expect a decision within ten (10) working days from editorial deliberation. There may be instances when decisions can take longer: in such cases, the Editorial Coordinator shall inform the authors.
- The editorial decision for manuscripts shall be one of the following: (a) acceptance without further revision, (b) acceptance with minor revisions, (c) major manuscript revision and resubmission, or (d) non-acceptance.
- Accepted manuscripts are subject to editorial modifications to bring them in conformity with the style of the journal. Copyediting and layout shall take five (5) working days, after which the manuscript is published online.
- All online articles from the last six (6) months shall be collated and published in print as a full issue.

EDITORIAL OFFICE CONTACT INFORMATION:

The Philippine Journal of Pathology
2nd Floor, Laboratory Research Division
Research Institute for Tropical Medicine
Filinvest Corporate City
Alabang, Muntinlupa City 1781
Editor-in-Chief: **Amado O. Tandoc III, MD, FPSP**
Telefax number: (+632) 88097120
E-mail: philippinepathologyjournal@gmail.com
Website: http://philippinejournalofpathology.org

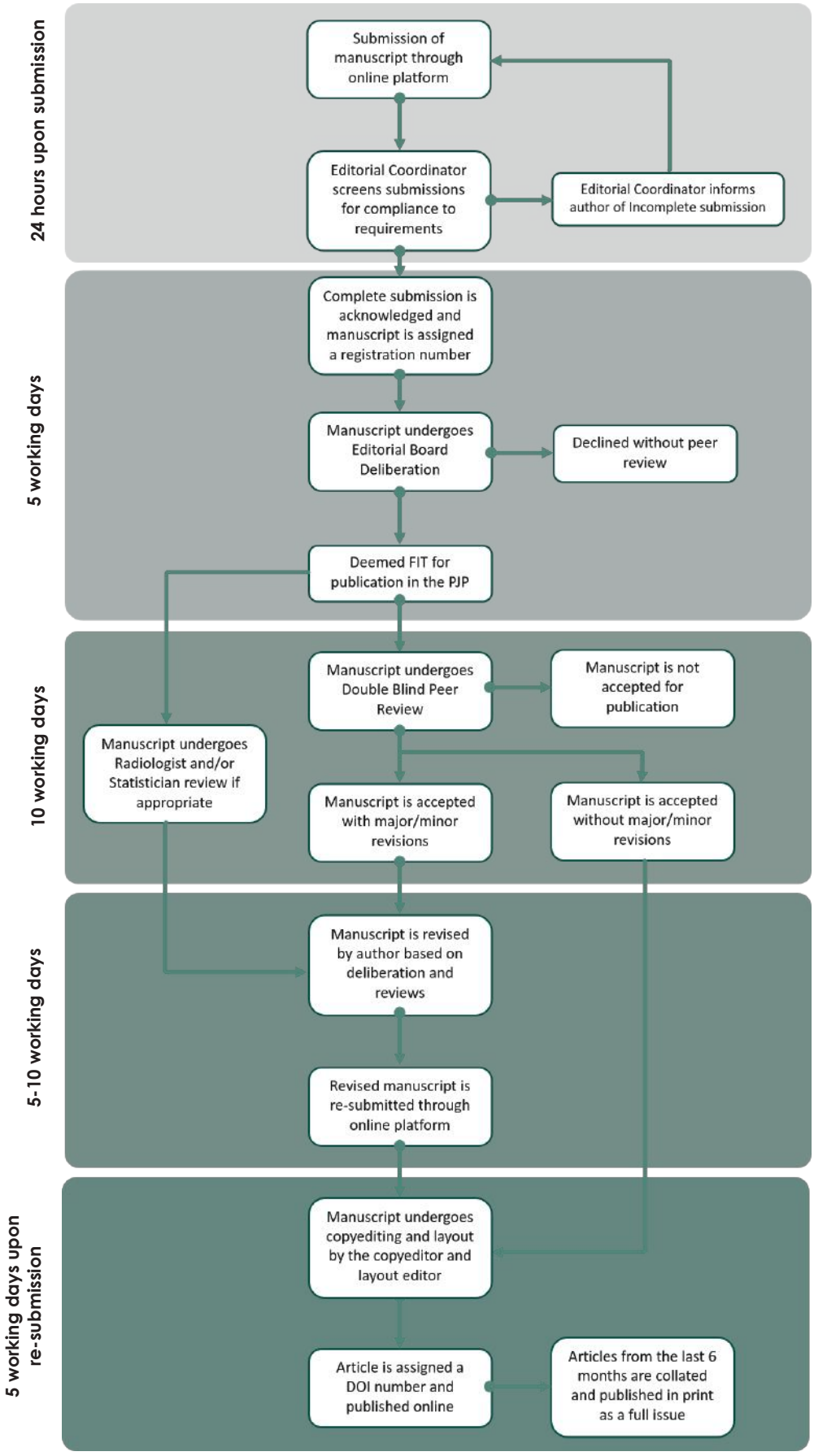

Figure 1. Editorial Process Flow.

PHILIPPINE JOURNAL OF PATHOLOGY

PJP-2024-AF-001: PJP Author Form v.2024

PJP AUTHOR FORM (PJP-2024-AF-001)

For submissions to the PJP to be accepted, all authors must read and sign this PJP Author Form consisting of (1) the Authorship Certification, (2) the Author Declaration, (3) the Author Publishing Agreement, and (4) the Statement of Disclosure of Conflicts of Interest. The completely accomplished PJP Author Form shall be scanned and submitted along with the manuscript. No manuscript shall be received without the PJP Author Form.

COMPLETE TITLE OF MANUSCRIPT

_____

_____

_____

AUTHORSHIP CERTIFICATION

☐ In consideration of our submission to the Philippine Journal of Pathology (PJP), the undersigned author(s) of the manuscript hereby certify, that all of us have actively and sufficiently participated in (1) the conception or design of the work, the acquisition, analysis and interpretation of data for the work; AND (2)drafting the work, revising it critically for important intellectual content; AND (3) that we are all responsible for the final approval of the version to be published; AND (4) we all agree to be accountable for all aspects of the work in ensuring that questions related to the accuracy or integrity of any part of the work are appropriately investigated and resolved.

AUTHOR DECLARATIONS

☐ The undersigned author(s) of the manuscript hereby certify, that the submitted manuscript represents original, exclusive, and unpublished material. It is not under simultaneous consideration for publication elsewhere. Furthermore, it will not be submitted for publication in another journal, until a decision is conveyed regarding its acceptability for publication in the PJP.

☐ The undersigned hereby certify that the study on which the manuscript is based has conformed to ethical standards and/or has been reviewed by the appropriate ethics committee.

☐ The undersigned likewise hereby certify that the article had written/informed consent for publication from involved subjects (for case report/series only) and that in case the involved subject/s can no longer be contacted (i.e., retrospective studies, no contact information, et cetera), all means have been undertaken by the author(s) to obtain the consent.

AUTHOR PUBLISHING AGREEMENT

☐ Furthermore, the undersigned author(s) shall retain ownership of copyright and intellectual rights for the journal article published in the PJP AND grants publishing rights to the journal which licenses all published manuscripts to be used for building on and expanding knowledge, for non-commercial purposes, so long as the manuscripts are properly cited and recognized (Attribution-NonCommercial-ShareAlike 4.0 International Creative Commons License [CC BY-NC-SA 4.0].

AUTHOR DISCLOSURE OF CONFLICTS OF INTEREST

To ensure scientific objectivity and independence, the PJP requires all authors to make full disclosure of areas of potential conflict of interest. Such disclosure will indicate whether the person and/or his/her immediate family has any financial relationship with pharmaceutical companies, medical equipment manufacturers, biomedical device manufacturers, or any companies with significant involvement in the field of health care. Place all disclosures in the table below. An extra form may be used if needed.

Examples of disclosures include but are not limited to ownership, employment, research support (including provision of equipment or materials), involvement as a speaker, consultant, or any other financial relationship or arrangement with manufacturers, companies or suppliers. For any relationships identified, the author(s) must provide sufficiently detailed information to permit assessment of the significance of the potential conflict of interest (for example, the amount of money involved and/or the identification of any value of goods and services).

AUTHOR NAME	RELATIONSHIP	MANUFACTURER/ SUPPLIER/ COMPANY

All disclosures shall remain confidential during the review process and the nature of any final printed disclosure will be determined by the PJP. If there are no conflicts of interest to disclose, the author(s) should check the box below.

☐ I/We do not have any conflicts of interest to disclose.

Author Name	Signature	Date (MM/DD/YYYY)
_____	_____	_____
_____	_____	_____
_____	_____	_____
_____	_____	_____
_____	_____	_____

ICMJE Form for Disclosure of Potential Conflicts of Interest

Date: _____

Your Name: _____

Manuscript Title: _____

Manuscript number (if known): _____

In the interest of transparency, we ask you to disclose all relationships/activities/interests listed below that are related to the content of your manuscript. "Related" means any relation with for-profit or not-for-profit third parties whose interests may be affected by the content of the manuscript. Disclosure represents a commitment to transparency and does not necessarily indicate a bias. If you are in doubt about whether to list a relationship/activity/interest, it is preferable that you do so.

The following questions apply to the author's relationships/activities/interests as they relate to the **current manuscript only.**

The author's relationships/activities/interests should be **defined broadly.** For example, if your manuscript pertains to the epidemiology of hypertension, you should declare all relationships with manufacturers of antihypertensive medication, even if that medication is not mentioned in the manuscript.

In item #1 below, report all support for the work reported in this manuscript without time limit. For all other items, the time frame for disclosure is the past 36 months.

		Name all entities with whom you have this relationship or indicate none (add rows as needed)	**Specifications/Comments (e.g., if payments were made to you or to your institution)**
Time frame: Since the initial planning of the work			
1	All support for the present manuscript (e.g., funding, provision of study materials, medical writing, article processing charges, etc.) **No time limit for this item.**	____None	
Time frame: past 36 months			
2	Grants or contracts from any entity (if not indicated in item #1 above).	____None	
3	Royalties or licenses	____None	

4	Consulting fees	____None	
5	Payment or honoraria for lectures, presentations, speakers bureaus, manuscript writing or educational events	____None	
6	Payment for expert testimony	____None	
7	Support for attending meetings and/or travel	____None	
8	Patents planned, issued or pending	____None	
9	Participation on a Data Safety Monitoring Board or Advisory Board	____None	
10	Leadership or fiduciary role in other board, society, committee or advocacy group, paid or unpaid	____None	
11	Stock or stock options	____None	
12	Receipt of equipment, materials, drugs, medical writing, gifts or other services	____None	
13	Other financial or non-financial interests	____None	

Please place an "X" next to the following statement to indicate your agreement:

____ I certify that I have answered every question and have not altered the wording of any of the questions on this form.

PHILIPPINE JOURNAL OF PATHOLOGY
PJP

PATIENT CONSENT FORM

For case report and image submissions to the PJP to be accepted, the author/s must ensure that patients or patients' legal guardian/relative have provided informed consent to publish information about them in the journal. The completely accomplished PJP Patient Consent Form shall be scanned and submitted along with the manuscript. No case report and image shall be received without the PJP Consent Form.

Name of person described in article or shown in photograph:_____

_____

Subject matter of photograph or article (brief description):

_____

_____

_____

(The Subject matter of the photograph or article is hereafter termed as the "INFORMATION.")

Title of article:

_____

_____

I, _____ , give my consent for this information
[please insert your full name]

about MYSELF/MY CHILD OR WARD/MY RELATIVE relating to the subject matter
[please underline correct description]

above to appear in the Philippine Journal of Pathology (PJP) subject to its publication policies and ethical standards.

I have seen and read the material to be submitted to the PJP and thoroughly understand the following:

- The Information will be published in the PJP without my name. It is the obligation of the PJP to make all attempts, within its reasonable jurisdiction and authority, to ensure my anonymity.
- The Information may also be placed on the PJP website.
- The PJP shall not allow the Information to be used for advertising or packaging or to be used out of context (i.e., used to accompany an entirely different article or topic).
- I can withdraw my consent at any time before publication, but once the Information has already been sent to press, it is my understanding that it will not be possible to revoke the consent.

Signed:_____ Date:_____
[signature over complete name]

Witness:

Signed:_____ Date:_____
[signature over complete name]

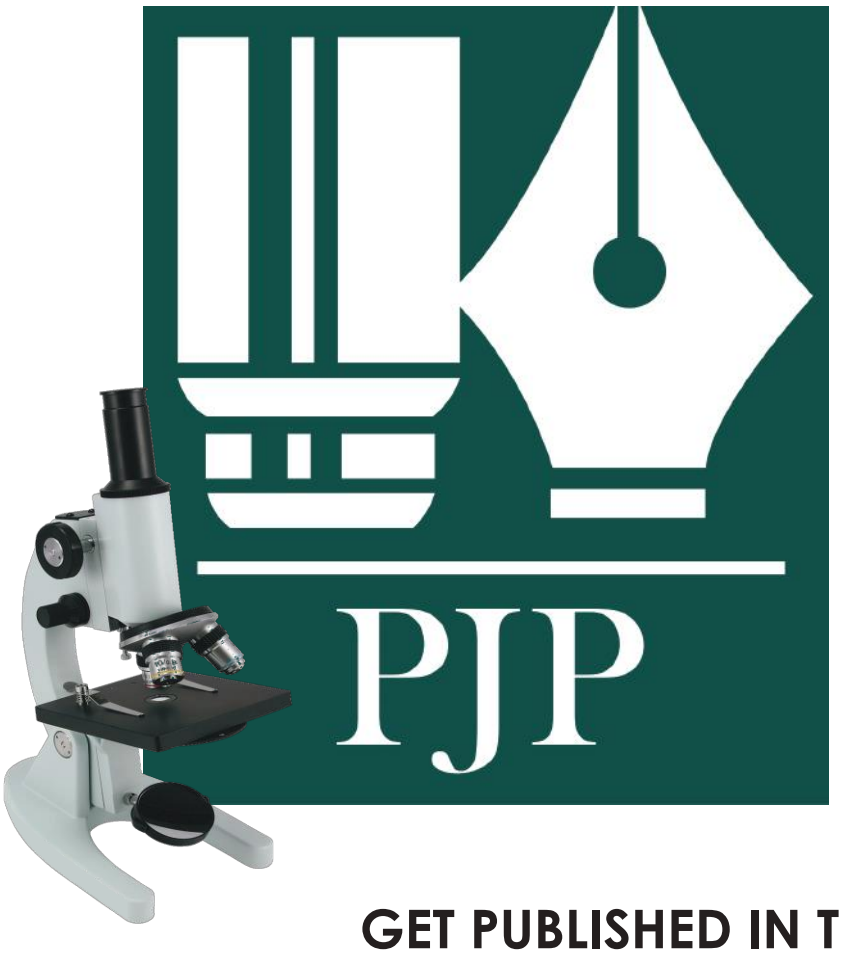

- *Online and Printed*
- *100% Open Access*
- *Peer Reviewed*
- *Continuous Publication model*
- *No Author Processing Fees*
- *Streamlined process from submission to publication*
- *24/7 web-based technical support*

GET PUBLISHED IN THE NEW PHILIPPINE JOURNAL OF PATHOLOGY!

The Philippine Journal of Pathology (PJP) is an open-access, peer-reviewed, English language, medical science journal published by the Philippine Society of Pathologists, Inc. It shall serve as the official platform for publication of high quality original articles, case reports or series, feature articles, and editorials covering topics on clinical and anatomic pathology, laboratory medicine and medical technology, diagnostics, laboratory biosafety and biosecurity, as well as laboratory quality assurance.

The journal's primary target audience are laboratorians, diagnosticians, laboratory managers, pathologists, medical technologists, and all other medical and scientific disciplines interfacing with the laboratory. For instructions and more information, visit our Official Website at:

http://philippinejournalofpathology.org

PJP Philippine Journal of Pathology

Philippine Society of Pathologists, Inc.

ICMJE COPE DOAJ equator network Crossref Scopus PAMJE

TONGUE SWAB SAMPLE FOR MYCOBACTERIUM TUBERCULOSIS

PLUSLIFE MINIDOCK

SMALL: PALM-SIZED,
WEIGHT LESS THAN IPHONE14 (~240G)
ACCURATE: COMPARABLE PERFORMANCE TO PCR RAPID:
RESULT IN 7-35 MINUTES SIMPLE: WITHIN 2 MINS HANDS-ON TIME FLEXIBLE: FREE FROM COLD-CHAIN

WHO-PREQUALIFIED FOR MTB;
OTHER TEST: CT/NG/UU; HPV 16/18/45
GROUP B STREPTOCOCCUS;
INFLUENZA A/B/RSV; STREP A

ALLIED HOSPITAL SUPPLY INTERNATIONAL CORP.

6 LEONARD WOOD LOOP, BAGUIO CITY
UNIT 1, BSC BLDG. 144 MINDANAO AVE, QC
TEL NO.: (02) 8-928-4649;
FAX NO.: (02) 3-455-4323

WEBSITE

Philippine Journal of Pathology
Committee on Publications | Philippine Society of Pathologists, Inc.
E-mail: philippinepathologyjournal@gmail.com
Website: https://philippinejournalofpathology.org